

UNIVERSITÀ DEGLI STUDI DI BOLOGNA
FACOLTÀ DI SCIENZE MATEMATICHE, FISICHE E NATURALI

Dottorato di Ricerca in Dottorato di ricerca in Scienze Ambientali: tutela e gestione delle
risorse naturali
XIX ciclo
GEO/08

**Destino del carbonio organico di apporto
fluviale sulle piattaforme continentali:
Adriatico centro-settentrionale e Golfo del
Leone**

Dottorando:
Tommaso Tesi

Relatore:
Dott.ssa Rossella Pistocchi

Correlatore:
Dr. Stefano Miserocchi
Dr. Leonardo Langone

Coordinatore:
Dr. Carlo Ferrari

| | |
|---|----|
| 1. INTRODUCTION | 3 |
| 2. STUDY AREAS | 6 |
| 2.1. ADRIATIC SEA | 6 |
| 2.2 GULF OF LIONS | 9 |
| 3. SAMPLING..... | 12 |
| 3.1 ADRIATIC SEA | 12 |
| 3.2. PO PRODELTA AREA | 14 |
| 3.3. GULF OF LIONS | 16 |
| 4. METHODS..... | 18 |
| 4.1. PRETREATMENT | 18 |
| 4.2. ELEMENTAL ANALYSES..... | 18 |
| 4.3. STABLE ISOTOPIC ANALYSES | 18 |
| 4.4. ALKALINE CUO OXIDATIONS (LIGNIN, BENZOIC ACIDS, P-HYDROXYBENZEBES)..... | 19 |
| 4.5. GRAIN SIZE ANALYSES..... | 21 |
| 4.6. AMS ¹⁴ C ANALYSIS | 21 |
| 5. ADRIATIC SEA | 22 |
| 5.1 RESULTS..... | 22 |
| 5.1.1 TSS, OC and TN | 22 |
| 5.1.2 Isotopic data..... | 22 |
| 5.1.3 CuO oxidation products..... | 23 |
| 5.1.4 Grain-size analyses | 23 |
| 5.1.5 Hydrographic data | 24 |
| 5.2 DISCUSSION | 26 |
| 5.2.1 PCA..... | 26 |
| 5.2.2 Sources of OM in the Western Adriatic..... | 27 |
| 5.2.3 Influence of the river plume on primary productivity | 31 |
| 5.2.4 Sediment variability along shelf..... | 34 |
| 5.2.5 Quantitative assessment of OM contributes in the western Adriatic Sea | 38 |
| 5.2.6 End-member mixing models..... | 42 |
| 6. PO PRODELTA AREA | 48 |
| 6.1 RESULTS..... | 48 |
| 6.1.1 Elemental, carbon stable composition and CuO oxidation products..... | 48 |
| 6.1.2 Radiocarbon compositions ($\Delta^{14}\text{C}$) | 49 |
| 6.1.3 Grain size analyses..... | 49 |
| 6.2 DISCUSSION | 51 |
| 6.2.1. Soil-derived OC vs vascular plant fragments..... | 51 |
| 6.2.2 ¹⁴ C age and CuO oxidation products..... | 54 |
| 6.2.3 Effect of sediment dynamics on biogeochemical distributions | 56 |
| 7. GULF OF LIONS..... | 63 |
| 7.1 RESULTS..... | 63 |
| 7.1.1 OC, TN and $\delta^{13}\text{C}$ | 63 |
| 7.1.2 CuO oxidization products..... | 64 |
| 7.1.3 Grain size analyses..... | 64 |
| 7.2 DISCUSSION | 67 |
| 7.2.1. Organic matter origin | 67 |
| 7.2.2 Sediment sorting..... | 71 |
| 7.2.3 Surficial OM distribution in the Gulf of Lions | 76 |
| 8. CONCLUSIONS | 84 |
| BIBLIOGRAPHY | 88 |

1. Introduction

Burial of terrestrial and marine organic matter (OM) in marine sediments is an important reservoir representing the predominant long-term sink in the global biogeochemical cycle of organic carbon (OC) (Bernier, 1982, 1989). Deltas and continental shelves receive large inputs from both autochthonous and allochthonous sources and account for ~ 90% OC burial in the ocean (Bernier, 1982, 1989; Hedges and Keil, 1995). Several geochemical studies have characterized composition and evolution of terrigenous particulate organic matter (OM) in continental margins, resulting in several key insights. Nowadays, we have realized that allochthonous material supplied by rivers is a heterogeneous and complex mixture of organic compounds with different chemical characteristics, originating from different sources (reactive freshwater phytoplankton, soil, leaf debris, woody fragments, kerogen etc.) (Goñi and Hedges, 1990; Hedges et al., 1997; Goñi et al., 2003). The composition of the materials exported by rivers is also quite dynamic, changing in both seasonal and inter-annual time scales (Gordon and Goñi, 2003; Miserocchi et al., 2007). Much of the OM deposited in prodelta areas is aged due to both the preferential degradation of the marine-riverine labile fraction compared to refractory terrestrial material as well as continental denudation, which can introduce ancient OC (Blair et al., 2003, Gordon and Goñi 2003, Aller and Blair, 2004). Additionally, the benthic boundary layer (BBL) is a key zone for the transport, transformation and diagenesis of OC; in highly porous BBL, fluid and mobile muds can act as a “reactor” where oxic and anoxic biogeochemical cycles promote efficient OC remineralization (Wainright and Hopkinson, 1997; Aller, 1998; Aller and Blair, 2004).

During the EuroSTRATAFORM (EUROpean STRATA FORMation on Margins) project, a multidisciplinary research effort was carried out to investigate the transport and deposition of riverine material in the Mediterranean Sea. The Rhône and the Po rivers are

currently the two largest fresh water inputs to the Mediterranean Sea. The Adriatic Sea (Italy) and the Gulf of Lions (France) have various sources of particulate matter (Roussiez et al., 2005; Miserocchi et al., 2007) and potentially sequester a significant fraction of these materials in their seabed. The primary objective of this study, within the the EuroSTRATAFORM project, was to characterize the age and composition of allochthonous and autochthonous OM in surficial sediments and suspended material using CuO oxidation, elemental, $\delta^{13}\text{C}$ and $\Delta^{14}\text{C}$ analyses. In addition, this study investigated the processes and mechanisms responsible for the evolution of organic matter along the Western Adriatic shelf and Gulf of Lions, where sediment transport and biological activity are intimately coupled.

Factors such as the timing of the sediment input and transport in relationship with physical oceanographic conditions in the receiving basin (i.e. tides, wave height, shear stress, currents) have a critical effect on the efficiency of sediment deposition and OC accumulation (Fox et al., 2004; Wheatcroft et al., 2006). The mechanisms of sediment transport have been particularly well investigated in these regions from a group of American and European scientists as part of the EuroSTRATAFORM project (Palinkas et al., 2005; Frignani et al., 2005; Syvinsky and Kettner, 2007; Palinkas and Nittrouer, 2006; Fain et al., 2007; Milligan et al., 2007; etc.). Over the course of five years, integrated coastal studies have been conducted to understand the processes governing the input, transport and fate of sediments from the terrestrial to the oceanic environment via rivers in the Mediterranean continental margins. These efforts have significantly increased basic understanding of the physical, geological and chemical mechanisms responsible for the dispersal and deposition of riverine material. Consequently, the union of this information regarding sediment dynamic with our data set is an exclusive occasion that facilitates the interpretation of the biogeochemical distributions observed in these European margins.

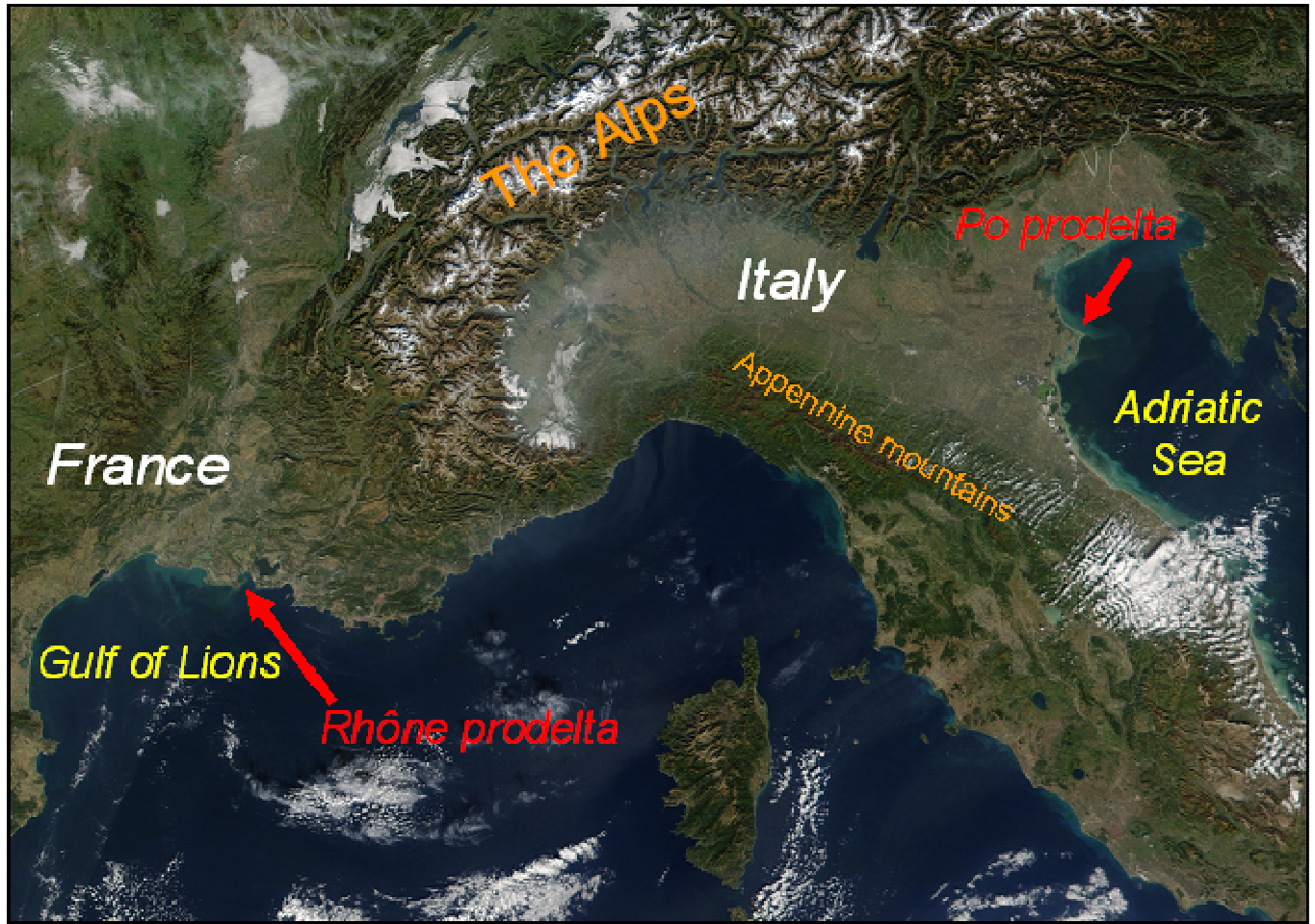


Fig.1.1 Studies areas in the Mediterranean Sea: Gulf of Lions (France) and Adriatic Sea (Italy).

2. Study areas

2.1. Adriatic Sea

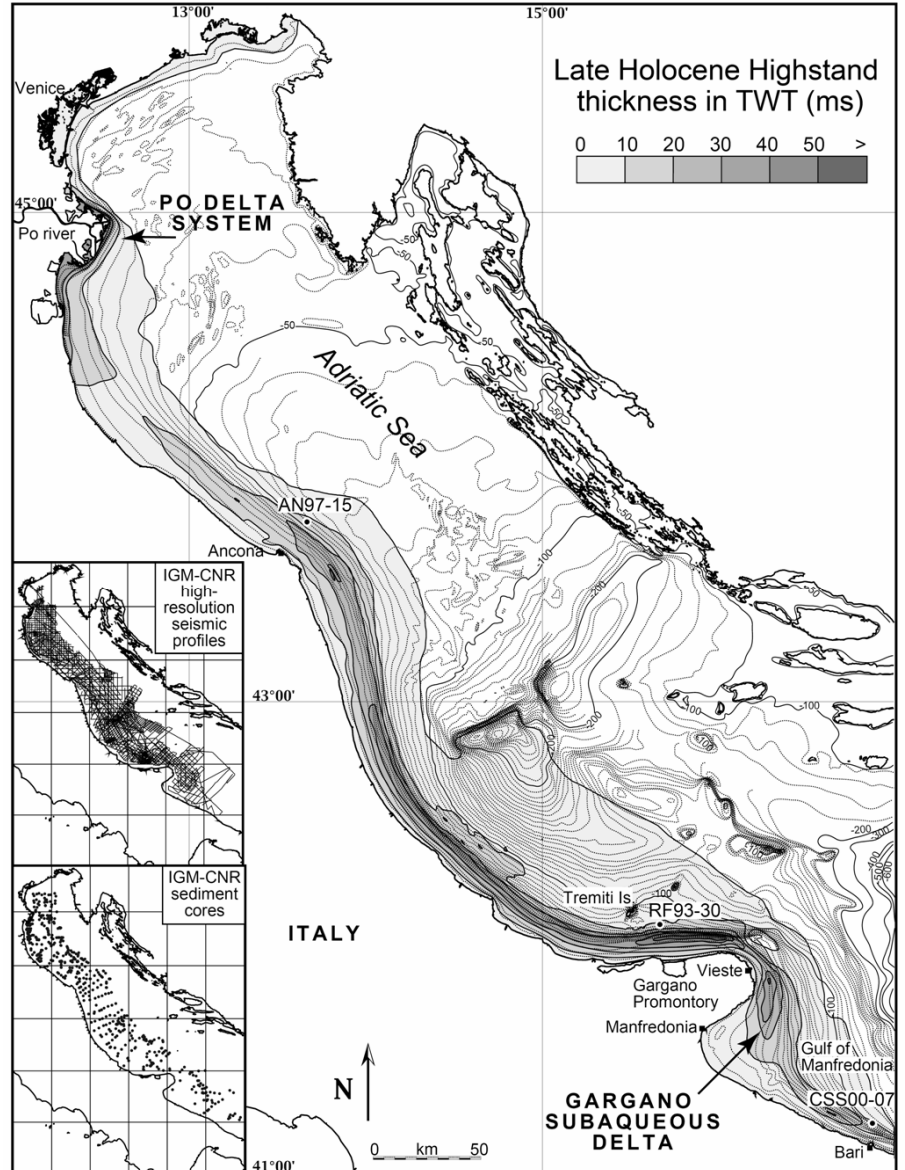
The Adriatic shelf is a shallow semi-enclosed basin (Cattaneo et al., 2003). The margin exhibits an extensive and continuous mud-dominated regressive wedge formed after the attainment of the modern high-stand in sea level (i.e. mid-late Holocene) under the combined influence of fluvial supply and marine processes (Correggiari et al., 2001; Cattaneo et al., 2003). This mud wedge, known as a clinoform, includes a continuous belt of deltaic and shallow-marine deposits up to 35 m thick (Correggiari et al., 2001). In sections perpendicular to the shore, it appears to be composed of forestepping sigmoides with gently dipping foresets (Correggiari et al., 2001). An important feature of the Adriatic basin is that its main clastic sources are not equally distributed but are primarily located along the western side (Cattaneo et al., 2003). The Po River, at 673 km long, is the largest Italian river and supplies over 50% of the fresh water input to the northern Adriatic basin (Degobbis et al., 1986). The Po delta includes 5 distributary mouths (the Maestra, Pila, Tolle, Gnocca, and Goro) each with different water discharges and solid loads. The Pila is the main mouth, accounting for 60% of water discharge and 74% of the sediment load (Nelson, 1970). The Po River is characterized by two annual floods associated with increased rainfall in autumn and snowmelt in spring. South of the Po, an array of rivers (Fig. 3.1) drain the Appennine Mountains along the eastern coast delivering approximately 22 Mt/y of sediment (Syvitski and Kettner, 2007). The Adriatic basin has a microtidal regime and is dominated by thermohaline currents. The surface circulation is characterized by cyclonic movement driven by buoyancy effects and wind patterns (Malanotte-Rizzoli and Bergamasco, 1983) which generate a southward flow along the eastern Italian shore (Western Adriatic Coastal Current, WACC Fig. 3.1; Zavatarelli et al., 2002).

Rapid accumulation after the Po floods (Fox et al., 2004) generates an ephemeral deposit of sediments that is subsequently remobilized by waves to form density flows (Traykovski et al., 2007). The sediments then travel southward in a series of wind-induced resuspension events promoted by Bora and Scirocco winds (Fain et al., 2006). South of the Po River, the amount of suspended sediment is increased by the Appennine Rivers through episodic high sediment discharges driven by climate conditions (Syvistski and Kettner, 2007). On the shelf, two transport pathways appear to be active: one occurs in shallow water and is dominated almost completely by along-shelf transport due to the WACC; the second takes place in deeper water and is driven by both along- and off-shelf transport due to Ekman veering (Fain et al., in press). Sediment erosion along the western Adriatic Sea varies both temporally and spatially. In wintertime, sediment in the vicinity of the Po delta (in the northern region) is less easily eroded than in the south. In summertime, the pattern is reversed, likely due to increased interparticle cohesion and binding of the sediment with exopolymeric substances released by microphytobenthos (Stevens et al., in press). Relatively high accumulation rates were recorded in the Po prodelta (up to $6.6 \text{ g cm}^{-2} \text{ yr}^{-1}$) and along a narrow belt between the Pescara and the Gargano peninsula (Frignani et al., 2005, Palinkas and Nittrouer, in press). There is not a geographical correlation between the sediment entry points and the depocenter locations because of the efficient transport of sediment (Cattaneo et al., 2003).

The load of particulate OC (POC) supplied by the Po River has been estimated at $13.4 \times 10^4 \text{ t yr}^{-1}$, making this river the most important contributor of OM and nutrients to the Mediterranean Sea (Pettine et 1998). Because the Po valley is one of the most productive agricultural areas in Italy, this river also accounts for ~50% of the total nutrient input into the northern Adriatic (Degobbis & Gilmartin, 1990). The highest average primary production values were measured in the northern region of the Adriatic Sea ($588 \text{ g C m}^{-2} \text{ yr}^{-1}$). In contrast, production in the middle and southern regions of the Adriatic is significantly

lower (137 and 97 g C m² y⁻¹, respectively), resulting in a strong eutrophic-oligotrophic gradient (Giordani et al., 2002).

Fig. 2.1. Thickness map of the HST wedge (from Correggiari et al., 2001). The HST wedge has three distinct depocentres: (1) offshore the Po river delta, (2) along the central Adriatic margin, and (3) eastwards of the Gargano promontory.



2.2 Gulf of Lions

The GoL is a modern wave-dominated continental shelf incised by a number of submarine canyons and characterized by a micro-tidal regime. The basin exhibits an extensive and continuous mid-shelf mud belt formed during the present high-stand in sea level under the combined influence of fluvial supply and re-suspension events (Aloisi et al., 1973, Fig 2.2). Maximum Holocenic mud belt thickness ranges from between 5 and 25 m; with the thickness decreasing from the Rhône river mouth towards the South West. This pattern of sedimentation confirms the major role of Rhône river during the post-glacial period in term of material inputs compared to the western rivers (Têt, Aude, Hérault, Orb) as well as underlines the influence of the westerly Liguro-Provençal current on particle dispersal (Aloisi et al., 1973). On the shelf, the granulometric distribution consists of a sandy band on the inner-shelf followed by a typical mid-shelf mud belt (Fig. 2.2) with a mix of relict sands and modern fine-grained sediments characterizing the outer-shelf (Roussiez et al., 2005).

Following the construction of the Aswan High Dam on the Nile River, the Rhône river represents the major fresh water and OC input to the Mediterranean Sea (Pettine et al., 1998; Sempéré et al., 2000). The Rhône catchment is one of the largest in Europe, with a drainage area of 97800 Km². The influence of discharge from the Alps is predominant, contributing to about 80% of the solid-liquid annual discharge. River regulation and damming are mostly located in the uppermost course (Arnau et al., 2004) while in its lower part the river crosses a succession of urban areas (Avignon, Beaucaire-Tarascon and Arles) (Arnaud-Fassetta, 2002). The Rhône river, upon entering the open sea, is stratified in a multi-layered system. The uppermost layer is thin (<1 m) and corresponds to the river plume, for which dilution depends on the physical regime. A second layer, much thicker at ~10 m, is present near the sea bed. This deeper layer

makes up the bottom nepheloid layer and is an important vector for offshore transport (Roussiez et al., 2005).

The hydrodynamic processes and mixing in the Rhône estuary are typical of a micro-tidal saltwedge estuary. The salt water forms a wedge near the bottom, beneath a layer of riverine fresh water. The inland extent of this wedge is primarily controlled by river discharge. The coarse particulate ($> 5 \mu\text{m}$) riverine material is trapped close to the landward limit of the salinity intrusion due to settling and dilution processes. The finest fraction (2-5 μm) has a more complex behavior displaying a poor average reactivity regarding salt induced flocculation (Thill et al., 2001).

The Rhône river is the dominant (80%) source of terrigenous material in the GoL (Durrieu de Madron et al., 2000) and its water discharge varies from $5 \cdot 10^2$ to $10^4 \text{ m}^3 \text{ s}^{-1}$, with an annual mean flow of $1715 \text{ m}^3 \text{ s}^{-1}$ (Naudin et al. 1997) and with a mean solid discharge of $6.2 \cdot 10^6 \text{ t y}^{-1}$ (Thill et al., 2001). The annual riverine OC input delivered to the GoL by the Rhône is $19.2 \pm 6 \cdot 10^4 \text{ t C y}^{-1}$ (Sempéré et al., 2000), comprising the majority of the total annual riverine contribution to the GoL, evaluated at around $24 \pm 10 \cdot 10^4 \text{ t C y}^{-1}$ (Durrieu de Madron et al., 2000). The GoL is characterized by phosphorus deficiency, which limits nitrate uptake by phytoplankton and overall primary productivity (Diaz et al., 2001), which was estimated to be about $71 \pm 7 \text{ g C m}^{-2}$ (Raimbault and Durrieu de Madron, 2003).

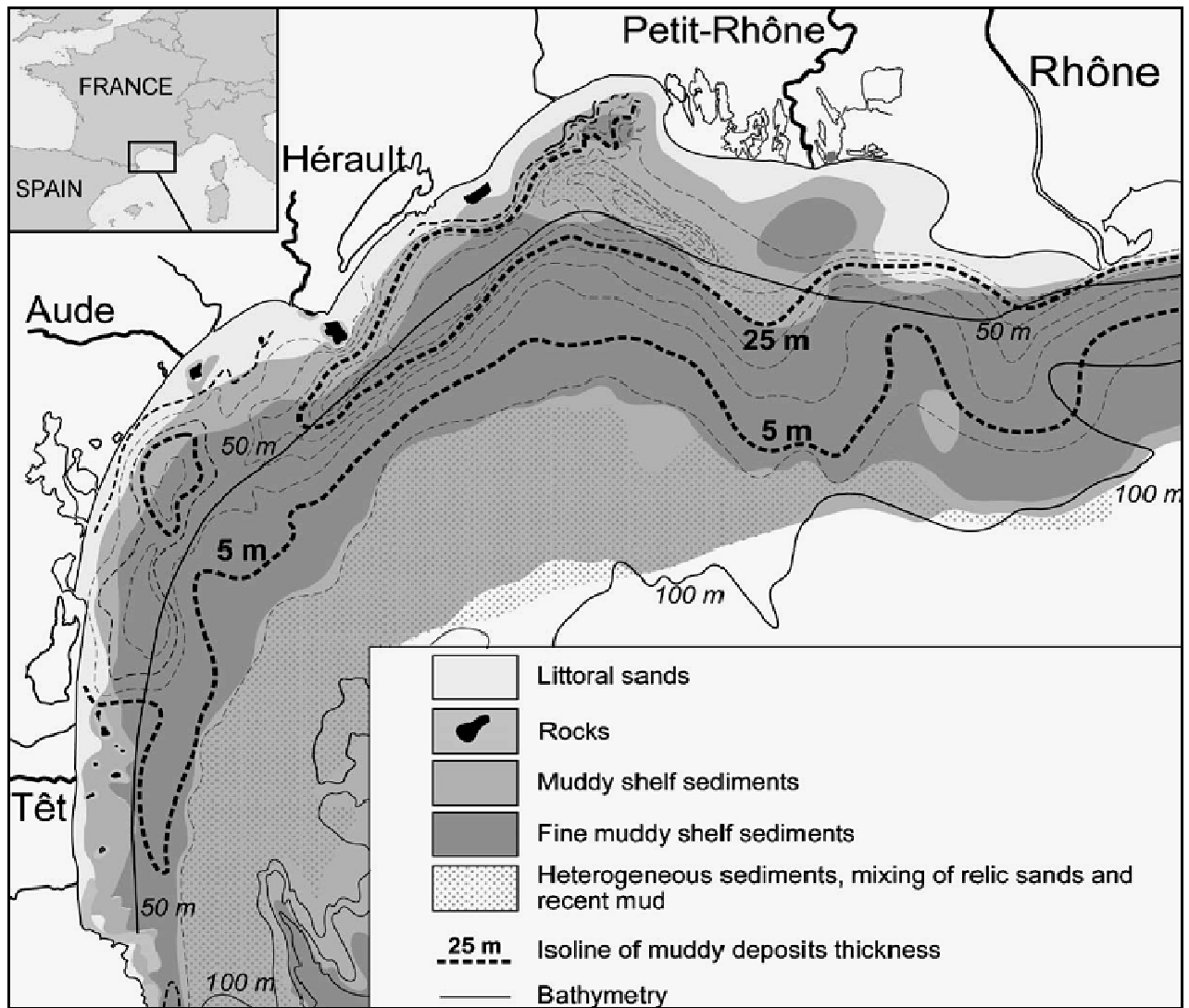


Fig. 2.2. Grain size distribution of surface sediments of the Gulf of Lions (Aloisi et al., 1973)

3. Sampling

3.1 Adriatic Sea

Suspended matter in the water column were collected in February 2003 along transects perpendicular to the shore (Fig. 3.1). Known volumes of water for elemental and isotopic analyses was filtered onto pre-combusted, 25-mm Whatman GF/F glass fiber filters. Total suspended material (TSM) samples were filtered onto pre-weighed, 25-mm Whatman GF/F glass fiber filters. All filters were stored at -20 °C until analysis. In the laboratory, the filters were oven-dried at 60 °C. Vertical water column profiles were acquired along the same transects. Data include depth, potential temperature, salinity, density (σ_t) and chlorophyll fluorometry.

Surficial sediments were collected in May 2003. The samples were collected in the Po prodelta area and several cores were taken on the mud-wedge along cross-shelf transects in order to sample three different portions of the clinoform: topset, foreset and bottomset (Fig. 3.1). The sediments were collected using a large diameter box corer. The cores were then sub-sampled using a 15-cm PVC liner. Surface sediments from the upper horizon (0–1 cm) were sampled and analyzed for this study. Besides the marine sediments, additional surficial sediments from the Po and Biferno rivers were collected in order to better delineate the composition of the riverine source.

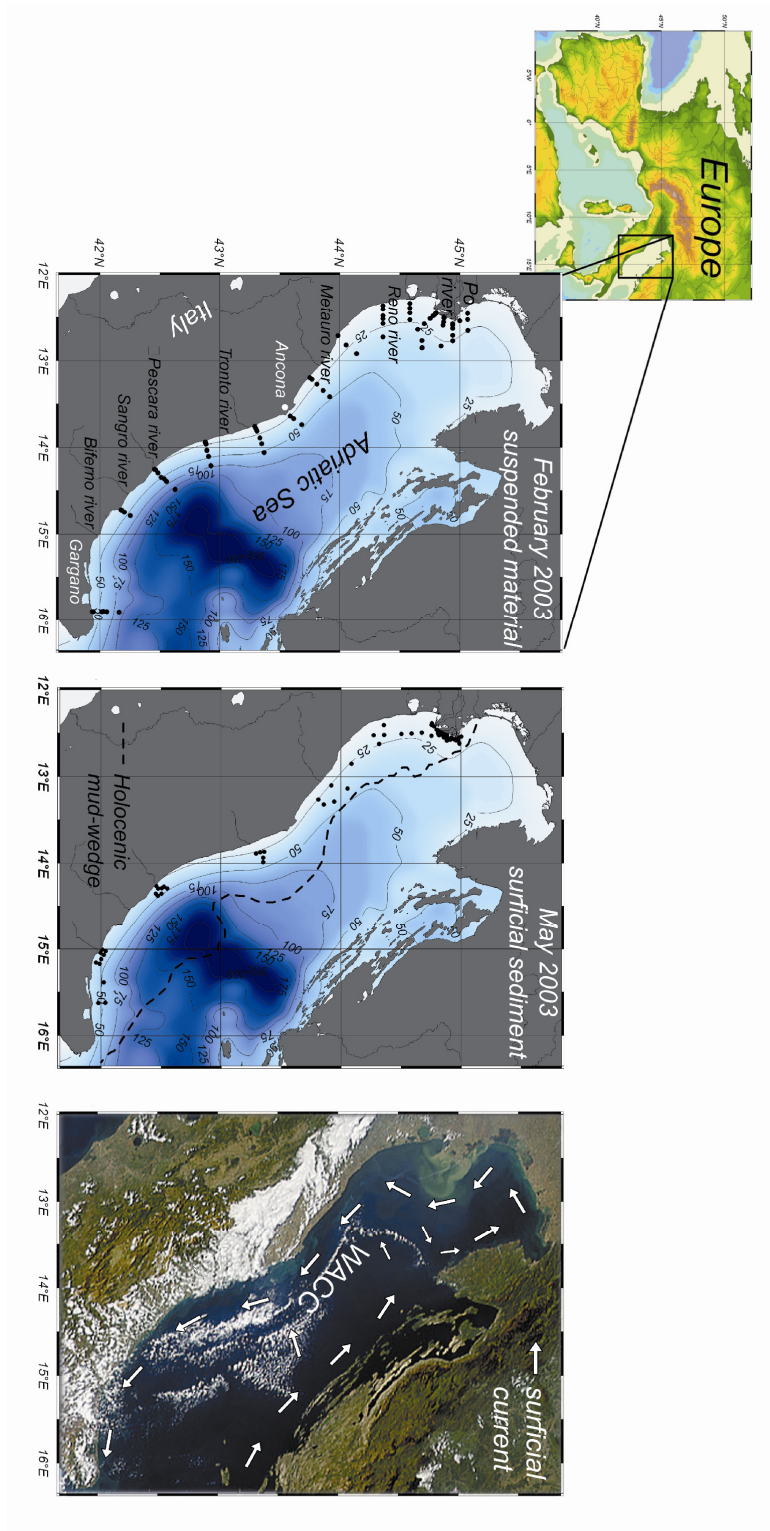


Fig. 3.1. Map of the study area in the Adriatic sea. Each station is indicated by enclosed circles for both suspended and surficial sediment samples. The figure shows the locations of rivers, the mud-wedge extension (Correggiari et al., 2001) as well as the surface circulation.

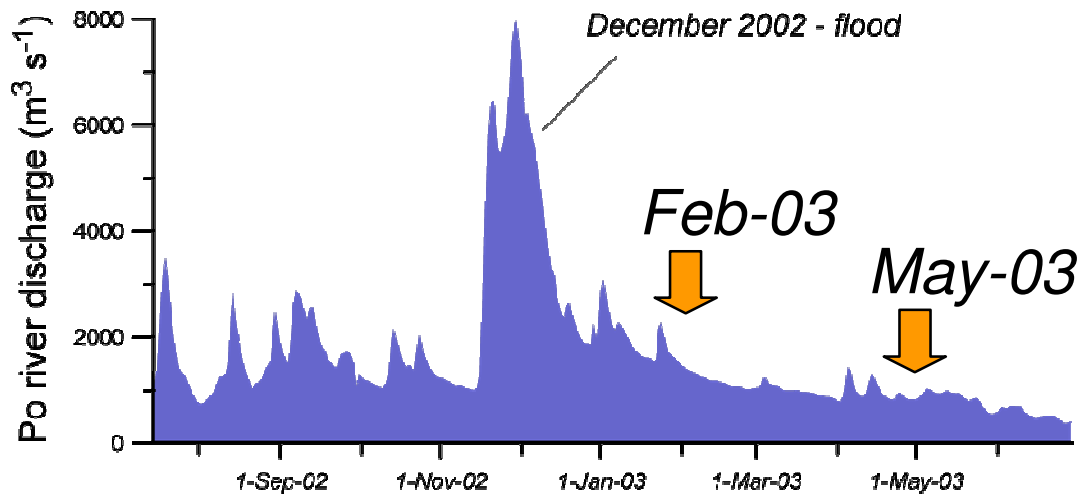


Fig. 3.2. Po river energy discharge. The arrows display the sampling periods (February 2003 and May 2003).

3.2. Po prodelta area

In early December 2000, shortly after the event, a rapid-response survey was carried out to describe the resulting October 2000 flood deposit. During this cruise, 33 box cores were collected at sampling sites located along shore-normal transect to investigate the initial distribution and location of the deposit. Using GPS location, in order to facilitate evaluation of the temporal variability, the prodelta area was re-sampled 1 year after the flood, October 2001, and in April 2002 during low river discharge (Fig. 3.3 and Fig. 3.4).

Sediment was collected in 8–31m water depth with a 20×30 cm Ocean Instruments box corer. Box-cores were sub-sampled using a 15-cm PVC liner and only the uppermost layer (0-1 cm) was used in this study.

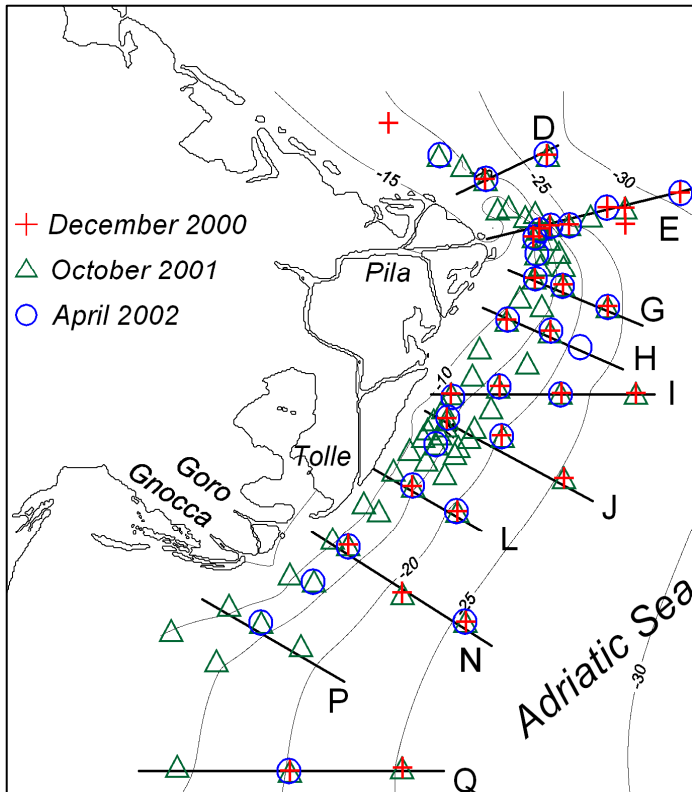


Fig. 3.3. Po prodelta area. The sampling sites are located along shore-normal transect and indicated by symbols. Red cross represent the samples collected in December 2000. Open green triangles represent the samples collected in October 2001. Open blue circles represent the samples collected in April 2002.

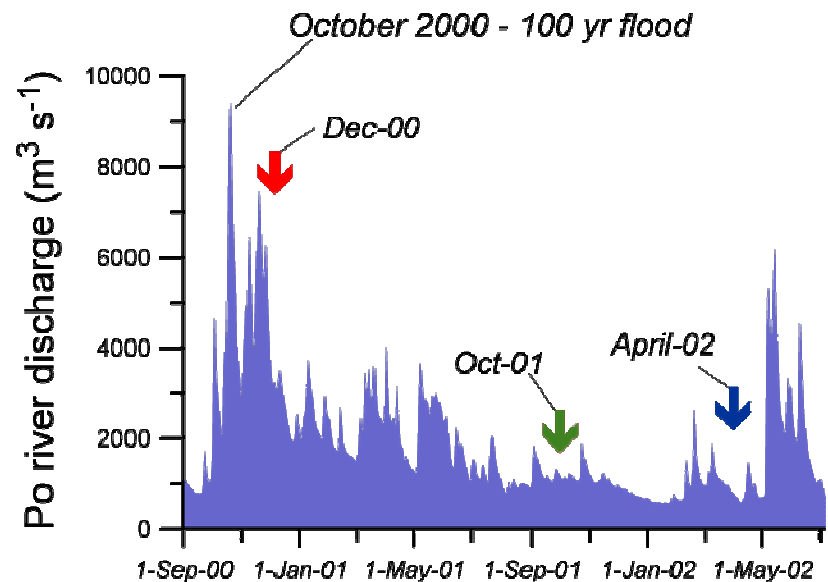


Fig. 3.4. Po River discharge from September 2000 to July 2002, arrows indicate the cruise periods. Red December 2000, green October 2001 and blue April 2002.

3.3. Gulf of Lions

Surficial sediments were collected during two oceanographic cruises, in October 2004 on the R/V Oceanus (cruise OC0904) and in April 2005 on R/V Endeavor (cruise EN0405) (Fig.3.5; Fig 3.6; Tab. 1). For the first cruise, the sampling areas were the Rhône prodelta and the S-W portion of the shelf, close to the head of the western canyons (Lacaze-Duthiers and Cap de Creus). In the second cruise, the prodelta area was re-sampled and several cores were collected on the mud-wedge along the sediment dispersal system (~60-80 m). Surface sediments were collected using a large diameter box corer. The cores were then sub-sampled using a 15-cm PVC liner. Surface sediments from the upper horizon (0–1 cm) were sampled and analyzed in this study.

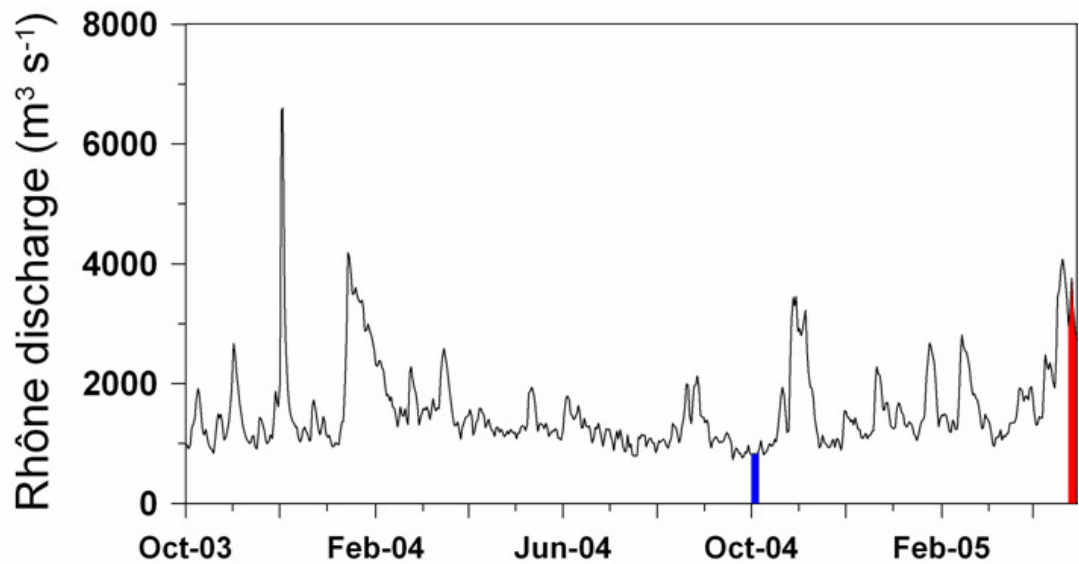


Fig.3.5. Mean daily Rhône river discharge. Data were provided by Université de Perpignan, Laboratoire de Sédimentologie et Géochemie Marines. The arrows mark the cruises and the shaded regions indicate sampling dates.

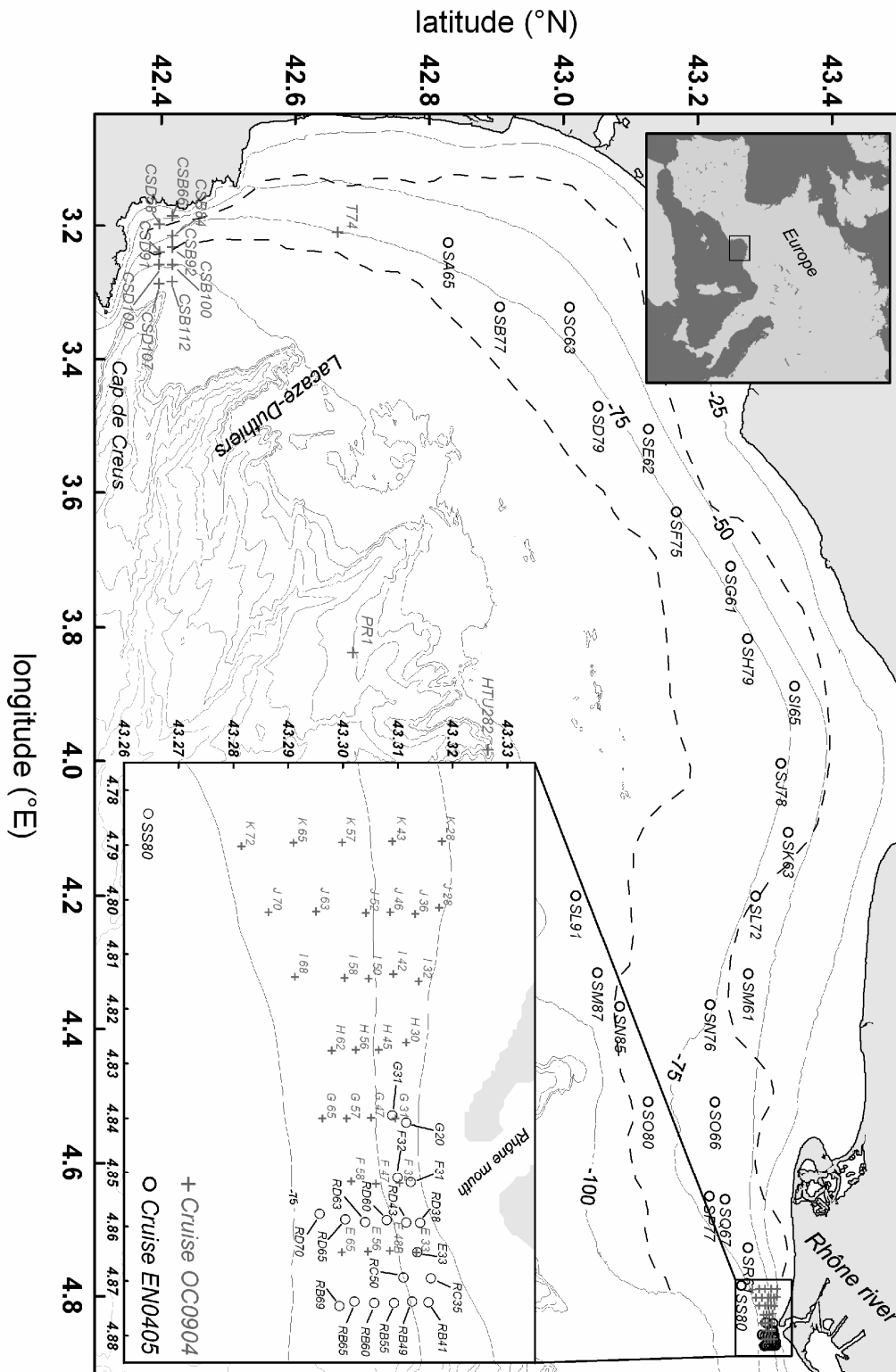


Fig. 3.6. Map of study area in the Gulf of Lions. Each box core station is indicated by a black crosshair (October 2004) and by open circle (April 2005). The dashed line displays the location of the mid shelf mud belt (Aloisi et al., 1973). The bathymetry was supplied by Serge Berné (Ifremer, Brest, France). The inset is a zoom in the prodelta.

4. Methods

4.1. *Pretreatment*

Once onboard, sediment samples were immediately frozen, and they were refrigerated during transport back to the laboratory where they were oven-dried (55 °C). A portion of the dried sediment was then ground to carry out elemental, isotopic and biomarker analyses. A fraction of unground sediment was used for the grain size analyses.

4.2. *Elemental analyses*

The sediments were pretreated with 1.5 N HCl solution in silver capsules to remove inorganic carbon. The filter samples were treated with 1.5 N HCl solution in glass containers and then enclosed in tin capsules. OC and total nitrogen (TN) contents were measured using a FISON NA2000 Element Analyzer. The average standard deviation of each measurement, determined by replicate analyses of the same sample, was $\pm 0.07\%$ for OC and $\pm 0.009\%$ for TN. In the laboratory the TSM filters were oven-dried at 60 °C and then weighed. The OC content of filtered material was calculated as ratio between particulate OC (POC, mg l^{-1}) and TSM (mg l^{-1}).

4.3. *Stable isotopic analyses*

Stable isotopic analyses of OC were carried out on the same samples by using a FINNIGAN Delta Plus mass spectrometer, which was directly coupled to the FISON NA2000 EA by means of a CONFLO interface for continuous flow measurements. The IAEA standard NBS19 (limestone, 1.95 ‰ vs VPDB) was acidified to produce CO₂ which was used as reference gas for the mass spectrometer calibration. Uncertainties were lower than $\pm 0.2\%$, as determined from routine replicate measurements of the IAEA

reference sample IAEA-CH7 (polyethylene, -31.08 ‰ vs VPDB). All isotopic compositions are reported as parts per thousand (‰) relative to variation (δ) from the PDB standard.

$$\delta^{13}C_{oc} = \left[\frac{(^{13}C/^{12}C)_{sample}}{(^{13}C/^{12}C)_{PDB}} - 1 \right] \times 1000$$

4.4. Alkaline CuO oxidations (lignin, benzoic acids, p-hydroxybenzebes)

Around 300 mg of dried sediment was ground and oxidized with CuO under basic conditions (8% NaOH) in an oxygen-free atmosphere at 150 °C for 90 min using a microwave digestion system with Teflon bombs (Goñi and Montgomery, 2000). After the oxidation, recovery standards (ethyl vanillin, trans-cinnamic acid) were added, after which the samples were acidified to pH 1 and extracted twice with ethyl acetate. After removing the excess solvent by evaporation under nitrogen, the extracts were re-dissolved in pyridine and derivatized with bis trimethylsilyl trifluoroacetamide (BSTFA) + 1% trimethylchlorosilane (TMCS) to silylate exchangeable hydrogens prior to injection in the GC/MS.

The yields of individual lignin and non-lignin oxidation products were quantified by GC-MS using selective ion monitoring. The compounds were separated chromatographically in a 30 m x 250 μ m DB1 (0.25 μ m film thickness) capillary GC column, using an initial temperature of 100 °C, a temperature ramp of 4 °C/minute and a final temperature of 300 °C. The MS was run in electron impact mode, monitoring positive ions from a range of 50 to 650 amu. External calibration standards were determined for each individual compound using ions specific to each chemical structure. The calibrations, which were performed on a regular basis to test the response of the GC-MS, were highly linear ($r^2 > 0.99$) over the concentration ranges measured in the samples.

The yields of lignin-derived phenols can be classified into three distinct groups based on their alkaline CuO oxidation products (Goñi and Hedges, 1992). Vanillyl phenols (V-series), vanillin (VI), acetovanillone (Vn) and vanillic acid (Vd), are present in all lignin-bearing plants. In contrast, the syringyl phenols (S-series), syringaldehyde (SI), acetosyringone (Sn) and syringic acid (Sd), are representative of woody and non-woody angiosperms. The cinnamyl phenols (C-series), p-coumaric (p-Cd) and ferulic acids (Fd), are found in nonwoody angiosperms and gymnosperms. The carbon-normalized sum of the eight lignin phenols ($\Lambda = S + V + C$; units of mg/100 mg OC) is used as an estimate of total lignin contributions to the OM in each sample. The ratio of S to V phenols (S/V) is used to distinguish the contributions of angiosperm vs. gymnosperm plants to the lignin in the samples, whereas the ratio C to V phenols is used to differentiate between woody and nonwoody tissue contributions.

In addition to lignin-derived reaction products, CuO oxidation also yields compounds derived from non-lignin sources. The para-hydroxybenzene monomers (P-series), 4-hydroxybenzaldehyde (PI), 4-hydroxyacetophenone (Pn), 4-hydroxybenzoic acid (Pd), are derived in part from the oxidation of aromatic amino acids, which are widely present in protein-rich OM sources such as plankton and bacteria. Furthermore, the benzoic acids (B-series) such as 3-hydroxybenzoic acid (Bd) and 3,5-dihydroxybenzoic acid (3,5-Bd), are an important category of non-lignin oxidation products present in relatively high yields from degraded materials such as soils and humic substances (e.g., Prahl et al., 1994), as well as in brown macroalgae and in certain vascular plant tissues, such as tree barks (Goñi and Hedges, 1992, 1995). Both the carbon-normalized yields of P and B products can be used in geochemical samples to further discriminate among OM sources.

4.5. Grain size analyses

A portion of unground sediment was wet-sieved using the deflocculant sodium metaphosphate (0.05%) at 62.5 μm to separate the mud (silt and clay) from the sand fraction. The sample was then sonicated prior to analysis with a Sedigraph 5100. The silt and clay percentages were calculated based on these granulometric interval: silt (62.5-3.9 μm) and clay (<3.9 μm).

4.6. AMS ^{14}C analysis

Accelerator Mass Spectrometry (AMS) ^{14}C Analysis Radiocarbon measurements were carried out on samples collected along transect in front of Pila distributary (E transect) for all three cruises. The analyses were performed by the National Ocean Sciences Accelerator Mass Spectrometry (NOSAMS, Woods Hole Oceanographic Institution). Briefly, CO_2 samples were obtained from the combustion of bulk OC from preacidified sediments. The evolved CO_2 was purified cryogenically and converted to graphite using hydrogen reduction with an iron catalyst. Graphite is pressed into targets, which are analyzed on the accelerator along with standards and process blanks. Two primary standards are used during all ^{14}C measurements: NBS Oxalic Acid I (NIST-SRM-4990) and Oxalic Acid II (NIST-SRM-4990C). ^{14}C measurements are reported as fraction modern (F_{mod}) and ^{14}C age (ybp). AMS results are calculated using the internationally accepted modern value of $1.176 \pm 0.010 \times 10^{-12}$ (Karlen, et. al., 1968) and a final ^{13}C correction is made to normalize the sample F_{mod} to a $\delta^{13}\text{C}$ value of -25 ‰. By definition, any carbon reservoir currently having a $\Delta^{14}\text{C}$ value > 0‰ has taken up some of this “bomb ^{14}C .” This effect can lead to increased values of $\Delta^{14}\text{C}$ and decreased ^{14}C ages for samples containing contemporary biomass.

5. Adriatic Sea

5.1 Results

5.1.1 TSS, OC and TN

Within the water column, the TSS, POC and particulate TN (PTN) exhibited a clear correlation to the depth of the station. The highest values were measured in the shallow stations ~6 mg/l, ~450 µg/l and ~80 µg/l for TSS, POC and PTN respectively (Tab. 5.1). TSS, POC and PTN values did not display any trend with the latitude. The surficial Po prodeltic sediments, OC contents showed a broad range of values from 0.65 to 1.62% (Fig. 5.1 and Table 5.2). South of the Po region, the OC content decreased drastically, exhibiting a narrower range from 0.39 to 0.97%. The TN values followed the same OC trend displaying higher values in the Po prodelta area, from 0.08 to 0.19 %, and lower ones along the shelf from 0.14 to 0.05% (Table 5.2.).

A strong, linear relationship was detected between the OC and TN contents in all surficial sediments ($r^2=0.91$) and suspended material ($r^2=0.93$). The x-intercepts of these regressions were close to zero, which indicates that the majority of nitrogen in these sediments is associated with OM.

5.1.2 Isotopic data

The suspended material collected in February (Tab. 5.2) displayed a broad range of $\delta^{13}\text{C}_{\text{OC}}$ values (from -21.1 to -26.5 ‰) along the shelf in both top and bottom levels without showing a clear latitudinal variability (Fig. 5.2). However, the values exhibited a significant seaward trend which was reverse to the isotopic gradient observed in the sediments. The $\delta^{13}\text{C}_{\text{OC}}$ in the prodelta Po sediments displayed depleted values ranging from -24.0 to -26.9 ‰ (Fig. 5.2, Tab. 5.1). Along the shelf, the OC isotopic composition was relatively enriched exhibiting a mean value around -24 ‰. The $\delta^{13}\text{C}_{\text{OC}}$ values in the southern portion

(Gargano peninsula) were significantly depleted up to -25.2 ‰. Across shelf, there was a slight trend towards more enriched $\delta^{13}\text{C}_{\text{OC}}$ values with increasing water depth.

5.1.3 CuO oxidation products

Lignin-derived phenols dominated the products of the CuO oxidation in all samples, accounting for ~ 70% of the combined CuO yields. Carbon-normalized lignin phenol yields were inversely related to distance from the Po mouth, ranging from 3.36 to 1.00 mg/100 mg OC (Fig. 5.2, Tab. 5.3). In the southern region there was a slight but significant increase up to 2.36 mg/100 mg OC. Para-hydroxybenzene monomers displayed a similar decrease with the distance from the Po river mouth. The values ranged from 0.34 to 0.95 mg/100 mg OC. P yields represented the second most abundant reaction products accounting for ~20% of the CuO oxidation yields. Benzoic acids slightly increased in the southern portion and accounted for ~10% of the CuO oxidation yields. In the surface sediments, B yields ranged from 0.14 to 0.36 mg/100 mg OC.

5.1.4 Grain-size analyses

Relatively coarse-grained sediments were observed in the northern stations close to the Pila distributary mouth (Table 3), with a mean diameter ranging from 14.56 to 19.76 μm . The finer material, which characterized the southern portion of the Po prodelta, displayed a wider range of diameters, from 5.57 to 15.07 μm . The grain size of surficial sediments along the Adriatic shelf was generally coarser relative to those of sediments from the Po region. The samples collected in the topset region showed a range of mean diameter from 19.38 to 34.19 μm .

5.1.5 Hydrographic data

In February 2003 considerably stratification of the water column was measured, with fresher Po water flowing out over more saline Adriatic water (Tab. 5.1). South of the Po region, the salinity increased seaward with water depth. The σ_t , visibly influenced by the salinity, exhibited a similar trend. The highest turbidity and chlorophyll values were detected in the Po prodelta region. Along the Adriatic shelf, both parameters decreased rapidly seaward suggesting a correlation with the Po and Appennine plumes that flow southward along the coast.

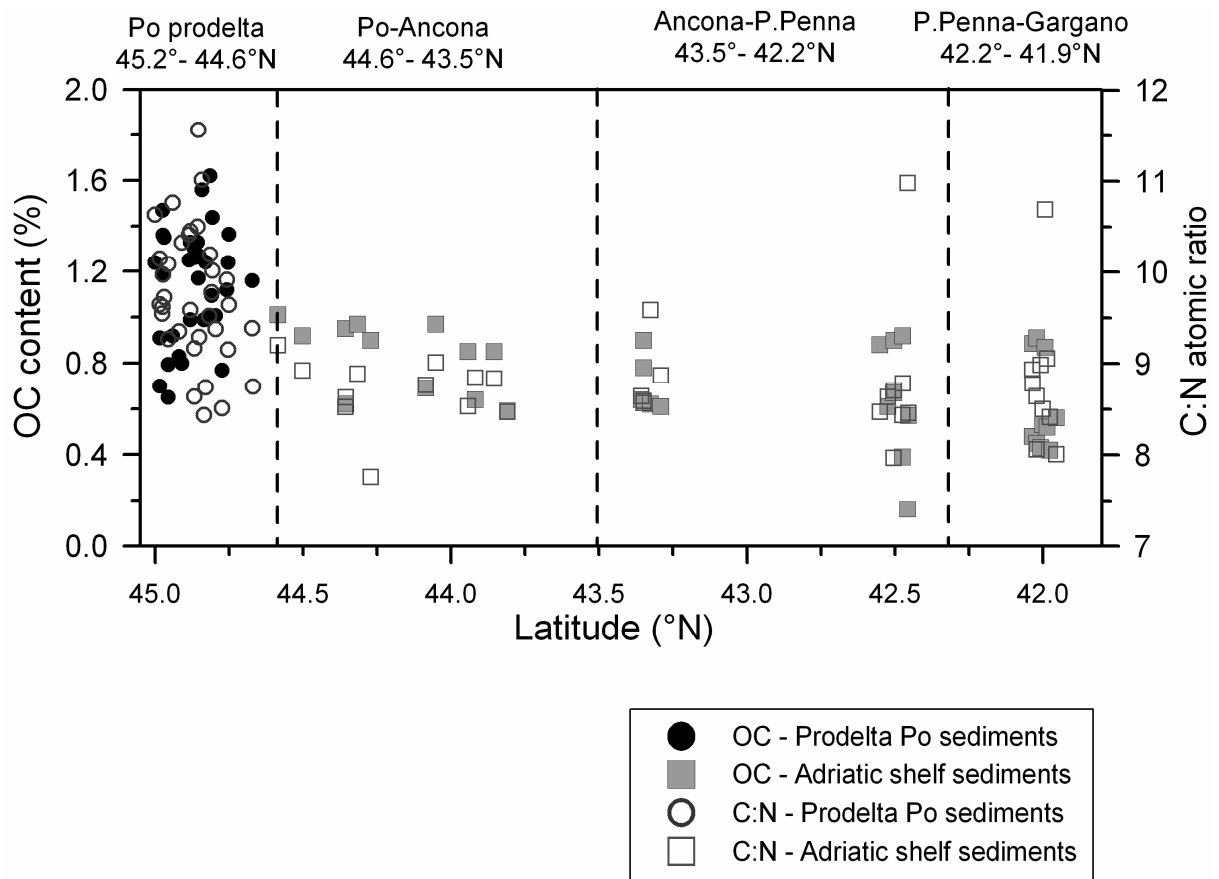


Fig. 5.1. Latitudinal distribution of OC content and OC:TN atomic ratio in surficial sediments (0-1 cm)

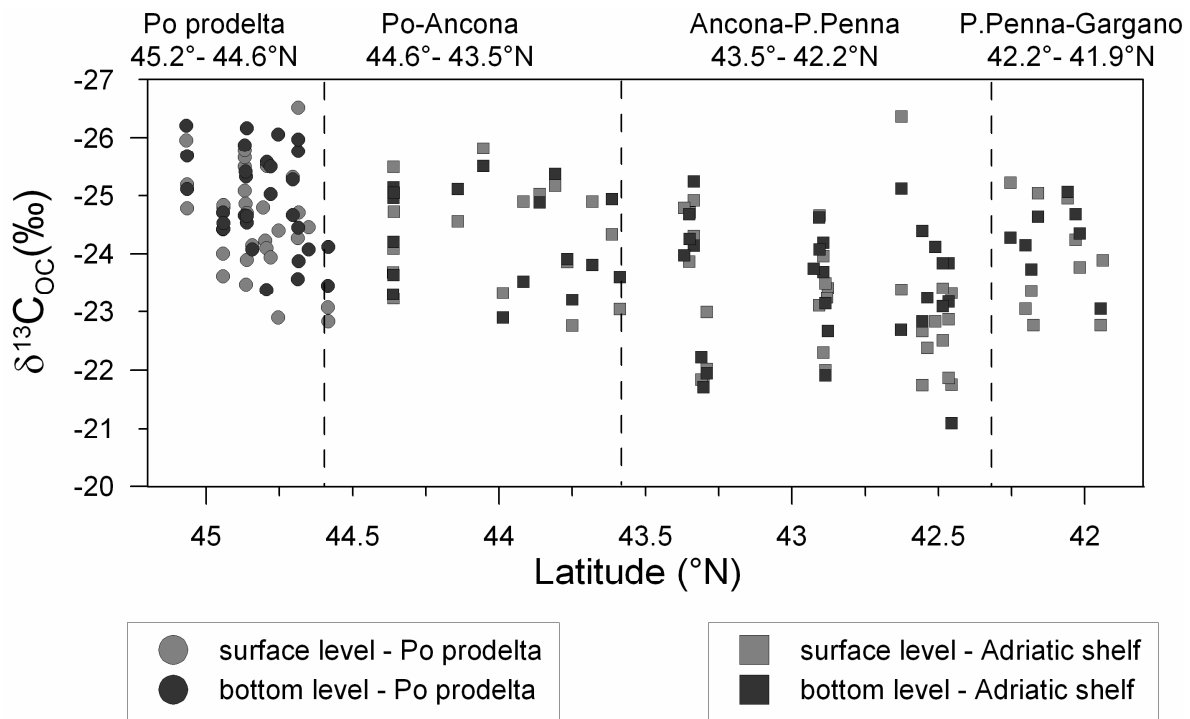


Fig.5.2. Latitudinal distribution of $\delta^{13}\text{C}_{\text{OC}}$ in suspended material collected in the water column in the Po prodelta and western Adriatic Sea

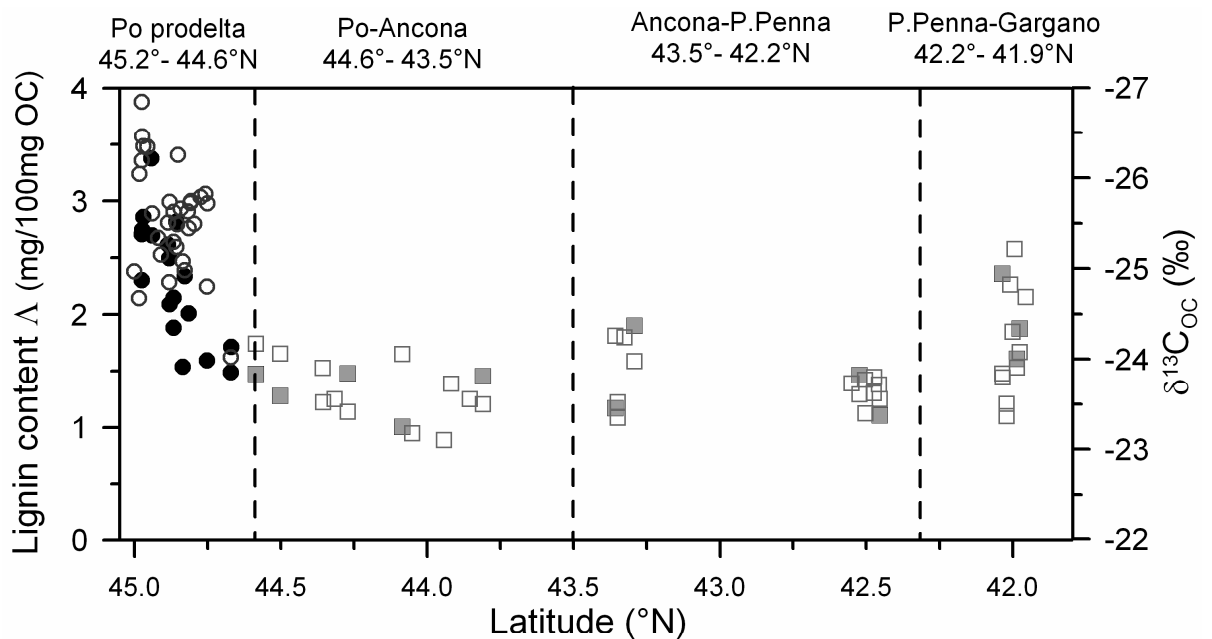
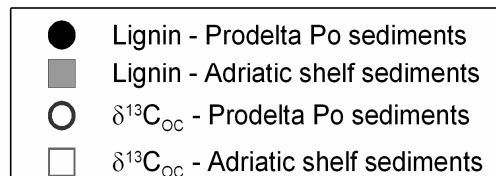


Fig. 5.3 Latitudinal distribution of $\delta^{13}\text{C}_{\text{OC}}$ and Δ in surficial sediments (0-1 cm).



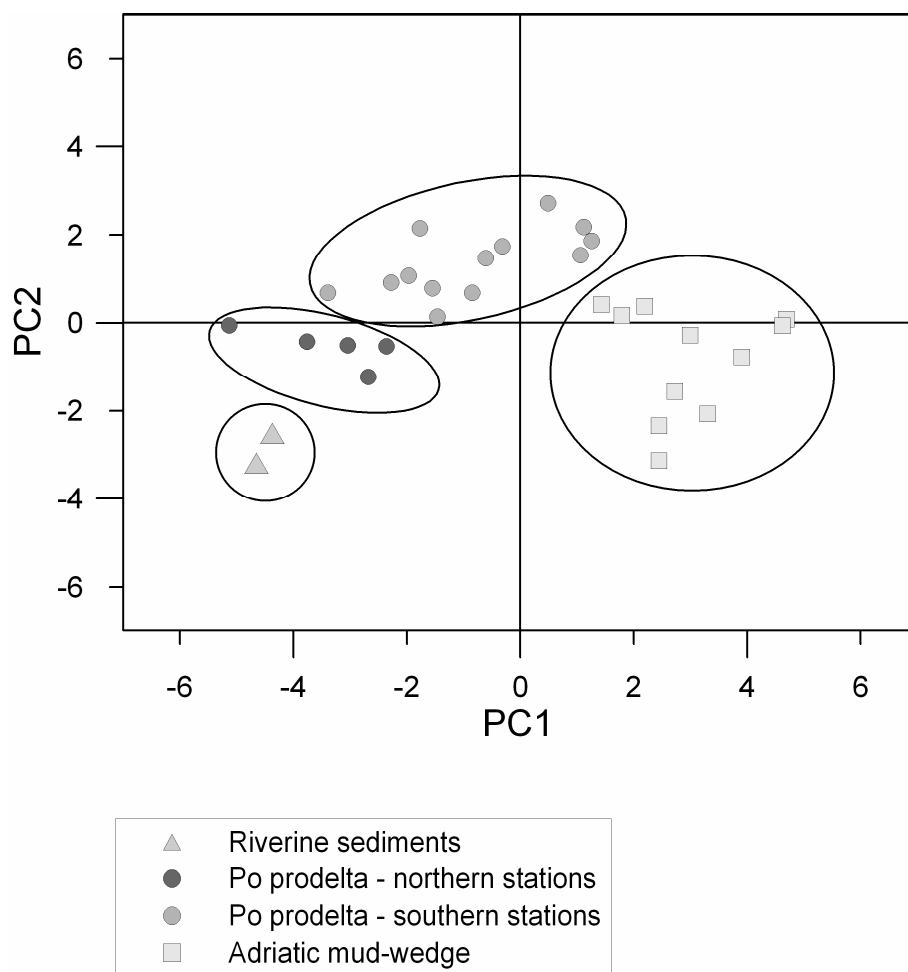
5.2 Discussion

5.2.1 PCA

PCA was performed on the station listed in table 5.3 on the basis of a complete data set. The five major principal components (PC) identified by PCA account for 84 % of the variation within the data set, with PC 1 and 2 together accounting for 63% (Tab. 5.4). The highest loadings of PC1 are displayed by VI, Vn, Vd, SI, Sd, and $\delta^{13}\text{C}_{\text{OC}}$ (Tab. 5.5). The $^{13}\text{C}_{\text{OC}}$ variable displays opposite loading relative to the lignin-derived phenols because of its depleted (negative) values. As the lignin monomers and the $^{13}\text{C}_{\text{OC}}$ are known biomarkers for the terrestrial origin, we deduce that the PC1 describes the terrigenous OM contribution in our samples. The highest coefficients for PC2 are displayed by Bd, Sn, p-Cd, Fd, 3,5-Bd as well as %OC and %N. Both, p-Cd and Fd are markers for non-woody lignin sources and Bd and 3,5-Bd have important soil/degraded sources (Prahl et al, 1994; Gordon and Goñi, 2003). It is possible that the opposite signs in the coefficients of these lignin and non-lignin compounds relative to the OC and TN contents may reflect contrasts in the contributions from OM-poor soil/ancient sources and fresh OM-rich plankton.

Fig. 5.4 shows the plot of the samples scores. An examination of the position of the samples in the coordinates of the first PCs suggests the presence of 4 major clusters, which separate river samples, northern Po prodelta stations influenced by the Pila distributary, southern Po prodelta station influenced by the other distributaries and Adriatic mud-wedge samples. These clusters subdivide the samples based on the similar organic characteristics, taking into consideration elemental, biomarkers and isotopic data. It is worth mentioning that the Adriatic shelf sediments exhibit a limited variability even if the sampling area covers a distance of almost 3° in latitude. In contrast, the Po prodelta area, which is much smaller in extent, displays a significant spatial variability and thus was divided into two sub-areas. In other words, the OM displays a much higher variability in the Po prodelta area relative to the whole Adriatic mud-wedge.

Fig. 5.4 Principal component analyses performed on elemental, isotopic and CuO oxidation products The plot shows the presence of 4 major clusters. Enclosed circles and enclosed square indicate the Po prodelta sediments and western Adriatic shelf respectively. Light grey enclosed triangles represent riverine surficial sediments.



5.2.2 Sources of OM in the Western Adriatic

The provenance of OM in the coastal environment can be assigned to several distinct sources, which include estuarine phytoplankton, marine phytoplankton, soil-derived OM, woody debris (Fry and Sherr, 1984; Mayer, 1994; Hedges et al., 1997; Goni et al., 2003; Gordon et al., 2003). Each source has distinct biogeochemical characteristics. The phytoplankton, which reside in environments where the dissolved inorganic carbon signature is variable, exhibit a wide isotopic range, as recently observed for the Adriatic Sea (Boldrin et al. 2005 and Tesi et al., 2006a). Typical values range from -19 to -21‰.

(Fry and Sherr, 1984) and from -30 to -25‰ (Goñi et al., 2006) for marine and estuarine phytoplankton respectively. Both plant debris and soil-derived OM display an isotopic range typical of the type of plants from which they originate ($\delta^{13}\text{C}$ values of C3 plant-derived carbon range from -25 to -28‰; $\delta^{13}\text{C}$ values of C4 plant-derived carbon range from -12 to 15 ‰; Fry and Sherr, 1984). C4 plants, which are most predominant in arid terrestrial environments (e.g. Teeri and Stowe, 1976), are not important in the Po and Apennine River basins and thought to contribute little to the POC load of these rivers. An additional characteristic of vascular land plants is the predominance of nitrogen-free biomolecules (molar C:N ratios >20, Hedges et al., 1997) as well as the elevated lignin content ($\Lambda > 6$ mg/100mg OC). Within soil, nitrogen is gained during microbial decay (molar C:N = 8-12; Hedges et al., 1997) and such degradation lowers the original lignin content (range from 1 to 4 mg/100mg OC).

Based on these biogeochemical ranges, we schematize these four OM sources in boxes in order to visually illustrate their contribution to the samples (Fig. 5.5, 5.6 and 5.7). Elemental and isotopic data suggest that riverine-estuarine and marine phytoplankton profoundly influence the suspended material in the Po prodelta and along shelf respectively, although soil-derived OM constitutes an important component, especially in the Po region. Conversely, the prodeltic and riverine sediments (Po and Biferno rivers) contain mainly terrestrial OM with a significant contribution from soil-derived OM. Woody plant fragments represent a reduced fraction of the terrigenous OC deposited in this area. The differences in POM sources between the water column and sediment could be described in terms of selective remineralization of algal-derived carbon. Within the sediment the organic material is remineralized with different efficiency depending on the OM origin (Aller, 1998; Aller and Blair, 2004). The refractory OC delivered by the rivers, especially in the partially degraded soil fraction, is more efficiently accumulated and preserved on surficial sediments than labile marine and estuarine phytoplanktonic detritus

(Hedges et al., 1997). The temporal factor is another key variable. One centimetre of surface sediment could represent up to 5 years of deposition depending on the area because sediment accumulation is highly variable along the Adriatic shelf (Frignani et al., 2005; Palinkas and Nittrouer, 2006). In other words, older sediment may contain higher proportion of terrestrial OM because of the efficient and selective degradation of the algal fraction.

Geochemical isotopic investigations have historically used mixing models between marine phytoplankton and isotopically depleted riverine-derived OM to quantify the terrigenous contribution to Adriatic sediments (Faganeli et al. 1988; Martinotti et al., 1997). In these studies, a common hypothesis was that the unidentified riverine material was diluted by phytoplankton detritus, and that this could explain the distribution of terrigenous material in marine sediments. Such a generalization has obscured the role of soil-derived OM in the compositions of Adriatic sediments as observed in this study. In recent years, several multi-proxy geochemical studies have characterized the content and composition of terrigenous particulate organic matter on continental margins in different areas of world. These studies emphasized the primary role of continental denudation in introducing ancient mineral-bound OC, in the form of soil-derived or bedrock-derived OM (Blair et al., 2003, Gordon and Goñi, 2003; Ogrinc et al., 2005; Goñi et al., 2005; Leithold et al., 2006).

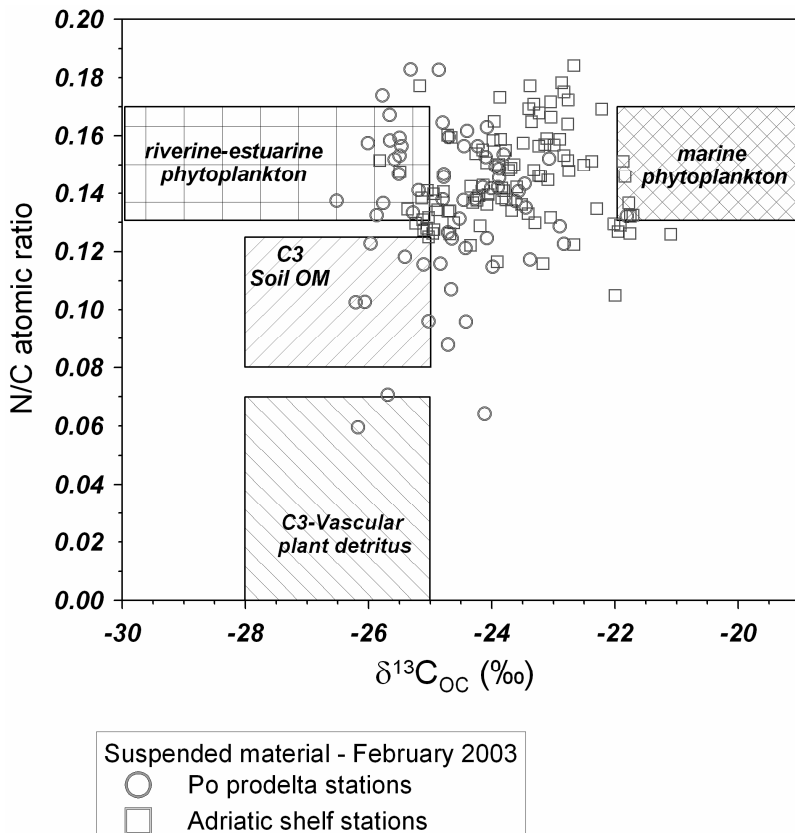
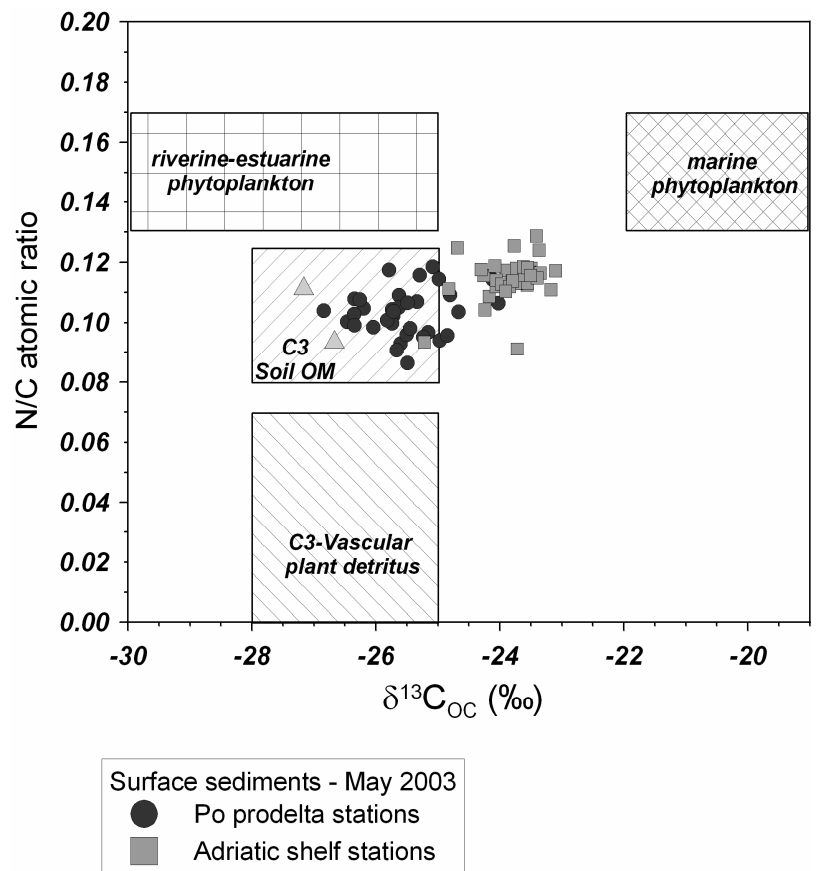


Fig. 5.5. $\delta^{13}\text{C}_{\text{OC}}$ vs TN:OC atomic ratio for suspended material collected within the water column. Both parameters are carbon-normalized. The compositions of four possible OC sources (C3 vascular plant detritus, C3 soil-derived OM estuarine phytoplankton detritus and marine phytoplankton detritus) are also plotted in the graph to illustrate the relative influence. Open circles and

Fig. 5.6. $\delta^{13}\text{C}_{\text{OC}}$ vs TN:OC atomic ratio for surficial sediments (0-1 cm). Both parameters are carbon-normalized. The compositions of four possible OC sources (C3 vascular plant detritus, C3 soil OM estuarine phytoplankton detritus and marine phytoplankton detritus) are also plotted in all graphs to illustrate the relative influence. Dark grey enclosed circles and light grey enclosed square indicate the Po prodelta and western Adriatic shelf sediments respectively. Light grey enclosed triangles represent riverine surficial sediments



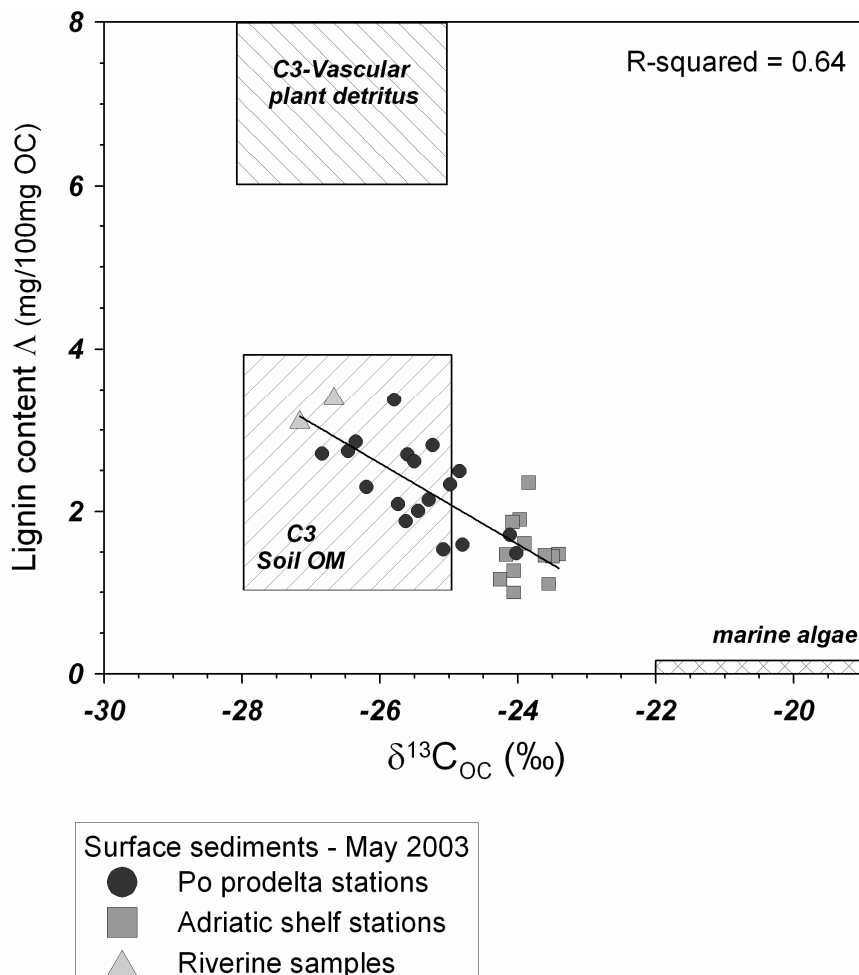


Fig. 5.7. $\delta^{13}C_{OC}$ vs Δ for surficial sediments (0-1cm). The compositions of three possible OC sources (C3 vascular plant detritus, C3 soil-derived OM and marine phytoplankton detritus) are also plotted in the graph to illustrate the relative influence. Dark grey enclosed circles and light grey enclosed square indicate the Po prodelta and western Adriatic shelf sediments respectively. Light grey enclosed triangles represent riverine surficial sediments.

5.2.3 Influence of the river plume on primary productivity

Along the Adriatic shelf, the buoyant discharge plume, identified by relatively low salinity, supplies land-derived nutrients that promote phytoplankton growth as shown by the fluorimetric surface water data (Fig. 5.8). In turn primary production influences the isotopic distribution of suspended particulates along the coastal regions. (Fig. 5.8). Conversely, in the distal stations, the lower OC contents and the relatively depleted isotopic values suggest a soil-derived OC contribution (Fig. 5.8). The presence of isotopically depleted OC on the distal shelf suggests that a fraction of very fine, OC-poor

terrigenous material leaves the plume and is exported southward, remaining suspended within the WACC. Even if the concentration of these particles is relatively low (Tab. 5.1), the quantity of material is sufficient to leave a terrestrial signal due to the absence of a significant marine contribution. It is reasonable to suppose that a considerable quantity of terrigenous material is also contained within the southward-moving plume. However, the contribution of fresh, OC-rich marine fraction is sufficient to partially obviate the terrestrial isotopic signal in the inshore Adriatic regions. This latitudinal isotopic gradient was not observed in the Po prodelta water column, although primary production profoundly influences suspended material as confirmed by fluorimetric data (Fig. 9). It is probable that, as algal estuarine material exhibits a more depleted isotopic composition than the marine contribution, the mixing between estuarine phytoplankton and terrigenous material does not generate a clear isotopic gradient.

An opposing seaward isotopic gradient was observed for the surface sediments, with the heaviest isotopic compositions measured in the distal stations (Tab. 5.1). The intensity of this trend is less evident than that observed in the suspended material. As previously mentioned, sedimentary dynamics are critical factors in OM diagenesis, which in turn influences surficial geochemical distributions. Frequent reworking and reoxidation of surficial deposits results in the preferential decomposition of reactive components (algal compounds) (Aller and Blair, 2004) leading to a “flat” isotopic gradient. Another important aspect to consider is Ekman veering; due to formation of an Ekman spiral, the sediment transport along the Adriatic shelf deviates from the direction of surface currents with an additional component across-shelf (Puig et al., 2007), homogenizing surficial isotopic distributions.

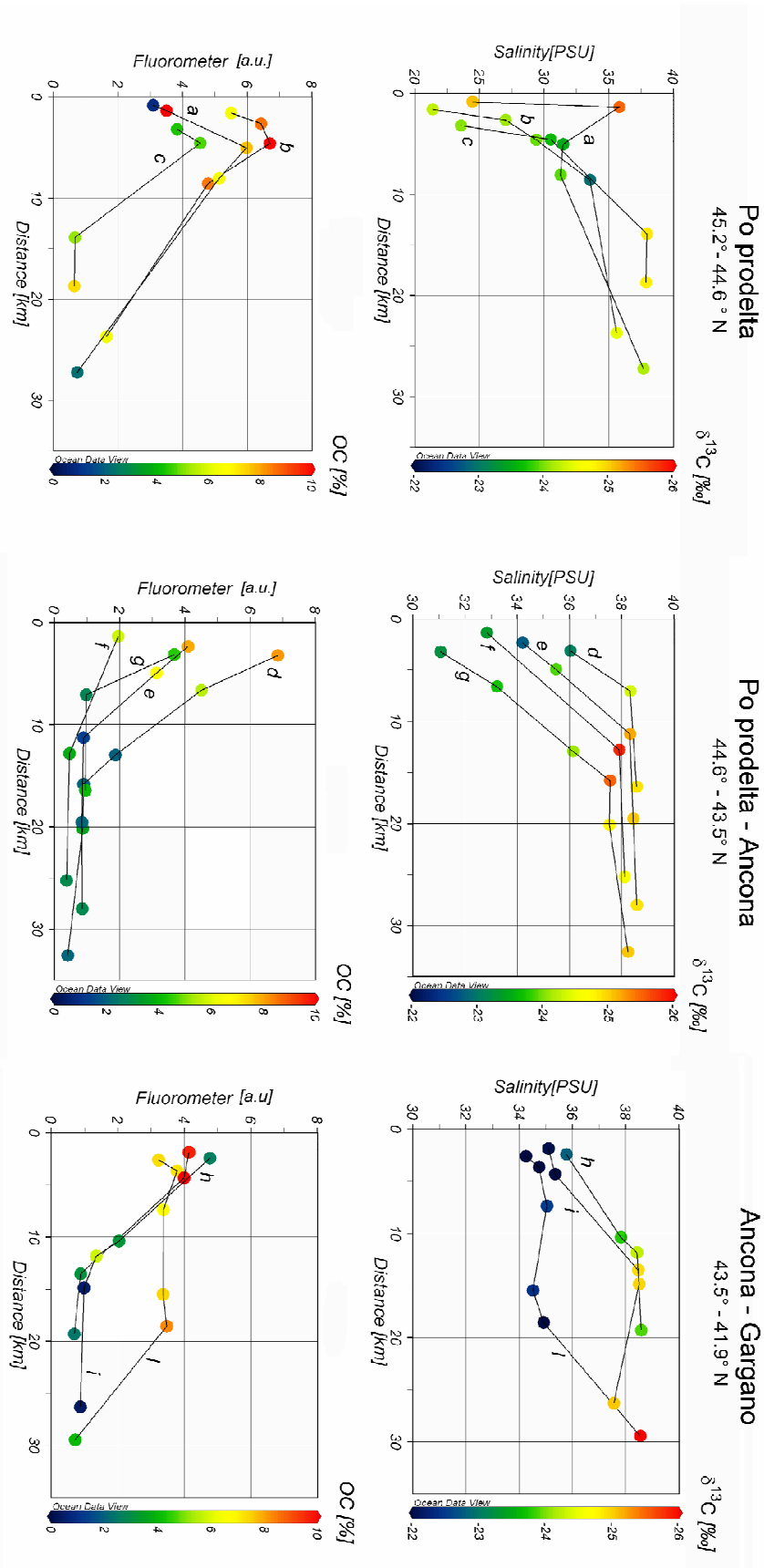


Fig.5.8. Variability of salinity, chlorophyll fluorimetry, $\delta^{13}\text{C}_{\text{OC}}$ and OC along shore normal transect from surface water samples (1m depth) for three different portion of the basin (a.u. stands. for arbitrary unit).

5.2.4 Sediment variability along shelf

The surficial sediments, south of the Po prodelta area, do not exhibit a latitudinal trend, showing a narrow range for elemental, isotopic and lignin values. In contrast, variable geochemical distributions were observed in the Po prodelta where a strong relationship was detected between grain size and lignin content (Fig. 5.9). The riverine material supplied by the Pila distributary (74% of the net sediment load), is steered southward by the coastal current. The vertical flux of particulates from this plume to the benthic region is mediated by hydraulic sorting according to size and density. High lignin content is generally associated with coarse material as plant fragments behave hydraulically like fine sand (Keil et al., 1998; Leithold and Hope, 1999). As result of these sediment dynamics, the northern prodeltaic stations are slightly richer in woody fragments (slightly higher lignin) relative to the southern stations. This implies that woody fragments tend to be trapped together with the coarse sediment in the prodelta area whereas the OM, adsorbed onto finer particles such as soil, is selectively transported out of the prodelta by the WACC.

In several studies elevated yields of 3,5-Bd relative to V phenols have been considered as evidence for humified soil-derived OM (Prahl et al., 1994; Gordon and Goñi, 2003). The 3,5-Bd is a common product of soil degradation processes through the humification of fresh vascular plant tissues (Goñi and Hedges, 1995) as well as a component of macroalgae. In this study, the marine origin of this phenolic compound was considered negligible on the basis of the PC1 loading (see previous discussion) and the linear correlation with Δ ($r^2=0.68$). Relatively high 3,5-Bd/V values were measured south of the prodelta Po area and they were interpreted to indicate humified soil-derived OM on fine particles (Fig. 5.10; Tab. 5.6). The changes in the ratio P:[V+S] offer further evidence of degradative processes affecting lignin, due to the demethylation of methoxylated vanillyl and syringyl phenols (brown rot) (Dittmar and Lara, 2001). Among the para-

hydroxybenzene monomers, only Pd exhibits a clear correlation with Δ ($r^2=0.65$), and consequently Pl and Pn were not considered because we were not certain of their terrestrial origin. The ratio Pd:[Vd+Sd] increases along the shelf (Fig.10), suggesting again the presence of degraded OM likely associated with fine material travelling southward in a series of wind-induced resuspension events (Fain et al. 2007). Paradoxically these southern stations, which displayed higher 3,5-Bd/V and Pd:[Vd+Sd] ratios, on average exhibited elevated sand concentration relative to the Po prodelta (Tab. 5.3). It is worth mentioning that this coarser shelf sediment is the result of intense seabed reworking in shallow topset region (Palinkas and Nittrouer, 2006) and therefore it is not associated with plant fragments as usually observed in prodelta areas (Leithold and Hope, 1999). Apparently the finer fraction, richer in OC because of the larger surface area, has a dominant influence on organic bulk composition. The decay of lignin by terrestrial fungi and other lignin-degrading organisms has been shown to raise the ratio of acid to aldehyde of vanillyl (Ad/Al)_v and syringyl (Ad/Al)_s phenols from the original plant values (Göni and Hedges, 1992; Opshal and Benner, 1995); these ratios can therefore provide an additional indication of degradative processes that dominate in terrestrial environments such as soil. The samples collected along the Adriatic mud-wedge do not display higher (Ad/Al)_v and (Ad/Al)_s relative to the Po prodelta as expected based on the 3,5Bd:V and P:[V+S] ratios. This could be due to the large error propagation associated with rationing small numbers (Göni et al., 1998).

The assessment of the distinct role of Po and Appennine rivers in feeding the Adriatic mud-wedge is not quantifiable through the syringyl:cinnamyl ratio (C/V) (Fig. 5.11; Tab. 5.6). The higher values measured on the Adriatic shelf, which suggested a major contribution from nonwoody plant tissues, could indicate different things. For example, the elevated C/V ratio (>0.2) has been interpreted as evidence for selective transport of fine sediment (Hedges and Mann, 1979; Prahl et al., 1985) which could derive from the Po

prodelta region. In addition it could signal differing vegetation (Alps vs. Appennine), as suggested by the dissimilar ratios observed for the Po and the Biferno rivers. Unfortunately, interpretation of the data is complicated by the fragmented bibliography regarding vegetation distribution in the Italian drainage basin.

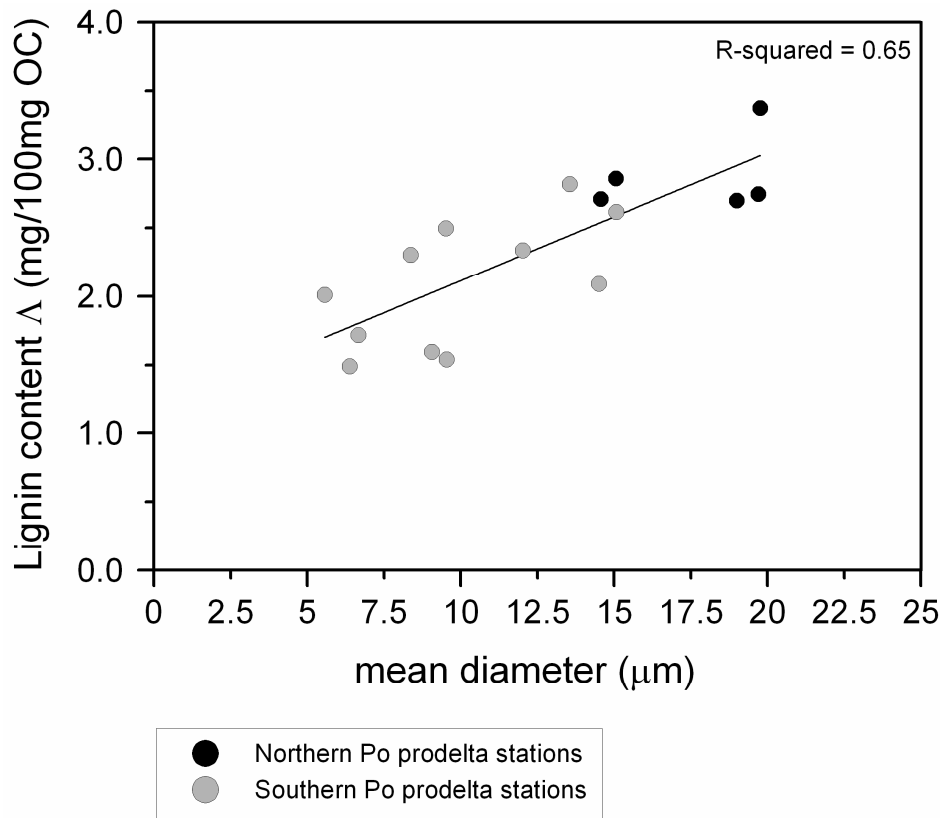


Fig. 5.9. Relationship among Δ and mean diameter in the Po prodelta 686 surficial sediments (0-1 cm). Dark grey and light grey enclosed circles display southern and northern station respectively.

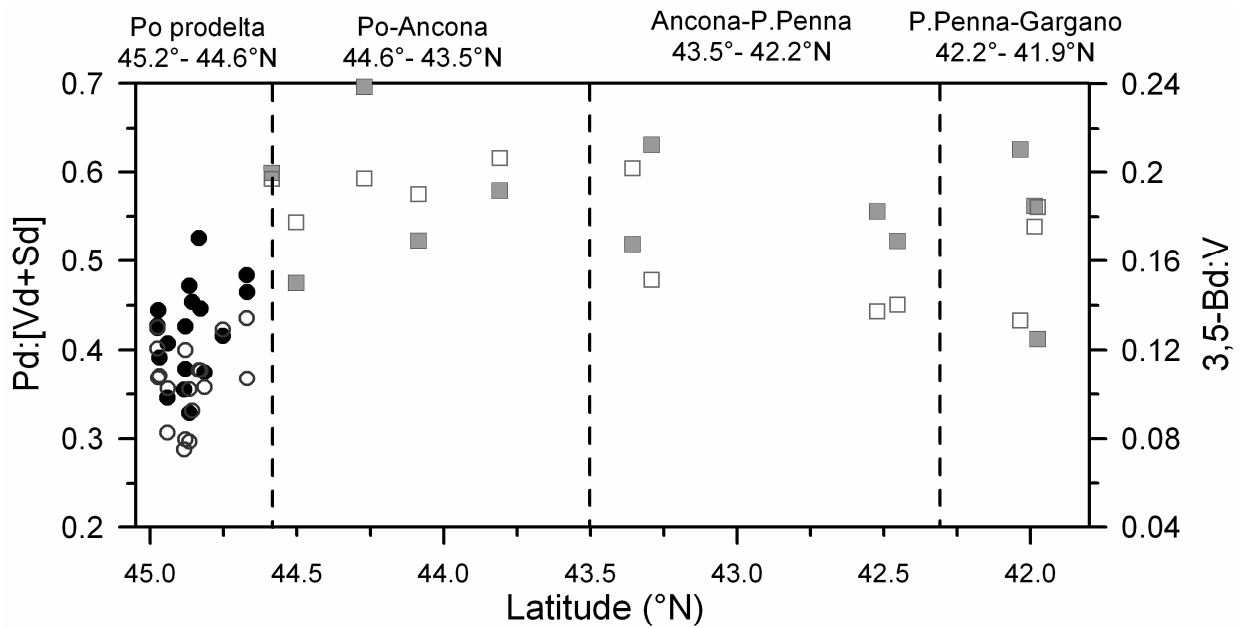


Fig. 5.10. Latitudinal distribution of 3,5-Bd/V and Pd:[Vd+Sd] ratios in surficial sediments. Dark grey enclosed circles and light grey enclosed square indicate Po prodelta and Adriatic shelf sediments (0-1 cm) respectively.

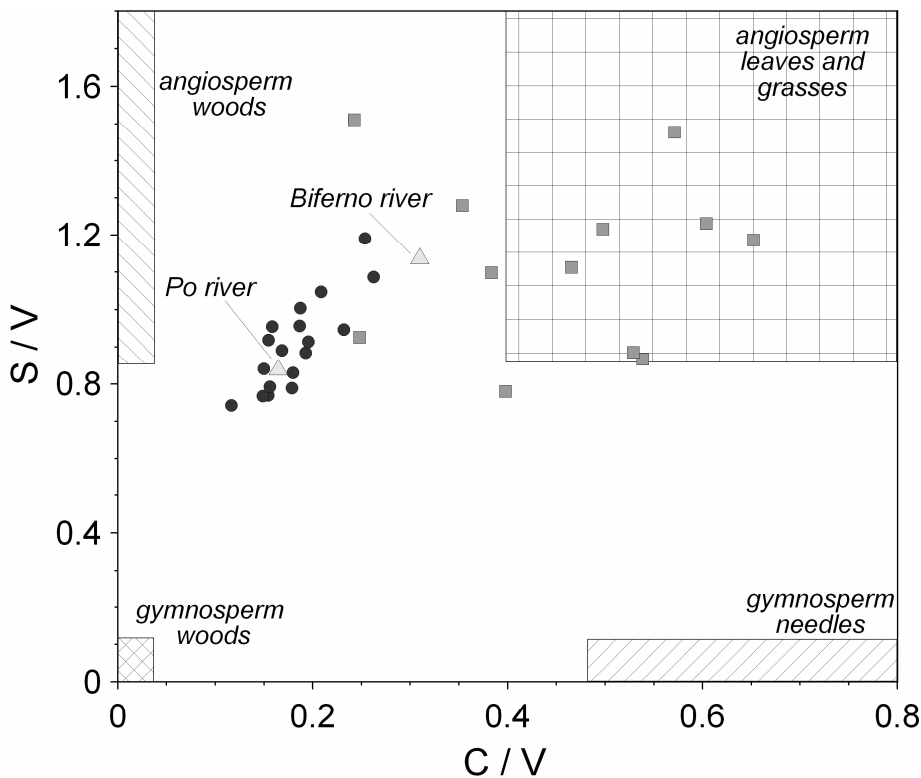
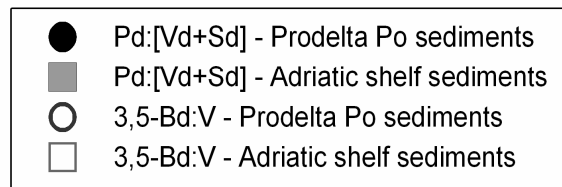
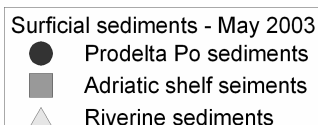


Fig. 5.11. Syringyl/vanillyl phenol ratio vs cinnamyl/vanillyl phenol ratio. Typical ranges for woody and nonwoody tissues of both angiosperm and gymnosperm vegetation are indicated. Dark grey enclosed circles and light grey enclosed square indicate the Po prodelta sediments and western Adriatic shelf respectively. Light grey enclosed triangles represent riverine surficial sediments.



5.2.5 Quantitative assessment of OM contributes in the western Adriatic Sea

In the previous section we used geochemical tracers to identify four main OC sources: marine phytoplankton, estuarine-riverine phytoplankton, soil-derived OM, and plant debris. To present a more quantitative evaluation of OM cycling in the western Adriatic Sea, three mixing models were applied to assess the relative proportions of these sources in the uppermost layer of the water column (1 m depth) and surficial sediments (0-1 cm). For suspended particles we used a three end-member mixing model based on elemental and stable carbon ratios and mass balance data, previously applied to suspended matter in the Po prodelta (Boldrin et al., 2005). In this model, OC mixing occurs between estuarine-riverine phytoplankton, marine phytoplankton and terrestrial-derived OC. Unexpectedly, when the model is applied to the Adriatic shelf samples it produces unrealistic results. According to the model, the estuarine-riverine phytoplankton OC contribution increases with distance seaward, reaching a maximum value of ~ 40%, with a similarly increasing seaward gradient observed for the terrestrial fraction. As the measurements performed at the distal stations indicate both low OC content and fluorimetric values, the presence of a significant estuarine phytoplanktonic contribution is highly improbable. The erroneous model results are probably due to the relatively low C/N values which characterized the distal stations. Fine terrigenous material exhibits a relatively low C/N ratio relative to bulk composition (Hedges and Oades, 1997). As the riverine sediment that travels southward is presumably fine, the terrestrial end-member used by Boldrin et al. (2005) does not reflect the real composition of this material. For this reason, the model underestimates terrestrial contribution and overestimates riverine-estuarine fraction. The choice of a different terrestrial end-member is complicated by the lack of specific analyses on the fine fraction of material collected in the drainage basin. In any case, the analytical errors which affect the elemental analyses would probably produce incorrect estimates in light of the subtle differences in C/N values between the

terrigenous and phytoplankton end-members. For this reason the assessment of suspended material along the Adriatic shelf was simplified to a two end-member mixing model with terrestrial and marine OC sources. In this model, we assume the riverine-estuarine phytoplankton contribution is negligible, justified by the observation that this phytoplanktic community is confined to the transition region between fresh and salt water (Cloern et al, 1985). For the suspended material collected from the Po prodelta, we kept the three end-member mixing model proposed for this area by Boldrin et al. (2005).

For the assessment of OM contribution to surficial sediments, we initially used the three end-member mixing model that again produced unrealistic results. The model predicted a marine OM contribution of ~ 10% in the riverine stations and, for most prodelta stations, the predicted riverine-estuarine OC contribution was highly negative. For these reasons, the calculations were carried out with a four end-member mixing model based on elemental, isotopic, lignin, and mass balance data. In this model, the OC mixing occurs between marine phytoplankton, riverine-estuarine phytoplankton, soil-derived OM, and plant debris.

For each mixing model, the contribution of all sources was calculated using a system of linear equations. In the appendix section we show the matrixes used for each mixing model in detail. The small negative contributions obtained from the mixing models were treated as null values. The difference was redistributed between the other end-members to obtain 100% from the sum of the remaining fractions. The marine, riverine-estuarine phytoplankton, and soil-derived OC end-members were chosen on the basis of published values (Boldrin et al., 2005; Tesi et al., 2006b; Tesi et al., 2006a) for the same study area; more detail is available in the next section. As plant fragments hydraulically behave like fine sand, we use soil values for the terrestrial end-member in the suspended-material mixing model. The plant debris end-member was chosen based on typical values for C3 plants (Fry and Sherr, 1984; Hedges et al., 1997; Goñi and Montgomery, 2000;

Gordon and Goñi, 2003, Opsahl and Benner, 1995). The sensitivity of the mixing model depends on the end members (Gordon and Goñi, 2003), and therefore the contributions of each source can change based on end-member values. However, these models are useful to summarize the data set and to understand the major OC distribution patterns on the shelf.

With regards to suspended material, we grouped the samples based on distance from the coast, as the strongest gradients were observed across-shelf (Tab. 5.7). The cumulative phytoplanktonic fraction in the uppermost layer decreases in the deepest stations, as supported by the fluorometric data (Fig. 5.8). In the surface water, phytoplankton is the prevailing source of OC in the Po prodelta area, ranging from ~50-80%. Its contribution decreases in the lowermost layer (1 m depth). The estuarine-riverine phytoplankton decreases with increasing water depth, probably as a result of increasing salinity (Tab. 5.7). The marine fraction does not exhibit any clear trend with water depth. The soil-derived OC contribution increases with the water depth in the uppermost layer, ranging from ~20-50%. In the lowermost layer it represents on average the prevalent source, probably as a result of sediment resuspension. For the shallowest stations along the Adriatic shelf, soil-derived OC and marine phytoplankton contribute equally to suspended material. Moving seaward, the marine fraction decreases up to 30%, probably because the nutrient availability is limited far from the plume. For the same distal stations, the soil-derived OC exhibits the highest contribution at ~70%. This terrigenous material is probably a fraction of the very fine, OC-poor sediment exported southward, suspended within the WACC.

The relative contributions of plant fragments, soil-derived OC, riverine-estuarine phytoplankton, and marine phytoplankton to the surficial sediments are shown in Fig. 5.12. Along the Adriatic shelf, the samples were grouped according to different depositional settings along the Adriatic shelf as defined by Frignani et al. (2005); an additional

subdivision has been made for the Po prodelta based on information from the PCA analysis. With regards to the riverine samples (Po and Biferno rivers), the average composition is ~74% soil-derived OC, ~7% plant fragments, and ~19% riverine phytoplankton. The mixing model did not show a marine contribution. The model-derived riverine phytoplankton contribution for Po sediment is ~28%. This value is in agreement with the annual estimate for the Po river derived from total pigments (~20%; Pettine et al., 1998). Soil-derived OC is the major constituent in all surficial sediments, ranging from ~50-94%. On average, the soil-derived OC contribution slightly decreases with distance southward from the Po prodelta, ranging from ~75% in the proximal Po prodelta to ~64% in the Biferno area. Plant fragments, due to their hydrologic behavior, are trapped in Po prodelta, where the highest concentrations (~5%) were observed in the northern portion, close to the mouth of the Pila distributary. Furthermore, along the shore-normal transect in front of Pila mouth, the plant debris contribution decreases seaward as expected based on the sediment settling velocities. The absence of fresh woody material along the Adriatic shelf is consistent with the 3,5-Bd:V and Pd:[Vd+Sd] ratios. The riverine-estuarine fraction is the second most important source in the proximal Po prodelta, at ~9% on average. In the distal prodelta, the riverine-estuarine fraction decreases, and along the shelf there is no evidence of the an estuarine contribution. The marine fraction is the smallest constituent in the proximal prodelta (~1%), however south of this region the marine contribution increases, eventually reaching a constant value of ~30% along the shelf. In the southern portion of the basin, the presence of a small plant-fragment OC contribution to surficial sediment (~3%) is probably attributable to local input from the Biferno river.

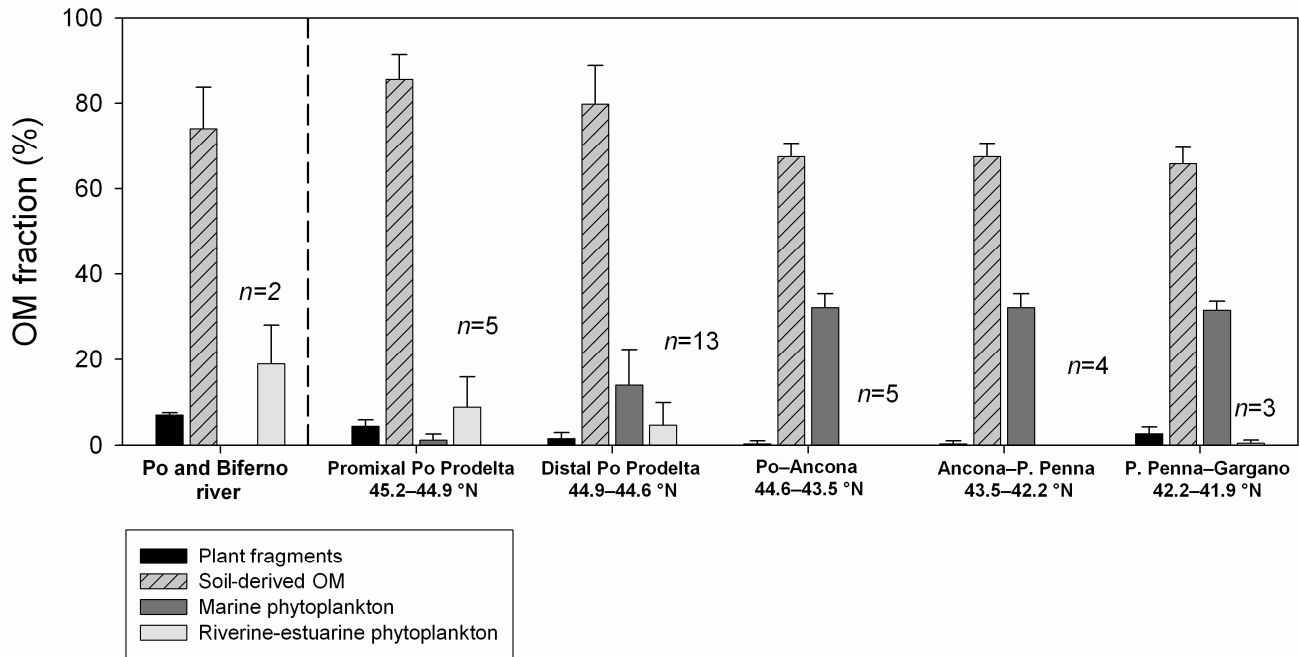


Fig. 5.12. Contributions of soil-derived OC, plant fragments, riverine-estuarine and marine phytoplankton in surficial sediments (0-1 cm). The samples were clustered in compartments (Frignani et al. 2005) which have different depositional settings

5.2.6 End-member mixing models

The end-member mixing models are based on a system of linear equations. All constants ($\delta^{13}\text{C}$, N/C , Λ) used in the equations are carbon-normalized. Linear systems for each mixing model can be represented in matrix form as the matrix equations:

$$1) \begin{bmatrix} \delta^{13}\text{C}_S & \delta^{13}\text{C}_M \\ 1 & 1 \end{bmatrix} \begin{bmatrix} F_S \\ F_M \end{bmatrix} = \begin{bmatrix} \delta^{13}\text{C}_{\text{sample}} \\ 1 \end{bmatrix} \text{ two-end members}$$

$$2) \begin{bmatrix} \delta^{13}\text{C}_S & \delta^{13}\text{C}_M & \delta^{13}\text{C}_E \\ \text{N}/\text{C}_T & \text{N}/\text{C}_M & \text{N}/\text{C}_E \\ 1 & 1 & 1 \end{bmatrix} \begin{bmatrix} F_S \\ F_M \\ F_E \end{bmatrix} = \begin{bmatrix} \delta^{13}\text{C}_{\text{sample}} \\ \text{N}/\text{C}_{\text{sample}} \\ 1 \end{bmatrix} \text{ three-end members}$$

$$3) \begin{bmatrix} \delta^{13}\text{C}_S & \delta^{13}\text{C}_P & \delta^{13}\text{C}_M & \delta^{13}\text{C}_E \\ \text{N}/\text{C}_S & \text{N}/\text{C}_P & \text{N}/\text{C}_M & \text{N}/\text{C}_E \\ \Lambda_S & \Lambda_P & \Lambda_M & \Lambda_E \\ 1 & 1 & 1 & 1 \end{bmatrix} \begin{bmatrix} F_S \\ F_P \\ F_M \\ F_E \end{bmatrix} = \begin{bmatrix} \delta^{13}\text{C}_{\text{sample}} \\ \text{N}/\text{C}_{\text{sample}} \\ \Lambda_{\text{sample}} \\ 1 \end{bmatrix} \text{ four-end members}$$

where F_S , F_P , F_M and F_E and are the relative contributions of soil-derived OC, plant fragments, marine phytoplankton and riverine-estuarine phytoplankton respectively. $\delta^{13}C_S$ (-25.83 ‰), N/C_S (0.094) and Λ_S (2.24 mg/ 100 mg OC) are the carbon isotopic composition, atomic nitrogen:carbon ratio and lignin content for soil-derived OC end-member. The soil-derived OC end-member is defined on the basis of the average chemical composition of the uppermost layer (0-1cm) of Po river flood deposit characterized by fine-grained sediment (Tesi et al., 2006b). $\delta^{13}C_P$ (-27.00 ‰), N/C_P (0.05) and Λ_P (20 mg/ 100 mg OC) are the carbon isotopic composition, atomic nitrogen:carbon ratio and lignin content for plant fragments end-member. The plant debris end-member was chosen based on typical values for C3 plants (Fry and Sherr, 1984; Hedges et al., 1997; Goñi and Montgomery, 2000; Gordon and Goñi, 2003, Opsahl and Benner, 1995). $\delta^{13}C_M$ (-20.4 ‰) and N/C_M (0.167) are the carbon isotopic composition and atomic nitrogen:carbon ratio for marine phytoplankton end-member. $\delta^{13}C_E$ (-28.9 ‰), N/C_E (0.182) are the carbon isotopic composition and atomic nitrogen:carbon ratio for riverine-estuarine phytoplankton end-member. The marine and riverine-estuarine phytoplankton end-members were chosen on the basis of published values for the Adriatic Sea (Boldrin et al., 2005; Tesi et al., 2006a). The lignin content, for marine and riverine-estuarine phytoplankton end-member (Λ_M and Λ_E), were considered as null values (0 mg/ 100 mg OC) as this molecule is absent in phytoplankton (Ludwig, 2001; Goñi et al., 2003).

Table 5.1. Elemental, isotopic composition, chl fluorimetry and physical data collected in the water column along the western Adriatic sea – February 2003. The sample from each layer (uppermost, intermediate and lowermost) were grouped based on the seabed depth.

| | <i>n</i> | bottom depth range (m) | Temperature (°C) | Salinity (PSU) | Sigma-0 (kg/m ⁻³) | Fluorometer (a.u.) | TSM (mg/l) | POC (µg/l) | PTN (µg/l) | δ ¹³ C _{OC} (‰) | C:N atomic |
|--|----------|------------------------|------------------|----------------|-------------------------------|--------------------|------------|------------|------------|-------------------------------------|------------|
| Uppermost layer of the water column (~ 1 m below the surface) | | | | | | | | | | | |
| in-shore | 19 | 0-10 | 6.8±0.6 | 32.8±3.6 | 25.6±3.1 | 3.2±1.7 | 4.3±0.9 | 257.8±102 | 46.2±18.3 | -23.6±1.2 | 6.6±0.7 |
| | 38 | 10-25 | 7.5±1.0 | 34.47±3.4 | 26.9±2.6 | 2.6±2.0 | 3.4±1.2 | 154.1±83.1 | 26.6±12.4 | -23.8±1.1 | 6.7±0.7 |
| | 26 | 25-60 | 9.1±1.8 | 37.0±1.9 | 28.66±1.4 | 1.1±0.9 | 1.9±0.9 | 91.4±47.4 | 15.3±8.9 | -24.6±0.9 | 7.13±0.8 |
| off-shore | 10 | 60-110 | 10.2±2.7 | 37.2±1.5 | 28.6±0.8 | 1.7±1.1 | 1.9±1.0 | 113.7±88.2 | 20.1±14.8 | -23.9±1.6 | 6.5±0.7 |
| Intermediate layer of the water column | | | | | | | | | | | |
| in-shore | | 0-10 | - | - | - | - | - | - | - | - | - |
| | | 10-25 | - | - | - | - | - | - | - | - | - |
| | 4 | 25-60 | 12.4±0.8 | 38.4±0.1 | 29.2±0.1 | 0.8±0.1 | 1.5±0.7 | 55.8±10.5 | 9.2±3.2 | -24.2±1.3 | 7.7±2.4 |
| off-shore | 5 | 60-110 | 8.3±0.6 | 37.9±0.4 | 29.5±0.2 | 1.3±0.7 | 1.8±0.9 | 66.7±12.5 | 11.5±1.73 | -24.2±0.4 | 6.7±0.3 |
| Lowermost layer of the water column (~ 1m above the seabed) | | | | | | | | | | | |
| in-shore | 19 | 0-10 | 7.4±0.6 | 36.7±0.9 | 28.8±0.7 | 2.8±1.5 | 3.5±0.8 | 229.5±94.3 | 35.5±14.1 | -23.6±1.5 | 7.53±0.9 |
| | 38 | 10-25 | 7.9±1.0 | 37.5±0.6 | 29.3±0.4 | 1.4±0.9 | 2.7±1.2 | 148.9±66.2 | 22.4±11.5 | -24.4±1.1 | 8.3±2.5 |
| | 26 | 25-60 | 9.3±1.5 | 38.2±0.2 | 29.6±0.2 | 0.9±0.2 | 2.9±0.9 | 95.0±40.5 | 14.0±4.1 | -24.6±0.7 | 7.8±1.8 |
| off-shore | 10 | 60-110 | 11.0±0.9 | 38.4±0.1 | 29.4±1.5 | 0.7±0.1 | 2.5±0.9 | 61.9±20.8 | 10.7±2.9 | -24.0±0.9 | 6.6±0.7 |

Table 5.2. Summary statistic of elemental and isotopic compositions of surficial sediment samples (0-1) collected along the western Adriatic Sea – May 2003. The samples were grouped in compartments defined by Frignani et al. (2005) which have identified different depositional settings along the Adriatic shelf.

| | <i>n</i> | OC (%) | s.d. | TN (%) | s.d. | δ ¹³ C (‰) | s.d. | C/N atomic | s.d. |
|------------------------------------|----------|--------|------|--------|------|-----------------------|------|------------|------|
| Po prodelta (45.2°-44.6°N) | 36 | 1.16 | 0.25 | 0.14 | 0.03 | -25.54 | 0.62 | 9.79 | 0.73 |
| Po prodelta-Ancona (44.6°-43.5°N) | 12 | 0.83 | 0.15 | 0.11 | 0.02 | -23.65 | 0.35 | 8.70 | 0.37 |
| Ancona-P.Penna (43.5°-42.2°N) | 12 | 0.71 | 0.17 | 0.10 | 0.02 | -23.74 | 0.30 | 8.64 | 0.37 |
| P.Penna-Gargano pit (42.2°-41.9°N) | 10 | 0.61 | 0.20 | 0.08 | 0.02 | -24.15 | 0.60 | 8.81 | 0.75 |

Table 5.3. Molecular composition and grain size data of surficial sediment samples (0-1) collected along the western Adriatic shelf – May 2003. S = syringyl phenols; V = vanillyl phenols; C = cinnamyl phenols; Λ = (S+V+C); B = benzoic acids; P = p-Hydroxybenzenes. n.a.= data not available

| Station | V | S | C | Λ | | B | | P | | Sand | Silt | Clay | Mean diameter |
|---------------|-------------|-------------|-------------|-------------|----------------|-------------|----------------|-------------|----------------|------|------|------|---------------|
| | mg/100mg OC | mg/100mg OC | mg/100mg OC | mg/100mg OC | % Cuo products | mg/100mg OC | % Cuo products | mg/100mg OC | % Cuo products | (%) | (%) | (%) | μm |
| <i>E25</i> | 1.02 | 1.07 | 0.21 | 2.30 | 74.0 | 0.23 | 7.2 | 0.58 | 18.8 | 1.0 | 35.0 | 63.7 | 8.4 |
| <i>E20</i> | 1.11 | 1.32 | 0.28 | 2.71 | 74.5 | 0.25 | 6.9 | 0.68 | 18.6 | 5.9 | 45.2 | 48.9 | 14.6 |
| <i>E16</i> | 1.26 | 1.19 | 0.29 | 2.75 | 75.0 | 0.26 | 7.2 | 0.65 | 17.8 | 5.5 | 32.9 | 61.6 | 19.7 |
| <i>E11</i> | 1.22 | 1.32 | 0.32 | 2.86 | 77.9 | 0.23 | 6.3 | 0.58 | 15.8 | 3.3 | 31.8 | 64.8 | 15.1 |
| <i>G15</i> | 1.76 | 1.35 | 0.27 | 3.38 | 77.4 | 0.21 | 4.8 | 0.78 | 17.8 | n.a. | n.a. | n.a. | n.a. |
| <i>G10</i> | 1.36 | 1.14 | 0.20 | 2.70 | 75.2 | 0.15 | 4.2 | 0.74 | 20.6 | 6.7 | 37.9 | 55.4 | 19.0 |
| <i>I17</i> | 1.36 | 1.05 | 0.20 | 2.62 | 73.5 | 0.20 | 5.5 | 0.75 | 20.9 | 2.8 | 49.5 | 47.7 | 15.1 |
| <i>I22</i> | 1.27 | 1.00 | 0.23 | 2.50 | 74.8 | 0.19 | 5.8 | 0.65 | 19.3 | 0.4 | 41.5 | 58.2 | 9.5 |
| <i>I10</i> | 0.95 | 0.96 | 0.18 | 2.09 | 69.9 | 0.21 | 7.1 | 0.69 | 23.0 | 3.2 | 32.4 | 64.7 | 14.5 |
| <i>J10</i> | 0.94 | 0.78 | 0.17 | 1.89 | 69.1 | 0.19 | 6.8 | 0.66 | 24.1 | n.a. | n.a. | n.a. | n.a. |
| <i>J13</i> | 1.16 | 0.86 | 0.13 | 2.15 | 66.9 | 0.26 | 8.2 | 0.80 | 24.9 | n.a. | n.a. | n.a. | n.a. |
| <i>J20</i> | 1.33 | 1.27 | 0.21 | 2.82 | 69.5 | 0.29 | 7.1 | 0.95 | 23.4 | 2.5 | 29.5 | 68.0 | 13.6 |
| <i>L10</i> | 0.74 | 0.66 | 0.14 | 1.54 | 64.5 | 0.19 | 7.9 | 0.66 | 27.6 | 1.2 | 35.9 | 62.9 | 9.5 |
| <i>L16</i> | 1.09 | 1.04 | 0.20 | 2.34 | 69.8 | 0.22 | 6.6 | 0.79 | 23.6 | 4.8 | 42.2 | 53.0 | 12.0 |
| <i>L21</i> | 1.03 | 0.82 | 0.16 | 2.01 | 70.4 | 0.28 | 9.8 | 0.57 | 19.8 | 0.3 | 25.9 | 73.8 | 5.6 |
| <i>N22</i> | 0.76 | 0.69 | 0.15 | 1.60 | 68.2 | 0.22 | 9.5 | 0.52 | 22.3 | 0.7 | 24.9 | 74.5 | 9.1 |
| <i>Q25</i> | 0.72 | 0.64 | 0.12 | 1.49 | 66.0 | 0.19 | 8.2 | 0.58 | 25.8 | 1.0 | 27.7 | 71.3 | 6.4 |
| <i>Q21</i> | 0.83 | 0.76 | 0.13 | 1.72 | 63.0 | 0.22 | 8.1 | 0.79 | 28.9 | 0.1 | 30.2 | 69.8 | 6.7 |
| <i>S25</i> | 0.48 | 0.71 | 0.28 | 1.48 | 64.3 | 0.21 | 9.3 | 0.61 | 26.4 | n.a. | n.a. | n.a. | n.a. |
| <i>U25</i> | 0.50 | 0.55 | 0.23 | 1.28 | 69.4 | 0.22 | 11.9 | 0.34 | 18.6 | n.a. | n.a. | n.a. | n.a. |
| <i>CEA 15</i> | 0.54 | 0.81 | 0.13 | 1.48 | 65.2 | 0.24 | 10.4 | 0.55 | 24.4 | n.a. | n.a. | n.a. | n.a. |
| <i>CA 20</i> | 0.42 | 0.36 | 0.22 | 1.00 | 66.8 | 0.15 | 9.9 | 0.35 | 23.3 | 2.1 | 58.9 | 39.0 | 19.3 |
| <i>SE 20</i> | 0.51 | 0.61 | 0.33 | 1.45 | 62.6 | 0.30 | 12.9 | 0.57 | 24.5 | 1.8 | 60.4 | 37.8 | 20.8 |
| <i>CHB20</i> | 0.54 | 0.50 | 0.13 | 1.17 | 61.0 | 0.33 | 17.1 | 0.42 | 21.9 | n.a. | n.a. | n.a. | n.a. |
| <i>CHD20</i> | 0.79 | 0.70 | 0.42 | 1.90 | 74.1 | 0.14 | 5.5 | 0.52 | 20.4 | 10.1 | 53.0 | 36.9 | 28.6 |
| <i>PE25</i> | 0.59 | 0.65 | 0.23 | 1.47 | 68.8 | 0.22 | 10.4 | 0.44 | 20.8 | n.a. | n.a. | n.a. | n.a. |
| <i>PH23</i> | 0.51 | 0.40 | 0.20 | 1.11 | 66.1 | 0.16 | 9.7 | 0.41 | 24.2 | 7.3 | 51.5 | 41.2 | 29.2 |
| <i>BA22</i> | 0.90 | 1.15 | 0.32 | 2.36 | 71.8 | 0.34 | 10.4 | 0.59 | 17.8 | 9.2 | 55.8 | 35.0 | 30.4 |
| <i>BD22</i> | 0.59 | 0.72 | 0.30 | 1.61 | 69.0 | 0.27 | 11.4 | 0.46 | 19.7 | 9.4 | 50.1 | 40.5 | 31.2 |
| <i>BH20</i> | 0.66 | 0.81 | 0.40 | 1.88 | 71.3 | 0.33 | 12.6 | 0.42 | 16.1 | 11.0 | 61.4 | 27.6 | 34.1 |

Table 5.4. Eigenvalues. PCA

| PC | Eigenvalues | %Variation | Cum.%Variation |
|----|-------------|-------------|----------------|
| 1 | 8.34 | 49.1 | 49.1 |
| 2 | 2.36 | 13.9 | 63 |
| 3 | 1.45 | 8.5 | 71.5 |
| 4 | 1.21 | 7.1 | 78.6 |
| 5 | 0.942 | 5.5 | 84.1 |

Table 5.5. Coefficients in the linear combinations of variables making up PC's

| Variable | PC1 | PC2 | PC3 | PC4 | PC5 |
|-----------------------------------|---------------|---------------|--------|--------|--------|
| % C | -0.265 | 0.293 | 0.169 | -0.253 | 0.06 |
| % N | -0.231 | 0.348 | 0.236 | -0.212 | 0.135 |
| $\delta^{13}\text{C}_{\text{oc}}$ | 0.305 | 0.065 | -0.194 | 0.092 | -0.101 |
| Bd | 0.162 | -0.266 | 0.091 | 0.493 | 0.262 |
| PI | -0.212 | 0.26 | -0.035 | 0.126 | -0.364 |
| Pn | -0.187 | 0.003 | 0.607 | 0.17 | 0.011 |
| VI | -0.282 | -0.085 | -0.225 | 0.053 | -0.2 |
| M-Bd | -0.185 | 0.112 | 0.111 | 0.427 | -0.485 |
| Vn | -0.302 | -0.01 | 0.244 | 0.075 | 0.22 |
| Pd | -0.235 | 0.095 | -0.386 | 0.182 | 0.353 |
| SI | -0.283 | -0.092 | -0.124 | 0.14 | -0.325 |
| Sn | -0.226 | -0.34 | 0.138 | 0.277 | 0.262 |
| Vd | -0.295 | 0.053 | -0.259 | -0.049 | 0.179 |
| 3,5-Bd | -0.263 | -0.324 | -0.167 | 0.076 | -0.08 |
| Sd | -0.302 | -0.066 | -0.268 | -0.16 | 0.07 |
| P-Cd | -0.194 | -0.384 | 0.096 | -0.328 | 0.037 |
| Fd | -0.028 | -0.487 | 0.134 | -0.365 | -0.317 |

Table 5.6. Compositional parameters of Western Adriatic sedimentary OM. V =vanillyl phenols; C = cinnamyl phenols; 3,5-Bd = 3,5-dihydroxybenzoic acid; Pd = 4-hydroxybenzoic acid; Sd= syringic acid; Vd = vanillic acid

| Station | C/V | S/V | 3,5Bd/V | Pd:[Vd+Sd] |
|---------|------|------|---------|------------|
| E25 | 0.21 | 1.05 | 0.12 | 0.42 |
| E20 | 0.25 | 1.19 | 0.13 | 0.44 |
| E16 | 0.23 | 0.95 | 0.11 | 0.39 |
| E11 | 0.26 | 1.09 | 0.11 | 0.35 |
| G15 | 0.15 | 0.77 | 0.08 | 0.41 |
| G10 | 0.15 | 0.84 | 0.10 | 0.43 |
| I17 | 0.15 | 0.77 | 0.08 | 0.36 |
| I22 | 0.18 | 0.79 | 0.08 | 0.38 |
| I10 | 0.19 | 1.00 | 0.12 | 0.43 |
| J10 | 0.18 | 0.83 | 0.10 | 0.47 |
| J13 | 0.12 | 0.74 | 0.08 | 0.33 |
| J20 | 0.16 | 0.96 | 0.09 | 0.45 |
| L10 | 0.19 | 0.88 | 0.11 | 0.53 |
| L16 | 0.19 | 0.96 | 0.11 | 0.45 |
| L21 | 0.16 | 0.79 | 0.10 | 0.38 |
| N22 | 0.20 | 0.91 | 0.13 | 0.42 |
| Q25 | 0.17 | 0.89 | 0.13 | 0.48 |
| Q21 | 0.15 | 0.92 | 0.11 | 0.46 |
| S25 | 0.57 | 1.48 | 0.20 | 0.60 |
| U25 | 0.47 | 1.11 | 0.18 | 0.47 |
| CEA 15 | 0.24 | 1.51 | 0.20 | 0.70 |
| CA 20 | 0.54 | 0.87 | 0.19 | 0.52 |
| SE 20 | 0.65 | 1.19 | 0.21 | 0.58 |
| CHB20 | 0.25 | 0.93 | 0.20 | 0.52 |
| CHD20 | 0.53 | 0.89 | 0.15 | 0.63 |
| PE25 | 0.38 | 1.10 | 0.14 | 0.56 |
| PH23 | 0.40 | 0.78 | 0.14 | 0.52 |
| BA22 | 0.35 | 1.28 | 0.13 | 0.63 |
| BD22 | 0.50 | 1.22 | 0.18 | 0.56 |
| BH20 | 0.60 | 1.23 | 0.18 | 0.41 |

Tabella 5.7. Contributions of soil-derived OC, riverine-estuarine phytoplankton and marine phytoplankton in suspended material collected in the uppermost layer of the water column in the Po prodelta and Adriatic shelf. The samples were grouped based on distance from the coast.

| distance from the coast (km) | Prodelta Po area | | | Adriatic shelf | |
|------------------------------|---------------------|------------------------|-------------|---------------------|-------------|
| | Soil-derived OC (%) | Estuarine-Riverine (%) | Marine (%) | Soil-derived OC (%) | Marine (%) |
| uppermost layer | | | | | |
| 0-6 | 21.1 ± 14.6 | 38.2 ± 18.9 | 40.6 ± 6.2 | 46.7 ± 14.6 | 53.2 ± 14.6 |
| 6-12 | 28.6 ± 14.7 | 27.5 ± 14.6 | 43.7 ± 8.7 | 60.4 ± 16.0 | 39.5 ± 16.0 |
| 12-18 | 48.4 ± 12.6 | 21.6 ± 11.1 | 29.9 ± 10.9 | 65.7 ± 23.5 | 34.2 ± 23.5 |
| 18-40 | - | - | - | 69.0 ± 18.1 | 30.9 ± 18.1 |
| lowermost layer | | | | | |
| 0-6 | 52.0 ± 29.6 | 21.5 ± 24.7 | 26.3 ± 18.0 | 49.4 ± 19.1 | 50.5 ± 19.1 |
| 6-12 | 70.8 ± 28.6 | 14.9 ± 17.8 | 14.2 ± 13.3 | 71.0 ± 14.3 | 28.9 ± 14.3 |
| 12-18 | 52.9 ± 19.7 | 16.6 ± 11.7 | 30.4 ± 13.7 | 73.5 ± 14.8 | 26.4 ± 14.8 |
| 18-40 | - | - | - | 75.4 ± 10.0 | 24.5 ± 10.0 |

6. Po prodelta area

6.1 Results

6.1.1 Elemental, carbon stable composition and CuO oxidation products.

Table 6.1 shows the summary statistics for OM composition in surficial sediments collected in the prodelta area. The OC and TN did not exhibit any clear temporal and spatial variability. On average, the material collected in December 2000 showed the lowest OC content equal to 0.97 ± 0.15 . After the flood event, the mean values for OC content were 1.07 ± 0.31 and 1.00 ± 0.23 , for October 2001 and April 2002 respectively. A strong relationship ($r^2=0.88$) was detected between OC and TN, suggesting that organic material is the main source of N. TN exhibited the same variability observed for the OC, displaying the lowest mean value right after the flood event and the highest mean value in October 2001.

In all cruises, stable carbon isotopic composition displayed a marked spatial variability (Fig. 6.1). The $\delta^{13}\text{C}$ distribution in December 2000 exhibited a distinct depocenter (-25.5%) in front of Pila mouth and depleted values in the southern portion of the near-shore region. The mean values after the flood event was $-24.7 \text{ ‰} \pm 0.9$. With time, the evolution of the $\delta^{13}\text{C}$ distribution exhibited an increase in homogeneity, and by April 2002 the depocenter in front of Pila distributary was no longer visible. In all cruises, it was observed a general increase in $\delta^{13}\text{C}$ values with distance from the river distributaries. For October 2001 and April 2002 the mean isotopic values were $-25.0 \text{ ‰} \pm 0.6$ and $-24.6 \text{ ‰} \pm 0.6$ respectively (Tab. 6.1).

Lignin-derived phenols dominated the products of the CuO oxidation in all cruises, accounting for more than 65% of the combined CuO yields (Fig. 6.2). In general, the carbon-normalized lignin phenol yields were higher in the northern region and decreased southward with the distance from Pila distributary along-shore. The lignin distribution showed the remarkable temporal variability. The lowest mean lignin content was measured in December

2000 soon after the flood (1.96 ± 0.33 mg/100 mg OC). With time the mean content increased reaching the highest value in April 2002 (2.61 ± 0.63 mg/100 mg OC). Compositionally, vanillyl and syringyl phenols were present in about equal measure and were the most abundant lignin-derived CuO reaction products, combined accounting for ~80–90% of lignin yields. The remaining ~10% of the lignin yields was constituted by cinnamyl phenols. The p-hydroxybenzenes were the second most abundant category of CuO reaction products, accounting for ~20% of the total yields, followed by benzoic acids (~10%). The relative contribution of p-hydroxybenzenes and benzoic acid was slightly higher in the material collected in December 2000 relative to October 2001 and April 2002.

6.1.2 Radiocarbon compositions ($\Delta^{14}\text{C}$)

The radiocarbon compositions ($\Delta^{14}\text{C}$) of the surficial prodeltaic sediments ranged between -178.5 and -375.6 ‰, with corresponding ^{14}C ages that ranged between 1520 and 3730 year before present (ybp). Generally the ^{14}C ages increased with the distance from Pila mouth and decreased with time after the flood although the shallowest station (E11) did not display such temporal variability (Tab. 6.3).

6.1.3 Grain size analyses

Grain size data are consistent with observations from other studies (Palinkas et al., 2005; Milligan et al., 2007). Surficial sediments generally coarsen over the course of 2 years (Tab. 6.2). The material collected in December 2000 was finer relative to the other cruises. After the flood the mean contents of clay and silt fractions were $72.0\% \pm 4.8$ and $26.0\% \pm 4.7$, respectively; sand contribution was absent in most of these samples. With time after the flood, the relative percentages of silt and sand increased. In October 2001, the mean values for clay and silt fractions were $55.4\% \pm 9.3$ and $43.8\% \pm 9.4$, respectively. The coarser

material was observed in April 2002, when the clay and silt fractions were $44.6\% \pm 13.2$ and $53.0\% \pm 11.4$, respectively; on average the sand fraction contributed $2.3\% \pm 3.0$.

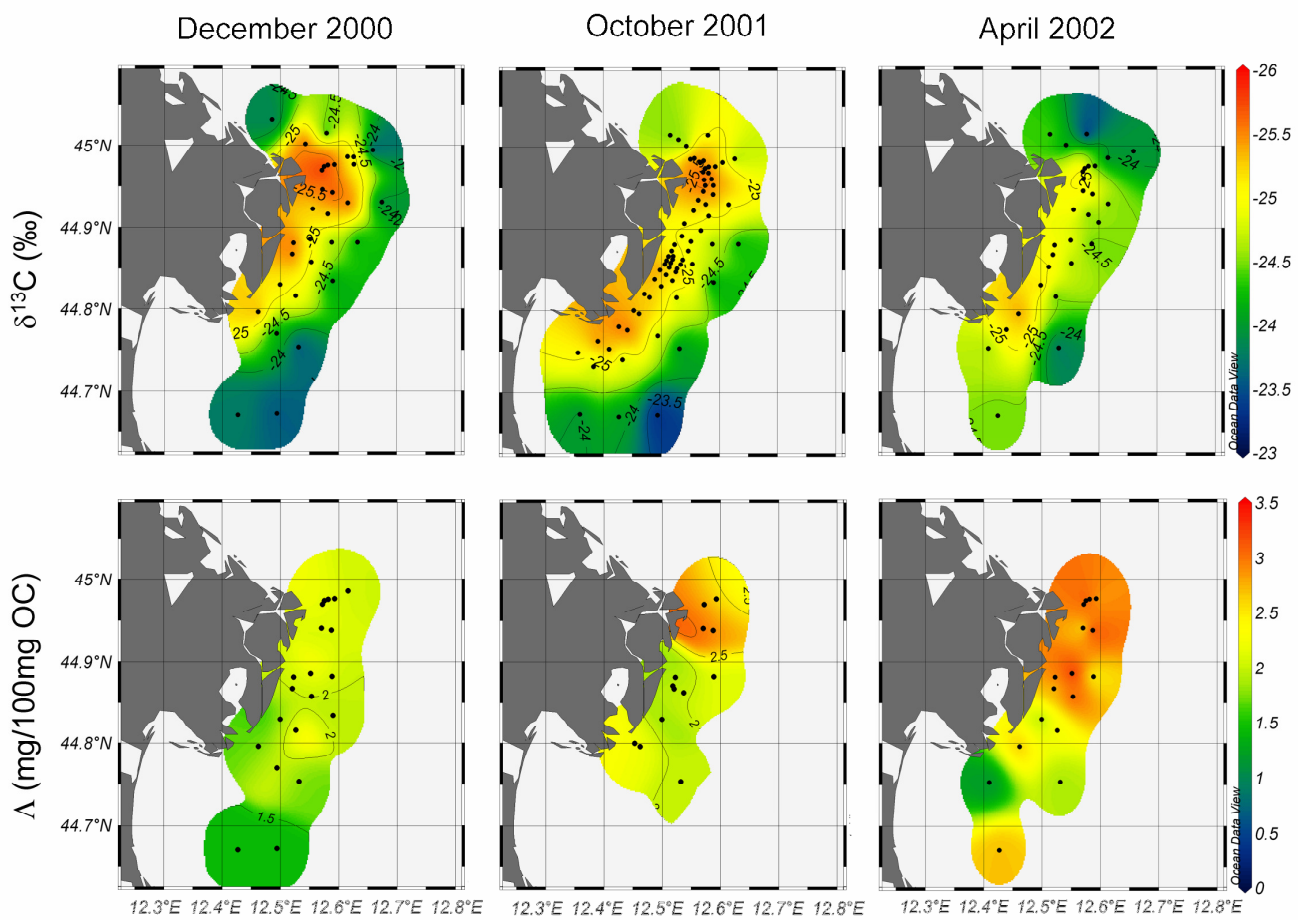


Fig. 6.1. Temporal and spatial evolution of stable isotope composition of OC and lignin content in surface sediments in the Po prodelta area. Station locations are indicated by enclosed circles.

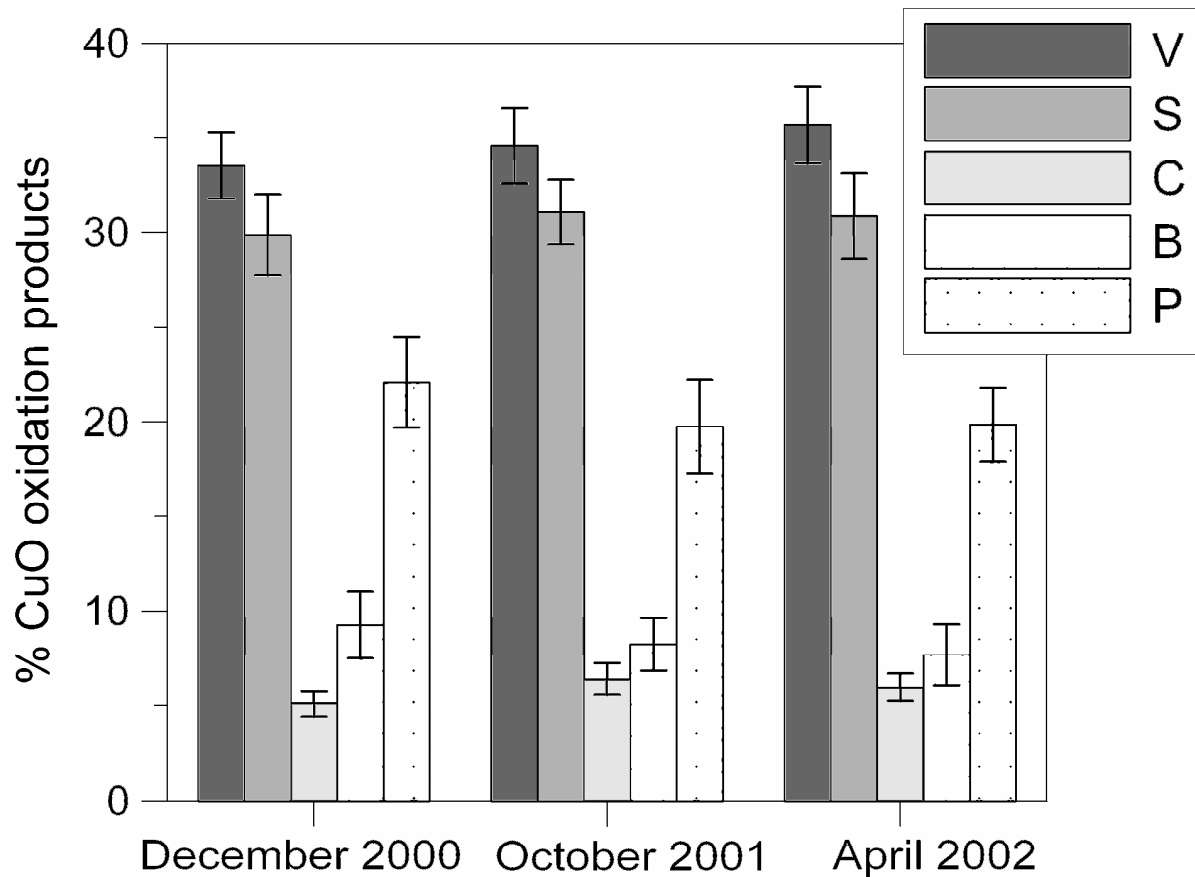


Fig. 6.2. Relative CuO reaction product abundance. The bar chart displays mean value and standard deviation for each cruise. S=syringyl phenols, V=vanillyl phenols, C= cinnamyl phenols, B= benzoic acids and P= p-hydroxybenzenes.

6.2 Discussion

6.2.1. Soil-derived OC vs vascular plant fragments

Soil-derived OC vs vascular plant fragments.

Carbon stable-isotope ratios and CuO alkaline oxidations have been utilized extensively in geochemical studies, as these biochemical tracers provide key details about the system being studied (Bianchi et al, 2001; Goñi et al 1993; Gordon and Goñi, 2001; Tesi et al., 2007). The

temporal evolution of the sedimentary OC within the Po prodelta, is exemplified in figure 6.3, wherein the sum of eight lignin-derived phenols is plotted versus $\delta^{13}\text{C}$. High variability was observed in the biogeochemical distributions over the course of 2 years. In December 2000, after the flood, soil-derived OC dominated bulk composition, in the form of organic film adsorbed to the surface of lithic particles (Mayer, 1994; Keil et al., 1994). However, with time after the flood event, the contribution of the woody fraction (i.e. vascular plant fragments), increased in surficial sediments. In April 2002, vascular plant fragments exhibited the highest concentrations during a period of low river discharge (figure 6.3 and figure 3.4). Correlation between lignin content and mean diameter (figure 6.4), suggests the observed geochemical distribution is tightly coupled to the coarsening of surficial sediment in the prodelta region. Fine sediment, due to its higher surface area, is rich in humified soil-derived OC relative to coarse sediment. Conversely, lignin-rich vascular plant fragments, which hydraulically behave like very fine sand (Keil et al., 1997; Leithold and Hope, 1999; Goni et al. 2006, Tesi et al., 2007), are associated with coarser material. In summary, our results imply that part of the evolution of the flood deposit involves the preferential concentration of relatively fresh, modern woody debris in the surface of the seabed, at the expense of aged, lignin.-poor humified, soil-derived OM.

According to Boldrin et al. (2005) in the suspended material, marine-estuarine phytoplankton is an important OC source to the Po prodelta area (>50%). Although the sediments were collected during diverse river energy conditions, the terrestrial contribution is always the dominant OC source. It is probable that oxygen exposure time is a control on algal OC preservation (Hedges and Keil, 1995). As bioturbation and resuspension create an oscillating oxic/anoxic environment, episodic physical and biological mixing affects the degradation of fresh algal compounds in prodeltaic marine sediments (Aller 2004).

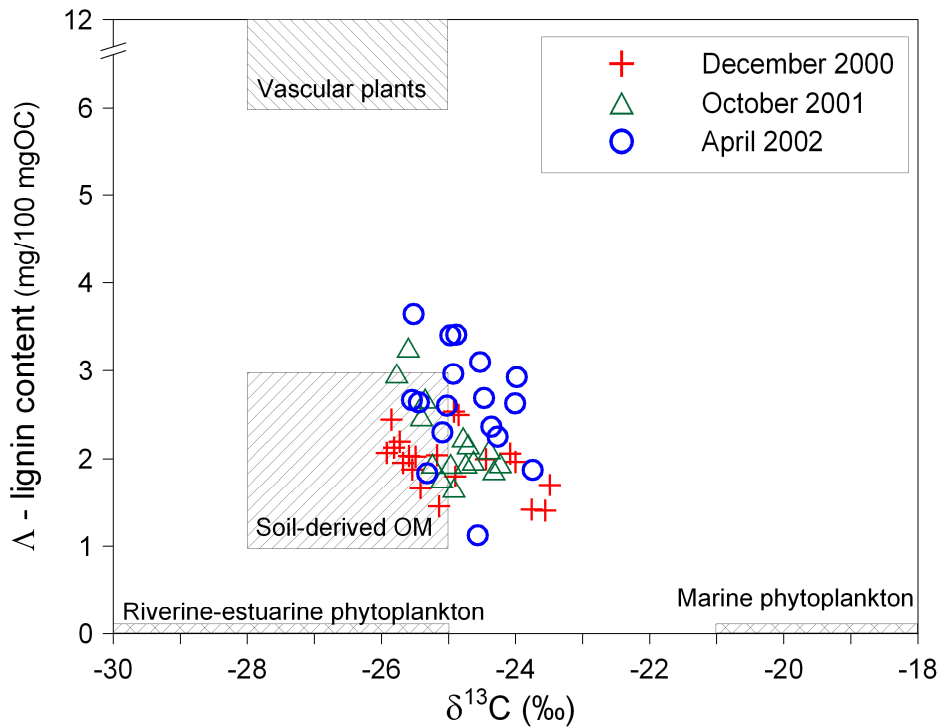


Fig.6.3. Stable isotopic compositions of OC vs carbon-normalized lignin phenol yields from surficial sediments. The compositions of four possible OC sources (C3 vascular plant detritus, C3 soil OM riverine-estuarine phyto-detritus and marine phyto-detritus) are plotted to show the relative contribution of allochthonous and autochthonous OM. Red cross represent the samples collected in December 2000. Open green triangles represent the samples collected in October 2001. Open blue circles represent the samples collected in April 2002.

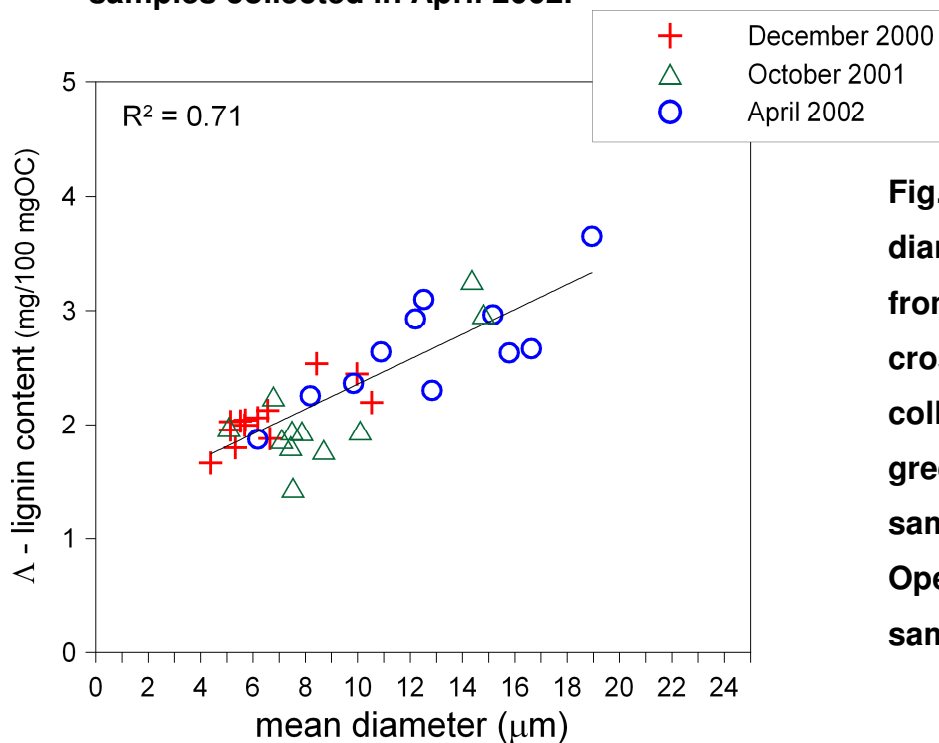


Fig. 6.4. Correlation among mean diameter and lignin phenol yields from surficial sediments. Red cross represent the samples collected in December 2000. Open green triangles represent the samples collected in October 2001. Open blue circles represent the samples collected in April 2002.

6.2.2 ¹⁴C age and CuO oxidation products

Figure 6.5 displays the temporal and spatial variability of the ¹⁴C age along E transect (Pila distributary). Because of the increase of modern vascular plant fragments, in less than 2 years after the initial emplacement of the flood deposit, the sedimentary OC significantly decreased in age. The shallowest station (E11), as constantly under the influence of Pila distributary, exhibits a relatively stable value. In addition, the ¹⁴C age was inversely related to distance from the Pila mouth (figure 6.5). An explanation for this trend may be that plant fragments, because of their hydrodynamic behavior, settle just off the Po mouths and so are retained in the shallowest stations together with coarse lithic material; conversely, lignin-poor, aged, soil-derived OC, adsorbed on fine material travels further, and is deposited in distal stations of the prodelta region. This hypothesis is supported by the strong correlation between the yield of lignin CuO products and ¹⁴C age (figure 6.6). The positive relationship ($r^2=0.88$) highlights the main factor governing OC age along the E transect: the higher the content of fresh, rich-lignin vascular plants fragments, the younger the OM. Additional information can be obtained by plotting the relative yield of lignin CuO products versus the F_{mod} (fraction modern carbon, with modern defined as the ¹⁴C/¹²C ratio in 1950 AD). In this study, values of $F_{\text{mod}} > 1$ indicate the presence of bomb-produced ¹⁴C and values < 1 correspond to atmospheric ¹⁴C levels before 1950 AD. For 100% yield of lignin CuO products, the F_{mod} is equal to 1.24 ($F_{\text{mod}} = 0.0173 \times \Lambda_{\%} + 0.495$). This implies that, although the overall OM is largely aged, the Po River delivers a small fraction of OC which incorporates anthropogenic ¹⁴C produced by the atmospheric testing of nuclear weapons.

The rest of the CuO oxidation products (i.e. p-hydroxybenzenes and benzoic acids) displayed a negative correlation with ¹⁴C age (figure x). High yields of these non-lignin oxidation products have been found for both fresh marine and terrestrial OM (Goni and Hedegs, 1995; Goni and Thomas, 2000), as well as in humified soil-derived OC (Chen and

Pawluk, 1995; Prahl et al., 1994; Baziramakenga et al., 1995;). As these CuO products are inversely correlated with ^{14}C age, we exclude a modern origin (e.g. fresh phyto-detritus) for both B and P oxidation products. The 3,5-Bd is a common product of soil degradation processes through the humification of fresh vascular plants tissues (Prahl et al., 1994; Goñi and Hedges, 1995). In addition, elevated p-hydroxybenzene products could offer further evidence of degradative processes affecting lignin, due to the demethylation of methoxylated vanillyl and syringyl phenols (brown rot) (Chen and Pawluk, 1995; Dittmar and Lara, 2001). It is worth mentioning that, besides degradative processes, selective adsorption to fine soil particles could affect the concentration of these phenolic compounds (Inderject et al., 2004; Cecchi et al., 2004). However, mean diameter does not exhibit any clear correlation either with B or P reaction products.

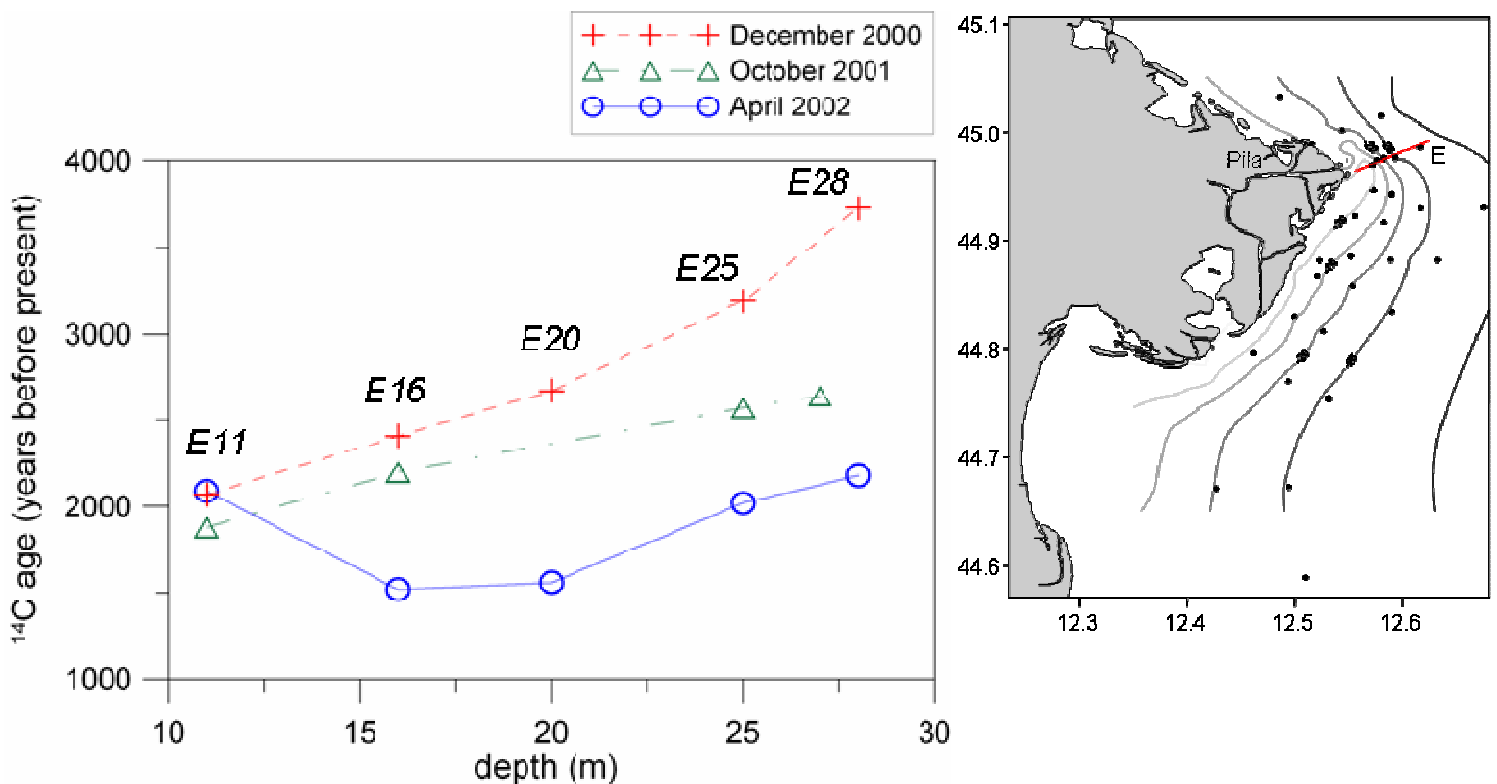


Fig. 6.5. Temporal and spatial evolution of ^{14}C ages along the E transect. Red cross represent the samples collected in December 2000. Open green triangles represent the samples collected in October 2001. Open blue circles represent the samples collected in April 2002.

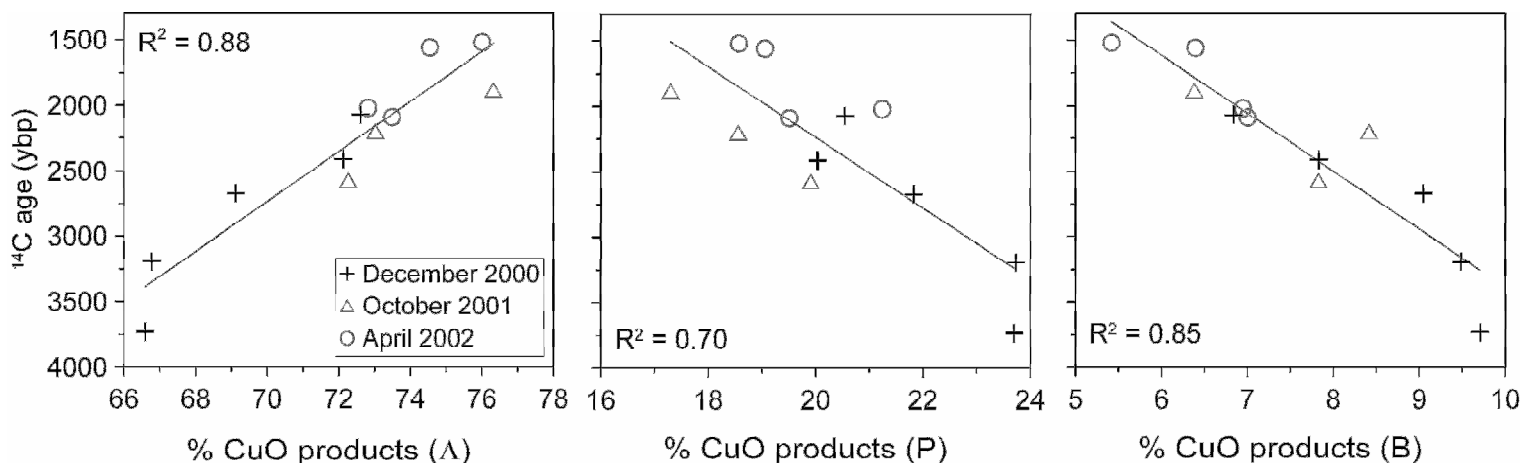


Fig.6.6. Correlation among relative CuO reaction product abundance and ^{14}C ages. Λ = sum of syringyl, vanillyl, and cinnamyl phenols, P=p-hydroxybenzenes and B=benzoic acids. Red cross represent the samples collected in December 2000. Open green triangles represent the samples collected in October 2001. Open blue circles represent the samples collected in April 2002.

6.2.3 Effect of sediment dynamics on biogeochemical distributions

This time-series biogeochemical study highlights important connections between sediment transport dynamics and cycling of terrestrial OM in prodeltaic environments. In the previous chapter we showed that fine and coarse sediments exhibit heterogeneous OC composition, and the evolution of seabed texture over time plays a central role in surficial biogeochemical distributions. The Po October 2000 flood occurred during relatively quiescent physical oceanographic conditions, which allowed for the formation of a fine-grained deposit. In the subsequent years this surficial flood deposit was altered by a number of processes, including bioturbation and winnowing/resuspension, as well as the addition of non-flood material. Resuspension and winnowing of fine particles during periods of high wave energy may have played a role in the coarsening the surface sediments, especially in the shallower

stations. Relatively high [3,5-Bd:V] ratios were measured along the Adriatic dispersal system and were interpreted as evidence of the resuspension and subsequent deposition of humified, soil-derived OM adsorbed on fine particles (Tesi et al., 2007). This is consistent with temporal variability observed in the prodelta area; in the two years following December 2000, [3,5-Bd:V] values increased, suggesting the winnowing of fine sediments (Tab. 2). Following December 2000, Fain et al. (2007) provided over 3 years of continuous data regarding the winnowing and resuspension events recorded via bottom boundary layer (BBL) tripods deployed in the subaqueous delta. In the BBL, Bora-wind resuspension events were found to make the dominant contribution to the net sediment flux. In quiescent conditions, the suspended solid concentration (SSC) near the seabed was generally less than 50 mg l⁻¹, however, during winter storms the observed nearbed SSC was often 10–60 times greater, up to 2.0 g l⁻¹.

An alternative explanation for the observed coarsening of surface sediments is biological activity, which can mix fine surficial sediments with coarser particles from lower layers that are also likely to contain higher amounts of lignin-rich vascular detritus. According to Palinkas et al. (2005), downward mixing of sediment by biological activity occurred after the initial emplacement of the flood deposit. This vertical mixing due to bioturbation could also explain the evolution of the surficial $\delta^{13}\text{C}$ distribution, which increases in homogeneity with time after the flood event (figure 3).

New deposition was observed after the October 2000 flood, in particular in the near-shore stations under the influence of the Pila distributary (Palinkas et al., 2005). The deposition of new material is supported by data from the short-lived cosmogenic nuclide ⁷Be, which indicates the presence of recently terrestrial material (<200 days). The introduction of fluvial material during non-flood periods of high river discharge is another possible mechanism to explain the changes observed at the sediment surface. During low energy

discharge, suspended particles in the surface plume are relatively diluted, inhibiting the flocculation of fine material (e.g., Milligan et al., 2007). Thus, the fine material may remain suspended in the surface plume for a much longer distance whereas the coarse material is deposited in the prodelta area together with vascular plant fragments. Conversely, during the October 2000 flood, flocculated material was rapidly deposited near the river mouth forming a thick deposit of fine sediment (Wheatcroft). In addition, during periods of low discharge, the river is likely to carry a particle load enriched in modern vascular plant detritus, as a result of decreased rates of soil erosion (e.g., Gomez et al., 2003).

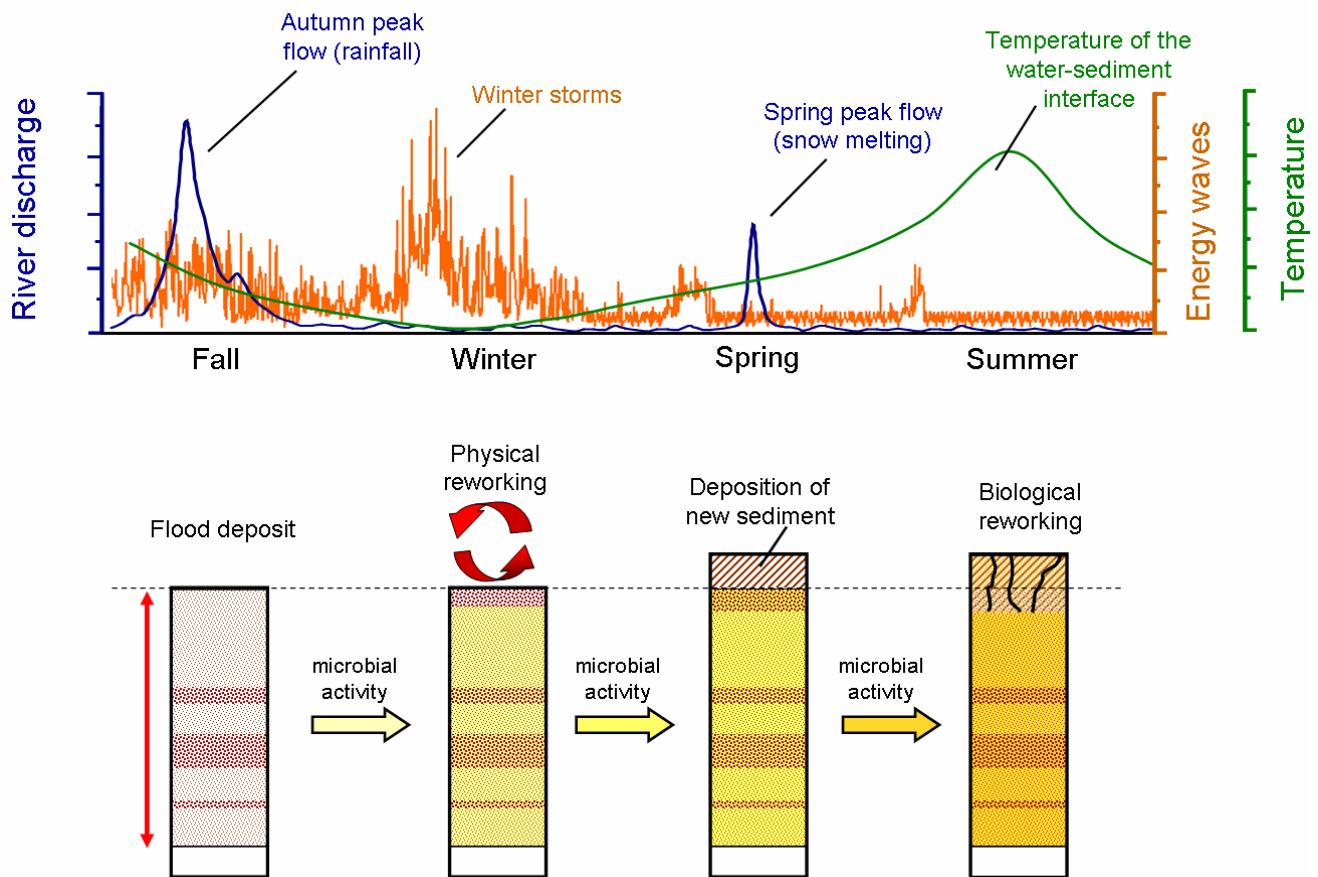


Fig.6.7. Conceptual model of the evolution of a flood deposit.

Table 6.1. Summary statistics of organic carbon content, total nitrogen content and carbon isotopic composition for Po prodelta sediments.

| | OC (%) | | | | TN (%) | | | | $\delta^{13}\text{C}$ (‰) | | | | <i>n</i> |
|--------|--------|------|------|------|--------|------|------|------|---------------------------|------|-------|-------|----------|
| | mean | s.d. | min | max | mean | s.d. | min | max | mean | s.d. | Min | Max | |
| Dec-00 | 0.97 | 0.15 | 0.44 | 1.24 | 0.11 | 0.02 | 0.05 | 0.14 | -24.7 | 0.9 | -25.9 | -23.1 | 33 |
| Oct-01 | 1.01 | 0.15 | 0.58 | 1.35 | 0.11 | 0.02 | 0.07 | 0.15 | -25.0 | 0.6 | -26.4 | -23.3 | 71 |
| Apr-02 | 1.07 | 0.20 | 0.65 | 1.52 | 0.13 | 0.02 | 0.08 | 0.17 | -24.6 | 0.6 | -25.5 | -23.1 | 30 |

Table 6.2. Bulk compositions of surficial sediments from Po prodelta transects. Grain size, CuO oxidation yields and lignin compositional parameters. n.a.= not available.

| Sample | Cruise | Sand | Silt | Clay | V | S | C | B | P | Λ | B | P | S/V | C/V | 3,5-Bd/V |
|--------|----------------|-------------|--------------|--------------|-------------|-------------|-------------|-------------|-------------|-------------|------------|-------------|-------------|-------------|--------------|
| | | (%) | | | mg/100mg OC | | | | | (%) | | | | | |
| E11 | Dec-00 | n.a. | n.a. | n.a. | 0.98 | 0.94 | 0.14 | 0.19 | 0.58 | 72.6 | 6.8 | 20.5 | 0.96 | 0.14 | 0.086 |
| E16 | Dec-00 | 0.0 | 21.8 | 78.2 | 1.15 | 1.11 | 0.18 | 0.27 | 0.68 | 72.1 | 7.8 | 20.0 | 0.97 | 0.16 | 0.107 |
| E20 | Dec-00 | 1.3 | 35.6 | 63.1 | 1.06 | 0.98 | 0.15 | 0.29 | 0.69 | 69.1 | 9.0 | 21.8 | 0.92 | 0.15 | 0.115 |
| E25 | Dec-00 | 0.1 | 29.7 | 70.2 | 0.97 | 0.78 | 0.13 | 0.27 | 0.67 | 66.8 | 9.5 | 23.7 | 0.80 | 0.13 | 0.101 |
| E28 | Dec-00 | 0.7 | 25.0 | 74.3 | 0.97 | 0.92 | 0.15 | 0.30 | 0.73 | 66.6 | 9.7 | 23.7 | 0.94 | 0.16 | 0.130 |
| G10 | Dec-00 | 0.3 | 26.8 | 72.9 | 0.98 | 0.90 | 0.15 | 0.34 | 0.73 | 65.4 | 11.0 | 23.6 | 0.92 | 0.16 | 0.122 |
| G15 | Dec-00 | 0.3 | 26.8 | 72.9 | 1.17 | 0.85 | 0.10 | 0.29 | 0.72 | 67.8 | 9.2 | 23.0 | 0.72 | 0.09 | 0.097 |
| I10 | Dec-00 | 0.0 | 25.5 | 74.5 | 0.95 | 0.88 | 0.12 | 0.27 | 0.70 | 66.7 | 9.2 | 24.0 | 0.92 | 0.13 | 0.146 |
| I17 | Dec-00 | n.a. | n.a. | n.a. | 1.20 | 1.12 | 0.18 | 0.22 | 0.80 | 71.0 | 6.3 | 22.7 | 0.93 | 0.15 | 0.109 |
| I22 | Dec-00 | 0.0 | 28.1 | 71.9 | 0.96 | 0.90 | 0.13 | 0.20 | 0.81 | 66.4 | 6.7 | 26.9 | 0.93 | 0.13 | 0.119 |
| J13 | Dec-00 | 0.3 | 26.9 | 72.8 | 0.95 | 0.91 | 0.17 | 0.30 | 0.57 | 70.0 | 10.5 | 19.5 | 0.96 | 0.17 | 0.124 |
| J20 | Dec-00 | 0.3 | 27.3 | 72.4 | 0.90 | 0.75 | 0.14 | 0.25 | 0.53 | 69.6 | 9.8 | 20.6 | 0.83 | 0.16 | 0.108 |
| J25 | Dec-00 | n.a. | n.a. | n.a. | 0.95 | 0.84 | 0.18 | 0.35 | 0.53 | 69.1 | 12.1 | 18.8 | 0.89 | 0.19 | 0.108 |
| L16 | Dec-00 | n.a. | n.a. | n.a. | 0.69 | 0.66 | 0.11 | 0.24 | 0.61 | 63.2 | 10.3 | 26.5 | 0.96 | 0.16 | 0.157 |
| L21 | Dec-00 | 0.0 | 23.5 | 76.5 | 1.21 | 1.14 | 0.19 | 0.22 | 0.69 | 73.6 | 6.5 | 20.0 | 0.94 | 0.15 | 0.092 |
| N14 | Dec-00 | 0.1 | 23.9 | 76.1 | 0.83 | 0.71 | 0.12 | 0.27 | 0.49 | 68.9 | 11.0 | 20.1 | 0.86 | 0.15 | 0.133 |
| N22 | Dec-00 | 0.0 | 38.5 | 61.5 | 1.01 | 0.90 | 0.15 | 0.27 | 0.58 | 70.7 | 9.4 | 20.0 | 0.89 | 0.15 | 0.096 |
| N25 | Dec-00 | n.a. | n.a. | n.a. | 0.77 | 0.77 | 0.16 | 0.25 | 0.54 | 68.4 | 10.0 | 21.6 | 1.00 | 0.21 | 0.119 |
| Q21 | Dec-00 | n.a. | n.a. | n.a. | 0.72 | 0.58 | 0.12 | 0.22 | 0.52 | 65.6 | 10.2 | 24.2 | 0.82 | 0.17 | 0.105 |
| Q25 | Dec-00 | n.a. | n.a. | n.a. | 0.76 | 0.54 | 0.11 | 0.25 | 0.50 | 65.2 | 11.7 | 23.2 | 0.71 | 0.15 | 0.105 |
| | Average | 0.26 | 27.64 | 72.09 | 0.96 | 0.86 | 0.14 | 0.26 | 0.63 | 68.4 | 9.3 | 22.2 | 0.89 | 0.15 | 0.114 |
| E11 | Oct-01 | 3.3 | 31.8 | 64.8 | 1.51 | 1.21 | 0.25 | 0.25 | 0.67 | 76.3 | 6.4 | 17.3 | 0.80 | 0.17 | 0.078 |
| E16 | Oct-01 | 0.5 | 56.1 | 43.4 | 1.42 | 1.43 | 0.26 | 0.36 | 0.79 | 73.0 | 8.4 | 18.6 | 1.01 | 0.18 | 0.075 |
| E25 | Oct-01 | 0.2 | 35.0 | 65.0 | 1.12 | 0.92 | 0.21 | 0.24 | 0.62 | 72.3 | 7.8 | 19.9 | 0.82 | 0.19 | 0.086 |
| E29 | Oct-01 | n.a. | n.a. | n.a. | 0.92 | 0.70 | 0.12 | 0.41 | 0.75 | 60.0 | 14.0 | 26.0 | 0.76 | 0.13 | 0.064 |
| G10 | Oct-01 | 0.8 | 61.4 | 37.8 | 1.51 | 1.44 | 0.32 | 0.26 | 0.68 | 77.6 | 6.2 | 16.2 | 0.95 | 0.21 | 0.075 |
| G15 | Oct-01 | n.a. | n.a. | n.a. | 1.22 | 1.19 | 0.27 | 0.30 | 0.63 | 74.3 | 8.3 | 17.4 | 0.98 | 0.22 | 0.087 |
| I10 | Oct-01 | n.a. | n.a. | n.a. | 0.83 | 0.72 | 0.12 | 0.22 | 0.65 | 65.9 | 8.6 | 25.6 | 0.86 | 0.14 | 0.086 |
| I22 | Oct-01 | n.a. | n.a. | n.a. | 1.09 | 0.87 | 0.16 | 0.21 | 0.60 | 72.3 | 7.2 | 20.6 | 0.80 | 0.14 | 0.077 |
| J10 | Oct-01 | 0.0 | 46.3 | 53.7 | 0.89 | 0.90 | 0.17 | 0.24 | 0.57 | 70.9 | 8.5 | 20.6 | 1.01 | 0.19 | 0.102 |
| J13 | Oct-01 | 0.4 | 44.8 | 54.8 | 0.90 | 0.85 | 0.19 | 0.25 | 0.53 | 71.2 | 9.2 | 19.6 | 0.94 | 0.22 | 0.087 |
| J17 | Oct-01 | n.a. | n.a. | n.a. | 1.02 | 0.94 | 0.21 | 0.27 | 0.52 | 73.3 | 9.0 | 17.7 | 0.93 | 0.20 | 0.103 |

| | | | | | | | | | | | | | | | |
|-----|----------------|-------------|--------------|--------------|-------------|-------------|-------------|-------------|-------------|-------------|------------|-------------|-------------|-------------|--------------|
| J20 | Oct-01 | n.a. | n.a. | n.a. | 0.87 | 0.85 | 0.23 | 0.30 | 0.52 | 70.5 | 10.7 | 18.8 | 0.98 | 0.27 | 0.110 |
| L16 | Oct-01 | 1.1 | 55.0 | 43.9 | 0.86 | 0.76 | 0.16 | 0.26 | 0.60 | 67.5 | 9.8 | 22.7 | 0.89 | 0.18 | 0.108 |
| L21 | Oct-01 | 0.6 | 37.2 | 62.2 | 0.83 | 0.81 | 0.23 | 0.34 | 0.49 | 69.3 | 12.7 | 18.0 | 0.97 | 0.28 | 0.120 |
| N10 | Oct-01 | n.a. | n.a. | n.a. | 1.19 | 1.09 | 0.20 | 0.27 | 0.73 | 71.4 | 7.6 | 20.9 | 0.91 | 0.17 | 0.096 |
| N14 | Oct-01 | 3.5 | 40.6 | 56.2 | 0.93 | 0.85 | 0.18 | 0.32 | 0.56 | 69.0 | 11.2 | 19.9 | 0.91 | 0.19 | 0.091 |
| N22 | Oct-01 | 0.0 | 31.8 | 68.2 | 0.95 | 0.86 | 0.17 | 0.19 | 0.49 | 74.3 | 7.3 | 18.5 | 0.91 | 0.18 | 0.090 |
| Q21 | Oct-01 | 0.1 | 48.0 | 51.9 | 0.73 | 0.84 | 0.25 | 0.26 | 0.54 | 69.2 | 10.1 | 20.7 | 1.16 | 0.34 | 0.136 |
| Q25 | Oct-01 | 0.7 | 43.5 | 55.8 | 0.60 | 0.64 | 0.21 | 0.28 | 0.44 | 66.6 | 12.9 | 20.5 | 1.05 | 0.34 | 0.153 |
| | Average | 0.94 | 44.29 | 54.81 | 1.02 | 0.94 | 0.21 | 0.27 | 0.60 | 70.8 | 9.3 | 20.0 | 0.93 | 0.21 | 0.096 |
| E11 | Apr-02 | 7.2 | 67.4 | 25.4 | 1.21 | 1.21 | 0.25 | 0.25 | 0.71 | 73.5 | 7.0 | 19.5 | 1.01 | 0.20 | 0.111 |
| E16 | Apr-02 | 3.6 | 64.2 | 32.2 | 1.58 | 1.75 | 0.32 | 0.26 | 0.89 | 76.0 | 5.4 | 18.6 | 1.11 | 0.20 | 0.102 |
| E20 | Apr-02 | 0.0 | 54.2 | 45.8 | 1.45 | 1.20 | 0.28 | 0.25 | 0.75 | 74.5 | 6.4 | 19.1 | 0.83 | 0.19 | 0.090 |
| E25 | Apr-02 | 3.3 | 54.2 | 42.6 | 1.29 | 1.11 | 0.23 | 0.25 | 0.78 | 72.8 | 6.9 | 21.2 | 0.87 | 0.18 | 0.087 |
| G10 | Apr-02 | 1.3 | 71.7 | 27.0 | 1.15 | 0.95 | 0.20 | 0.28 | 0.62 | 71.9 | 8.7 | 19.5 | 0.82 | 0.18 | 0.090 |
| G15 | Apr-02 | 9.3 | 65.9 | 24.8 | 1.69 | 1.42 | 0.29 | 0.30 | 0.71 | 77.0 | 6.8 | 16.2 | 0.84 | 0.17 | 0.053 |
| I10 | Apr-02 | 0.0 | 50.1 | 49.9 | 1.48 | 1.25 | 0.23 | 0.24 | 0.77 | 74.4 | 6.1 | 19.4 | 0.85 | 0.15 | 0.086 |
| I17 | Apr-02 | n.a. | n.a. | n.a. | 1.79 | 1.39 | 0.23 | 0.25 | 0.87 | 75.3 | 5.6 | 19.1 | 0.78 | 0.13 | 0.074 |
| I22 | Apr-02 | 0.4 | 50.7 | 48.9 | 1.28 | 0.93 | 0.15 | 0.24 | 0.76 | 70.2 | 7.1 | 22.7 | 0.73 | 0.12 | 0.088 |
| J13 | Apr-02 | 0.4 | 41.0 | 58.7 | 1.25 | 1.11 | 0.24 | 0.26 | 0.70 | 73.1 | 7.3 | 19.6 | 0.89 | 0.19 | 0.113 |
| J20 | Apr-02 | 0.7 | 47.6 | 51.7 | 1.50 | 1.33 | 0.26 | 0.31 | 0.75 | 74.6 | 7.4 | 18.1 | 0.89 | 0.17 | 0.113 |
| L16 | Apr-02 | n.a. | n.a. | n.a. | 0.89 | 0.81 | 0.14 | 0.26 | 0.61 | 67.9 | 9.7 | 22.4 | 0.92 | 0.16 | 0.139 |
| L21 | Apr-02 | 0.3 | 48.3 | 51.4 | 1.12 | 0.96 | 0.17 | 0.25 | 0.69 | 70.6 | 7.8 | 21.6 | 0.86 | 0.15 | 0.108 |
| N14 | Apr-02 | 3.3 | 35.9 | 60.7 | 1.29 | 1.17 | 0.18 | 0.30 | 0.58 | 74.8 | 8.6 | 16.5 | 0.90 | 0.14 | 0.082 |
| N25 | Apr-02 | 0.1 | 38.7 | 61.2 | 0.95 | 0.77 | 0.16 | 0.24 | 0.54 | 70.7 | 9.0 | 20.3 | 0.81 | 0.17 | 0.098 |
| P15 | Apr-02 | n.a. | n.a. | n.a. | 0.57 | 0.45 | 0.10 | 0.19 | 0.36 | 67.2 | 11.5 | 21.3 | 0.79 | 0.18 | 0.108 |
| Q21 | Apr-02 | n.a. | n.a. | n.a. | 1.30 | 1.16 | 0.23 | 0.36 | 0.89 | 68.1 | 9.2 | 22.7 | 0.89 | 0.18 | 0.105 |
| | Average | 2.30 | 53.07 | 44.63 | 1.28 | 1.12 | 0.21 | 0.27 | 0.71 | 72.5 | 7.7 | 19.9 | 0.87 | 0.17 | 0.097 |

Table 6.3. Temporal and spatial variability of $\Delta^{14}\text{C}$, F Modern and ^{14}C age in surficial sediment collected along the E transect

| Sample | Cruise | depth | $\Delta^{14}\text{C}$ (‰) | F Modern | ^{14}C age (ybp) |
|--------|--------|-------|---------------------------|----------|---------------------------|
| E11 | Dec-00 | 11 | -232.8 | 0.773 | 2070 |
| E16 | Dec-00 | 16 | -264.7 | 0.740 | 2410 |
| E20 | Dec-00 | 20 | -287.5 | 0.717 | 2670 |
| E25 | Dec-00 | 25 | -332.8 | 0.672 | 3190 |
| E28 | Dec-00 | 28 | -375.6 | 0.629 | 3730 |
| E11 | Oct-01 | 11 | -214.4 | 0.791 | 1880 |
| E16 | Oct-01 | 16 | -244.6 | 0.761 | 2200 |
| E25 | Oct-01 | 25 | -279.2 | 0.726 | 2570 |
| E27 | Oct-01 | 27 | -284.8 | 0.720 | 2640 |
| E11 | Apr-02 | 11 | -234.1 | 0.771 | 2090 |
| E16 | Apr-02 | 16 | -178.5 | 0.827 | 1520 |
| E20 | Apr-02 | 20 | -182.4 | 0.823 | 1560 |
| E25 | Apr-02 | 25 | -227.7 | 0.778 | 2020 |
| E28 | Apr-02 | 28 | -243.1 | 0.762 | 2180 |

7. Gulf of Lions

7.1 Results

7.1.1 OC, TN and $\delta^{13}\text{C}$

In the prodelta region, OC content was inversely related to distance from the Rhône mouth, such that the highest OC values were observed at station G31 for both cruises (Fig. 7.1; Tab. 7.1, 7.2). The surficial prodelta sediments showed a clear seasonal variability, exhibiting the highest OC content (up to 2.05 %) in April 2005 (Fig. 7.1; Tab. 7.1, 2). The OC values along the mud belt in April 2005 were low compared to the prodelta samples, and exhibited a narrow range between 0.81 and 1.16 %. The lowest OC contents measured in this study were observed in October 2004 at the offshore stations, located in the relict sand region close to the heads of the western canyons (Fig. 7.2; Tab. 7.1 and 7.2). The TN distribution was similar to that of surficial OC, showing the same seasonal and spatial variability (Tab. 7.1). The C:N atomic ratio generally decreased seaward and westward with the lowest values (from 4.8 to 7.3) measured at the offshore stations whereas the highest ones (from 10.2 to 14.5) were observed in the prodelta area during October 2004 (Tab. 1, 2). Depleted isotopic values ($\delta^{13}\text{C}$) were measured in the prodelta Rhône area, with the lowest values ($< -27\text{‰}$) observed in April 2005 (Fig. 7.1). The isotopic composition along the mud-wedge showed low spatial variability with values that ranged from -22.85 (SC63) to -23.94 ‰ (SO66). The “heaviest” isotopic composition was measured offshore in the relict sands (HTU282 and PR1) (Fig. 7.2).

7.1.2 *Cuo oxidization products*

The carbon-normalized yields of the major CuO reaction products for GoL sediments are presented in tables 7.3 and 7.4. The combined lignin phenol yields (Λ) showed the highest values in the prodelta area during October 2004 ranging from 1.81 (K72) to 4.07 (E33) mg/100 mg OC. Samples collected on the subsequent cruise showed a comparatively limited variability ranging between 2.36 (RD71) to 2.96 (RD60) mg/100 mg OC. In both cruises, considering the prodelta area, the combined lignin phenol yields were the most abundant CuO reaction products representing 70-80% of the total product yields for most prodelta samples (Tab. 3, 4). Compositionally, vanillyl and syringyl phenols were present in about equal measure and were the most abundant lignin-derived CuO reaction products, combined accounting for ~80-90% of Λ yields. Benzoic acids were the second most abundant category of reaction products, accounting for ~10-20% of the total yields, followed by p-hydroxybenzenes (~10%). On the shelf, there was a higher percentage of p-hydroxybenzenes and benzoic acids than on the prodelta, accounting for ~ 50 % of the CuO reaction products whereas the remaining ~50 % consisted of lignin-derived CuO yields.

7.1.3 *Grain size analyses*

Concerning the grain size analyses, coarse-grained surficial samples were observed in October 2004 in the prodelta area and percent sand was inversely related to distance from the Rhône mouth (Tab. 7.1). Samples collected in April 2005 were dominantly fine-grained without showing a clear granulometric trend (Tab. 7.2).

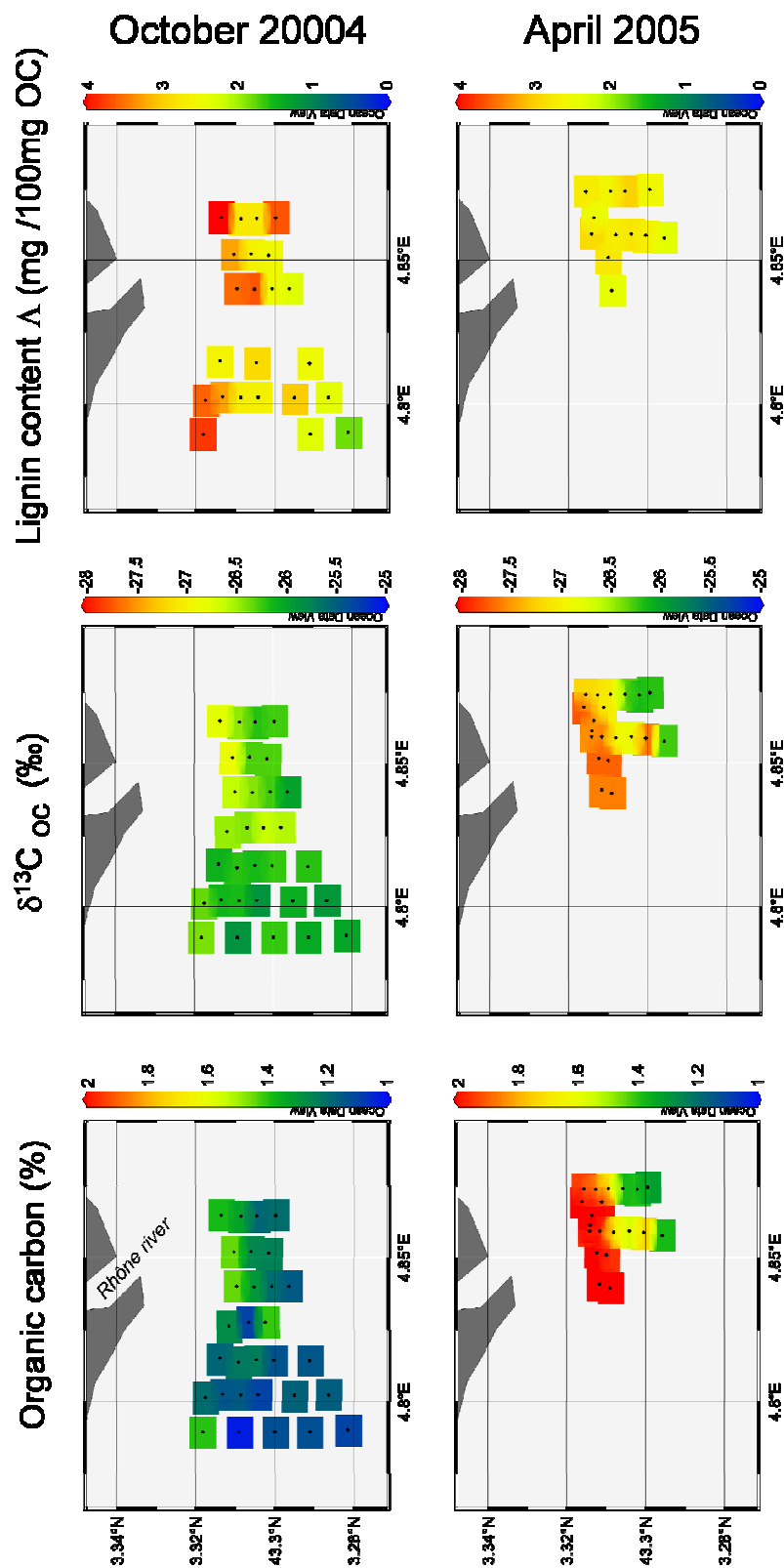


Fig. 7.1. Surficial distribution of organic carbon, stable isotope composition of organic carbon and lignin content of surface sediments in the prodelta Rhône area. Station locations are indicated by enclosed circles.

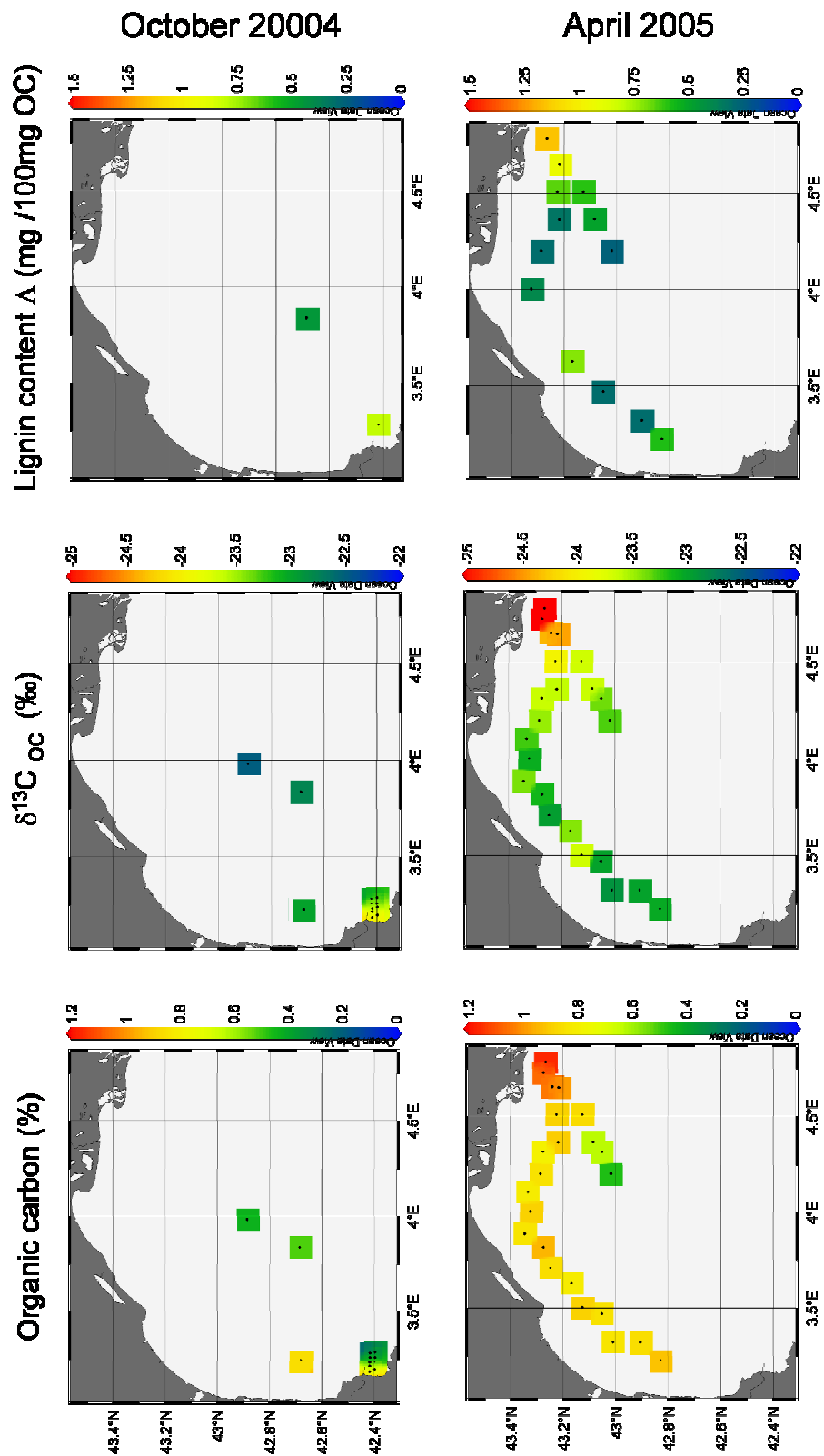


Fig.7.2. Surficial distribution of organic carbon, stable isotope composition of organic carbon and lignin content of surface sediments in the Gulf of Lions. Station locations are indicated by enclosed circles.

7.2 Discussion

7.2.1. Organic matter origin

Vascular plants exhibit many bulk chemical and isotopic properties that distinguish them from marine phytoplankton (Hedges et al., 1997). For example, as a result of contrasting inorganic carbon sources, distinct uptake processes and variable biosynthetic pathways (e.g., Park and Epstein 1961; Fry and Sherr, 1984; Popp et al., 1998), C₃ terrestrial plants exhibit more depleted $\delta^{13}\text{C}$ values (from -28 to -25 ‰) relative to temperate marine phytoplankton (from -22 to -19 ‰) (Hedges et al. 1997). Another characteristic bulk property of most terrestrial plants is the predominance of nitrogen-free biomacromolecules (Hedges and Oades, 1997), which results in a higher organic C/N ratio in vascular lands plant (C/N > 14; Goñi et al., 2003) relative to phytoplankton (C/N \approx 7; Redfield et al., 1963). Due to further fractionation along biosynthetic pathways, the isotopic composition of major biochemical classes can vary substantially. For example, lignin is depleted in ^{13}C relative to cellulose and hemicellulose (van Bergen and Poole, 2002) and consequently early diagenesis can also change the composition of OM sources prior to their sequestration in sediments (Benner et al., 1987; Benner et al., 1991). Conversely, addition of new microbial biomass, rich in proteins and carbohydrates which are “heavier” than refractory compounds, may raise the $\delta^{13}\text{C}$ values from the original plant value (Gleixner et al., 1993; Hobbie et al., 1999, Ehleringer et al., 2000). Furthermore, such existence of microorganisms (ex. bacteria, fungi), that decay the OM derived from vascular plants, can result in increases of nitrogen-rich biochemicals (proteins) (Hedges et al., 1997; Schneider et al., 2003), which in turn lower the C/N ratio from the original plant value.

Stable isotope and elemental data are commonly employed in biogeochemical investigations of coastal environments because of their potential to elucidate the roles of phytoplankton and vascular plants in the marine OC cycle (Faganeli et al., 1988; Hedges and

Oades, 1997; Leithold and Hope, 1999; Gordon and Goñi, 2003; Goñi et al., 2003; Boldrin et al., 2005; Miserocchi et al., 2007).

The OM in the GoL samples exhibited a broad range of C/N and $\delta^{13}\text{C}$ values (Tab. 1 and Tab.2), indicating both marine and terrestrial sources. Because of the heterogeneity of the riverine material, the Rhône prodelta surficial sediments showed additional seasonal variability reflecting diverse terrestrial OM sources. Specifically, the prodelta samples collected in April 2005 were characterized by relatively “light” isotopic compositions and lower C/N ratios compared to October 2004, suggesting a significant degraded soil-derived OM contribution. As previously cited, soil microbial biomass lowers the C/N ratio (soil values 8-14, Hedges and Oades, 1997), while the selective preservation of refractory compounds (such as lignin) lightens the isotopic composition of bulk OM (Benner et al., 1987; Benner et al., 1991). In contrast the higher C/N values of surficial sediments in October 2004 suggest a major influence fresher material such as plant fragments (C/N>14, Goni et al., 2003).

All these evaluations are summarized and graphically schematized in Figure 7.3, where $\delta^{13}\text{C}$ is plotted against the N/C ratio rather than the classical C/N ratio because the N/C parameter behaves linearly in a mixing model (Goñi et al., 2003). The majority of the samples collected along the mud-wedge (Fig. 5) showed a dominantly marine isotopic signature, although the C/N ratio was lower than the classical marine value of ~7 (N/C ~0.14) indicated by Redfield et al. (1963). In recent years many authors (Hedges et al., 1997; Schneider et al., 2003; Goñi et al., 2003) have pointed out the problems related to the nonconservative behavior of the C/N ratio. Variations from a constant value were explained in two ways: deviations during particle production (growth rate, availability of nutrients, etc) and changes during subsequent remineralization. The second process, which seems pertinent to the GoL offshore samples (Fig. 7.3), is driven by the presence of bacterial activity which increase the

nitrogen content of particulate material through microbial decay. This increase in nitrogen drops the elemental ratio of the marine particulate below the Redfield ratio.

Because lignin is a macromolecule uniquely synthesized by vascular plants, this tracer is a more sensitive biomarker for indirectly quantifying the marine fraction. Lignin has been used in many investigations to identify in detail the terrestrial OM contribution to a wide variety of environments including rivers (Hedges et al., 1984; Onstad et al., 2000; Cotrim da Cunha et al., 2001; Bianchi et al., 2004), estuaries (Reeves and Preston, 1989; Goñi et al., 2003), prodeltas and inshore regions (Goñi et al., 1998; Bianchi et al., 2002; Gordon and Goñi, 2003), offshore regions (Hernes and Benner, 2002), as well as deep sea fans (Cowie et al., 1995; Goñi, 1997; Buscail and Germain, 1997). Along the main dispersal system on the GoL shelf, the lignin contribution showed a drastic drop-off with increasing distance offshore (from 70-80% to 40-60% CuO products; Tab. 7.3 and 7.4) with a corresponding increase of the B yields (from 5-10% to 20-30% CuO products; Tab. 3,4). This trend reflects a reduction in direct terrestrial input, with a consequent enhancement of the marine OM contribution ($\Delta = 0$ mg/100 mg OC). Because of the low lignin content in soil ($\Delta = 1-4$ mg/100 mg OC; Hedges et al., 1997) relative to plant fragments ($\Delta > 6-8$ mg/100 mg OC; Hedges et al., 1997), the carbon-normalized lignin-derived sum eight is a powerful geochemical tool for identifying diverse terrestrial OM origins. This biomarker can be used to resolve the ambiguity that can result from simply using the isotopic signature, as sometimes isotopic differences between soil and woody material are not statistically significant. The lignin data confirm the variability detected in the prodelta concerning the terrestrial sources previously illustrated using N/C and isotopic values (Fig 7.4). Samples collected in April 2005 were isotopically depleted and displayed low lignin contents, indicating terrestrial soil-derived OM, whereas October 2004 showed higher lignin contents suggesting a greater contribution from plant debris.

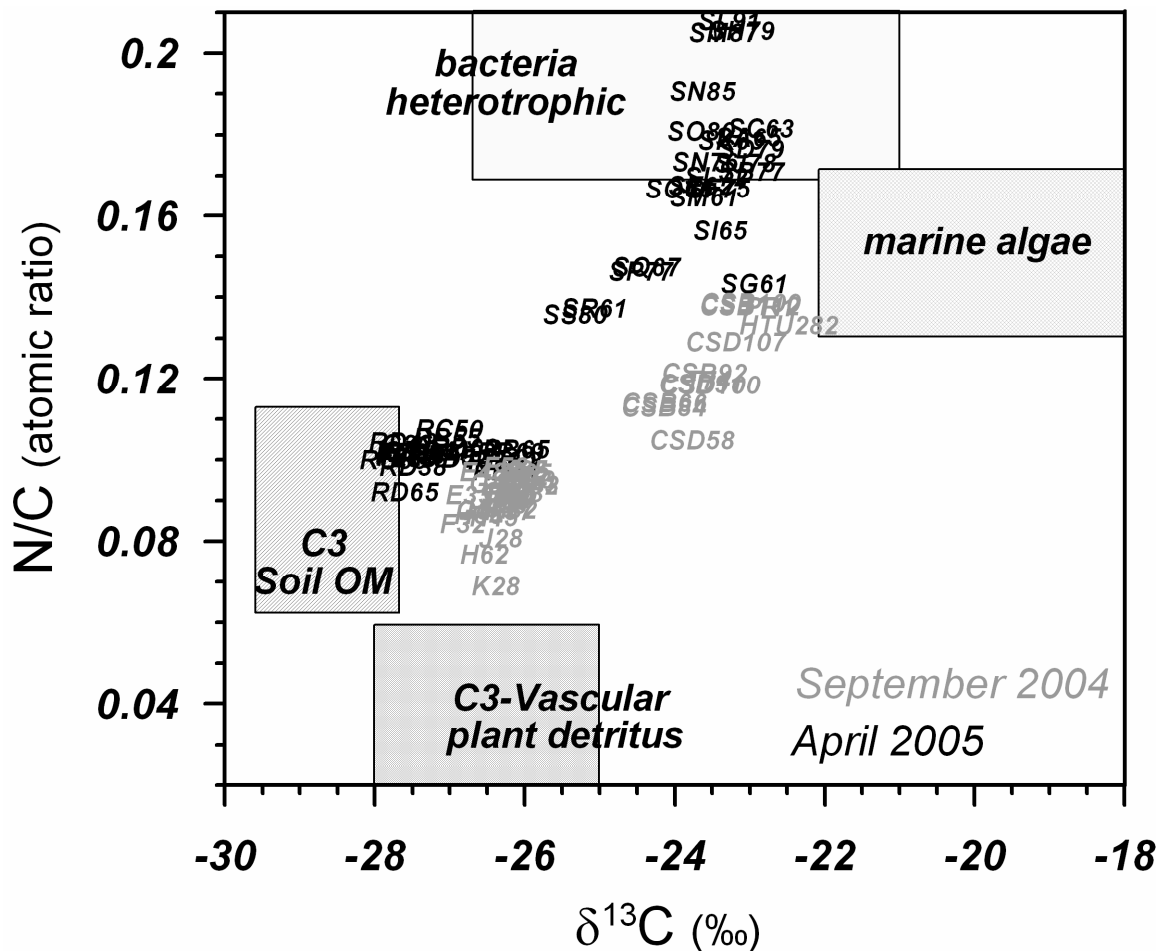


Fig.7.3. Stable isotopic compositions of organic carbon vs total nitrogen:organic carbon ratio from surficial sediments. The compositions of four possible OC sources (C3 vascular plant detritus, C3 soil OM riverine/estuarine phytoplankton detritus and marine phytoplankton detritus) are also plotted in all graphs to illustrate the relative influence. The N/C ratio was used rather than the classical C/N ratio because the N/C parameter behaves linearly in a mixing model (Goñi et al., 2003).

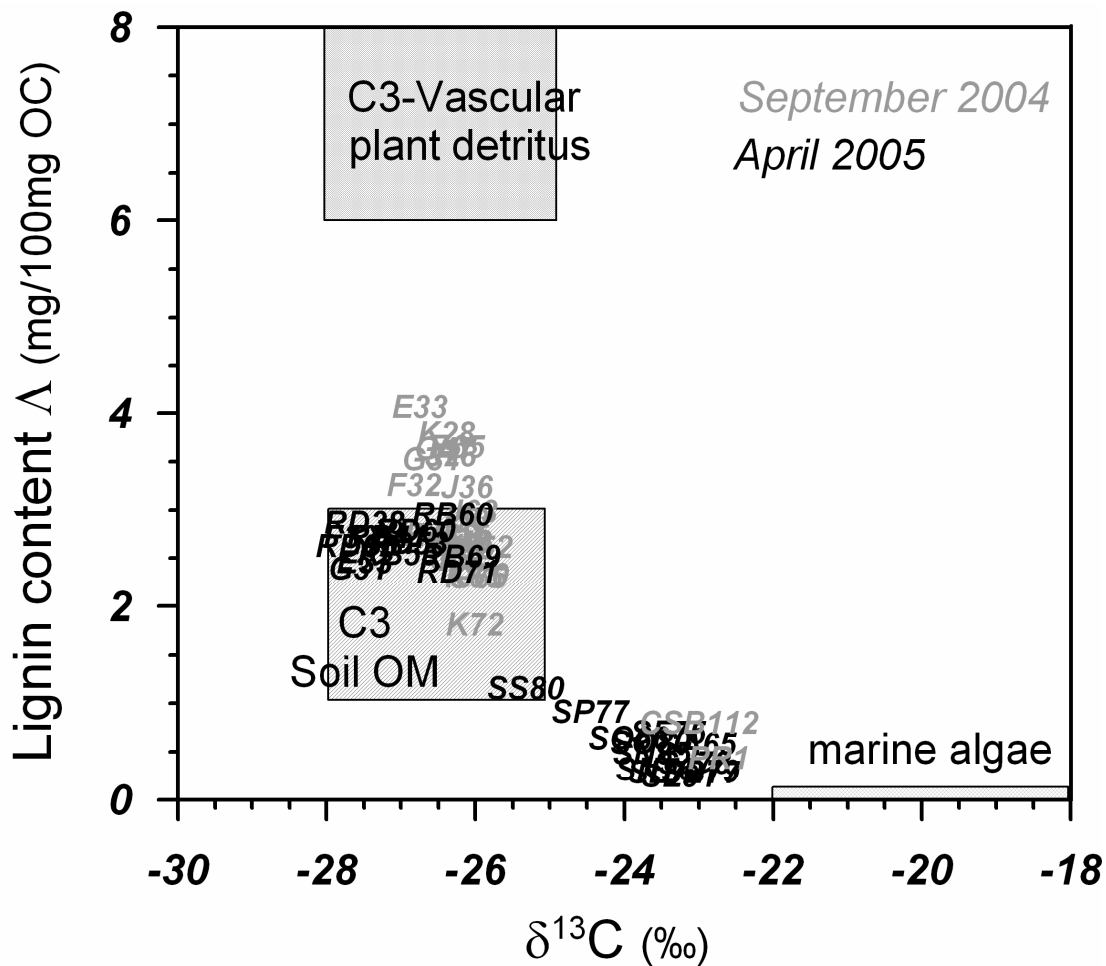


Fig. 7.4. Graph of the stable isotopic compositions of organic carbon vs carbon-normalized lignin phenol yields and from surficial sediments. The compositions of four possible OC sources (C3 vascular plant detritus, C3 soil OM riverine/estuarine phytoplankton detritus and marine phytoplankton detritus) are also plotted in all graphs to illustrate the relative influence.

7.2.2 Sediment sorting

Hydrodynamic sorting of the surface mixed layer (SML) has been shown to be a fundamental mechanism for the redistribution of riverine-derived organic matter along coastal margins (Prahl, 1985; Keil et al, 1998; Leithold and Hope, 1999). Riverine material, being heterogeneous with a broad variability in particle size, is not equally removed from the Rhône prodelta area and this in turn affects OC, N/C and lignin distribution in the surficial sediments. Therefore, the reason for the seasonal variability observed in the Rhône prodelta may lie in

the physical reworking and sorting of the SML. Recently, Roussiez et al. (2005) described the mechanisms that influence the transport of fine material in the basin. These authors showed that the large quantity of sediment introduced by the Rhône during flood events can lead to the formation of prodeltic structures of fine-grained sediments, termed “early muddy deposits”. These structures, being above the storm limit, are then exposed to resuspension events and can be actively redistributed along the entire margin. Sediment transport of this nature has implications for the surface distribution of geochemical parameters, and granulometric data can help in interpreting the geochemical gradients.

A positive correlation between percent sand and lignin content was detected in the surficial prodelta sediments (Fig. 7.5). Elevated lignin contents, associated with coarse material, were detected during the period of low river discharge (October 2004, Fig. 3.5), whereas after a period of high river discharge (April 2005, Fig. 3.5), the fine material exhibited lower lignin contents. The relationship between grain size and plant fragment content has been well documented in previous studies. For example, on the Washington-Oregon coast, Keil et al. (1998) found that the carbon-normalized yields of the major lignin phenol monomers and the C/N ratios increased with increasing grain size. On the northern Californian coast, Leithold and Hope (1999) showed that the surficial concentration of plant debris was coupled with the coarse-sized particles, reflecting vertical and lateral sorting in the plume and benthic boundary layer. In our hypothesis, as observed in the Gulf of Mexico (Goni et al., 1998), the riverine sediment, initially deposited in the prodelta area, is impacted by hydraulic sorting that preferentially removes the finest material. Thus, the OM associated with this fine fraction is selectively transported off the prodelta. Such physical sorting increases the concentration of the sand fraction as well as the amount of plants debris in the remaining deposits, which in turn increases the lignin content and drops the OC content (Fig. 7.1). Specific studies on the relationship between organic matter and particle size (Mayer, 1994;

Keil et al., 1997), indicate that the OC content in marine sediment increases with decreasing mean particle size, because of the larger specific surface area of finer particles such as clay.

The October 2004 and April 2005 GoL cruises represent two possible end-members in terms of the extent of post-depositional sediment sorting. Based on river discharge, the material collected during October 2004 probably represents reworked sediment initially supplied by the high-flow events of December 2003 and/or January 2004 (Fig. 3.5). In comparison, the April 2005 samples likely reflect the input of new fine material, as suggested by the fluvial regime and by the presence of terrestrially-supplied Be-7 (53-day half-life) in the surface sediment (Lomnický et al., 2006).

In addition to influencing lignin content, hydrodynamic sorting influences lignin composition in the prodelta region, due to the selective removal of woody-nonwoody tissues of both angiosperm and gymnosperm vegetation (Fig. 7.6). The S/V vs. C/V ratio (syringyl and cinnamyl phenols both normalized to vanillyl phenols) can provide information regarding the lignin origin. During the high-flow regime (April 2005), it was observed that the river supplied a homogeneous woody and non-woody mixture with a predominance of angiosperm tissues. In contrast, reworked surficial prodelta sediments (October 2004) exhibited a scattered distribution on the plot as well as a further increase in the angiosperm component of both woody and non-woody tissue. The prevalence of angiosperm tissues exhibited in both cruises is in contrast with previous studies (Bouloubassi et al., 1997), which emphasized the importance of gymnosperm-derived wood debris for the same region. This discrepancy may indicate a seasonal and spatial variability in riverine material that could depend on many factors, including the intensity of precipitation and runoff, as well as deviations in the character of the drainage basin (Onstad et al., 2000). Significant seasonal variability has been observed in the suspended material delivered by the nearby Tech, a French Mediterranean

river, where both gymnosperm and angiosperm plants have been found (Cotrim da Cunha et al., 2001).

The decay of lignin by terrestrial fungi and other lignin-degrading organisms has been shown to increase the ratio of acid to aldehyde of vanillyl $(Ad/Al)_v$ and syringyl $(Ad/Al)_s$ phenols relative to the range typical of fresh vascular plant tissues (Gõni and Hedges, 1992; Opshal and Benner, 1995); these ratios can therefore provide evidence of degradative processes that predominate in terrestrial environments such as soil. The samples collected on the mid-shelf mud belt do not display higher $(Ad/Al)_v$ and $(Ad/Al)_s$ as expected and concerning the Rhône prodelta there is no significant difference in the $(Ad/Al)_v$ and $(Ad/Al)_s$ between the two cruises in spite of the diverse nature of the riverine material. This could depend on the large error propagation associated with rationing small numbers (Gõni et al., 1998). The elevated yields of 3,5-Bd relative to V phenols $(3,5-Bd/V)$ was proposed as an additional evidence for a soil origin (Prahl et al. ,1994; Goñi et al., 2000). Although there are marine sources of 3,5-Bd acid such as plankton and macrophytes, which liberate large amounts of this compound upon CuO oxidation (Goñi and Hedges, 1995), the correlation between 3,5-Bd with Δ ($r^2 = 0.90$) and $\delta^{13}C$ ($r^2 = 0.83$) seems to suggest a terrestrial source (Gordon and Goñi, 2003). Most of the offshore samples display elevated 3,5-Bd/V ratios relative to the prodelta area and this may indicate a selective transport and subsequent deposition in the offshore region of soil derived OM adsorbed onto the fine fraction (Fig. 7.7).

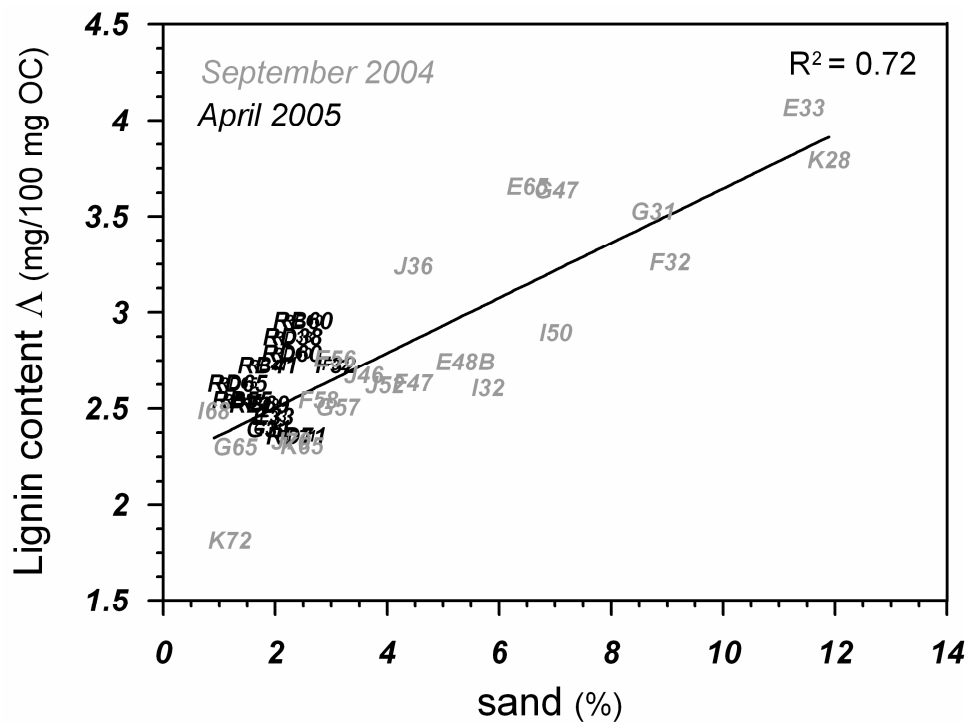


Fig. 7.5. Correlation between percent sand and lignin content in the surficial prodelta sediments.

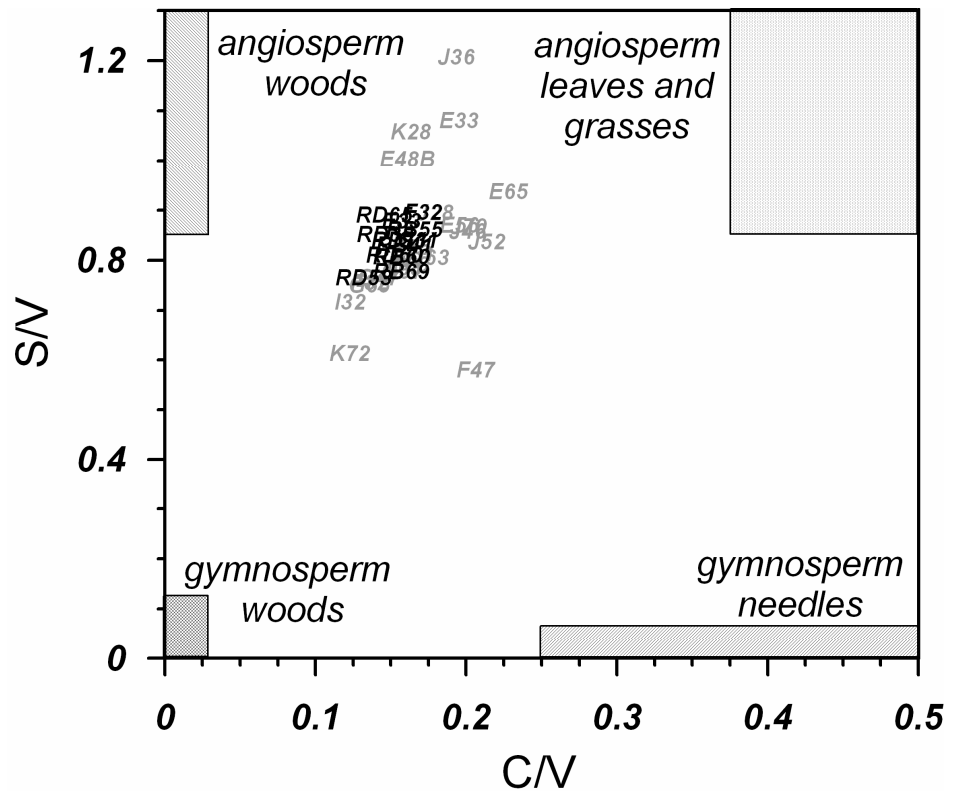


Fig. 7.6. Syringyl/vanillyl phenol ratio vs cinnamyl/vanillyl phenol ratio. Typical ranges for woody and nonwoody tissues of both angiosperm and gymnosperm vegetation are indicated.

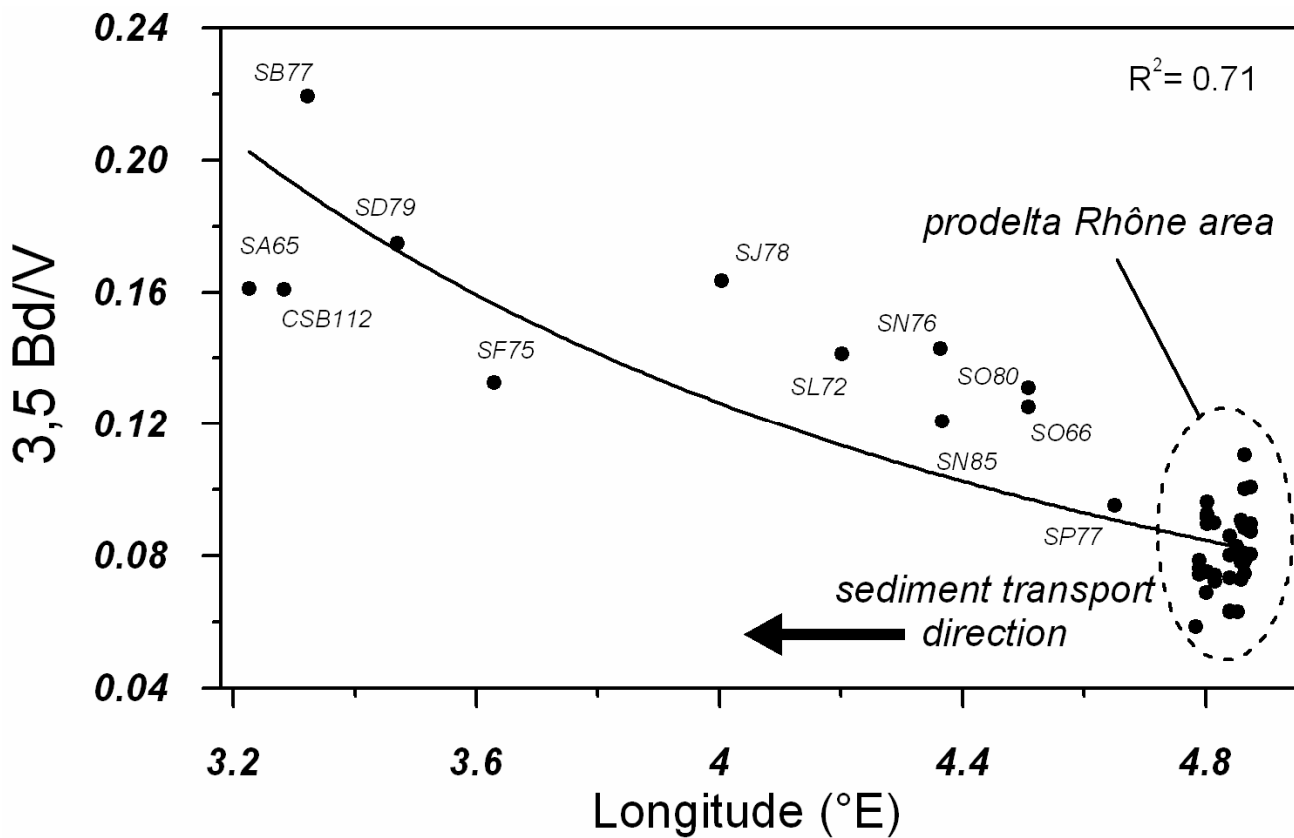


Fig. 7.7. Transport and subsequent deposition in the offshore region of humified soil-derived OM based on the 3,5-Bd/V ratios.

7.2.3 Surficial OM distribution in the Gulf of Lions

Shelf and prodelta environments play a significant role in the marine OC budget because they experience high sediment accumulation rates, accounting for almost 90% of OC burial (Berner et al., 1982, 1989; Hedges et al., 1997). Nevertheless, in the last few years it has been shown that the rate of this sequestration is not simply proportional to sediment accumulation rate and OC content, as many other physical and biological processes are involved (Aller, 1998). Because of their different reactivities (Hedges et al., 1997), terrestrial

and marine fractions are decomposed at different efficiencies in deltaic areas, with remineralization percentages reaching about 70% and 90%, respectively (Aller, 1998). For this reason, a coherent and articulate investigation of the OC burial in the marine environment should take into account the differences in chemical composition coupled with sediment accumulation that, on continental margins, are as highly variable as the OM source.

The composition of OM from surface sediments in different regions of the GoL, are shown in Fig. 7.8. The plot displays the relationships between $\delta^{13}\text{C}$, lignin and OC compositions of surficial sediments from diverse depositional settings in the GoL. These settings include the Rhône proximal prodelta, where high sediment accumulation rates reach 20 cm y^{-1} (Radakovitch et al., 1999), the distal prodelta area, the mid-shelf mud belt consisting of a fine-grained deposit of Holocene age, and finally the outer-shelf where relict sands are mixed with modern mud (Roussiez et al., 2005). The linear relationship highlighted in the graph identifies a possible mixing of fine soil-derived terrestrial material, isotopically depleted, rich in OC and relatively rich in lignin with marine phytodetritus characterized by low OC, “heavier” isotopic composition and the absence of lignin. Such a mixture is supported by the elevated coefficient of correlation ($r^2 = 0.92$). Along the dispersal system, a fraction of the OC adsorbed onto the fine material is diluted by marine OC that reaches the seabed and/or degraded by microbial activity. The retention time of fine sediments within the proximal and distal prodelta area seems to be a key variable. The geochemical surficial distributions observed in the GoL suggest a relatively elevated retention time allowing for significant microbial degradation and marine dilution; the advected material that reaches the slope and the head of the canyons has lost its original terrestrial signature and is dominantly marine. The extrapolation of the correlation line to $\Lambda = 0$ indicates a mean isotopic value -22.6 ‰ for lignin-free OM, which can include not only marine sources but also bedrock-derived kerogen (Blair et al., 2003; Leithold et al., 2006). The transport of soil derived OM adsorbed onto the

fine sediment does not take into account the coarser prodelta samples collected in October 2005. This exclusion is based on what was previously illustrated: the October 2005 prodelta samples have been reworked and altered, becoming depleted in the finest fraction. Coarse plant fragments, which are an additional important component of the carbon discharged by the Rhône, have a fate separate from the fine fraction due to their hydraulic behavior. Thill et al. (2001) have estimated that almost all 50-200 μm particles are removed from surface water just off the mouth by settling and dilution processes. As this coarse refractory carbon is likely to be trapped and degraded slowly, the distribution of vascular plant debris within flood layers may be an important predictor of where methane gas will accumulate on the continental margin (Leithold and Hope, 2001). It has been shown from a sampling performed on the same prodeltaic stations (EuroSTRATAFORM project, Garcia-Garcia et al, 2006) that elevated methane contents, up to 95720 ppm, characterize the Rhône proximal prodelta area, whereas the gas concentration drops drastically just outside the area influenced by the Rhône.

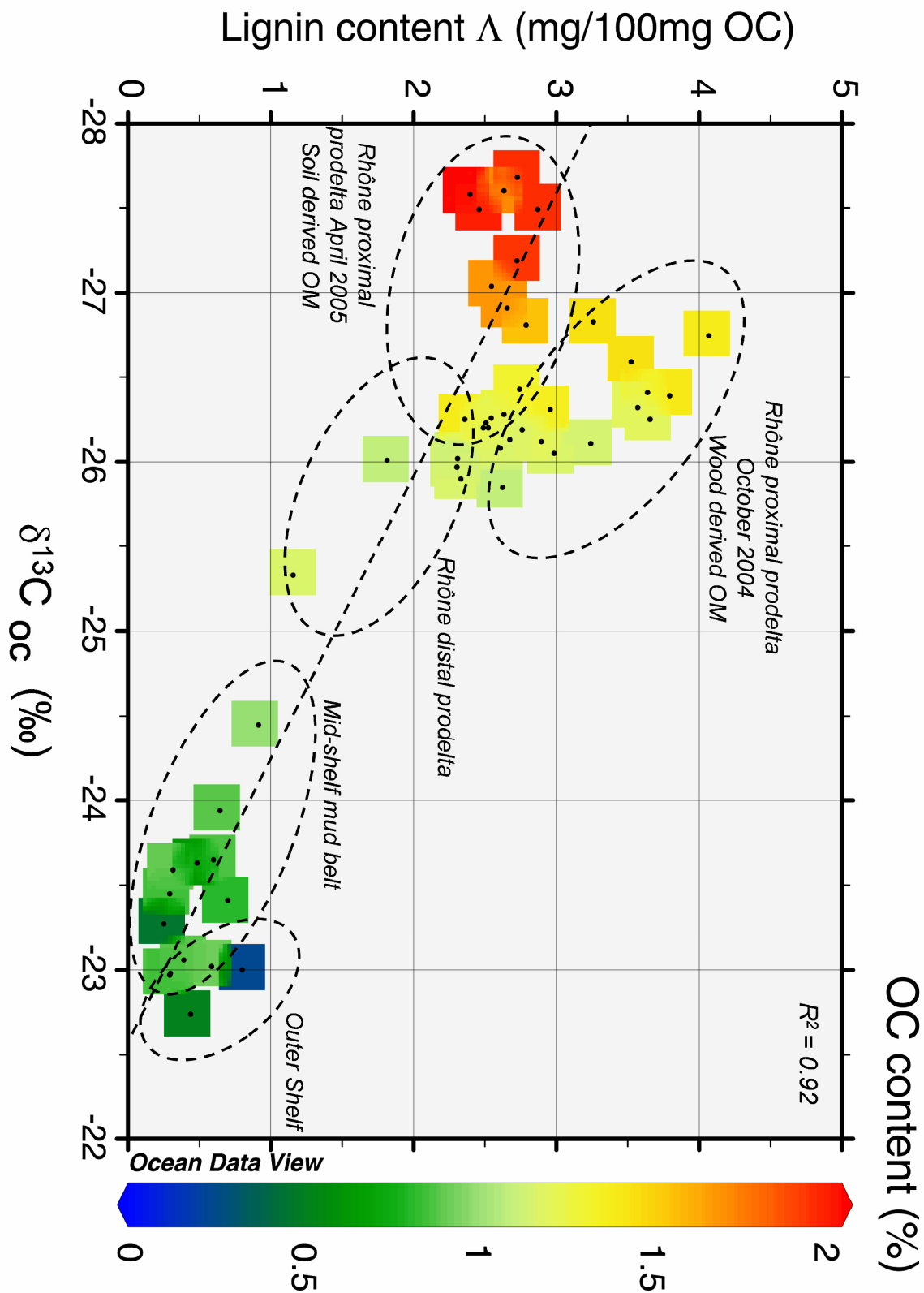


Fig.7.8. Surficial OC, $\delta^{13}C$ and Λ distribution for the GoL coupled with the sedimentary units characterized by different sedimentological features based on Durrieu de Madron et al. 2000.

Table 7.1. Station locations, elemental, isotopic compositions and grain-size data of surficial shelf sediments in the Gulf of Lions, October 2004

| core | latitude (° N) | longitude (° E) | water depth (m) | OC (%) | TN (%) | $\delta^{13}\text{C}_{\text{OC}}$ (‰) | C:N (atomic) | clay (%) | silt (%) | sand (%) |
|------------------------------|----------------|-----------------|-----------------|--------|--------|---------------------------------------|--------------|----------|----------|----------|
| <i>Rhône prodelta</i> | | | | | | | | | | |
| E33 | 43.313 | 4.865 | 33 | 1.38 | 0.147 | -26.75 | 10.94 | 49.56 | 39.01 | 11.43 |
| E48B | 43.309 | 4.864 | 48 | 1.32 | 0.149 | -26.43 | 10.31 | 47.02 | 47.59 | 5.39 |
| E56 | 43.305 | 4.865 | 56 | 1.18 | 0.13 | -26.19 | 10.89 | 23.37 | 73.57 | 3.06 |
| E65 | 43.3 | 4.865 | 65 | 1.2 | 0.126 | -26.25 | 11.11 | 52.89 | 41.39 | 5.72 |
| F32 | 43.31 | 4.852 | 31 | 1.44 | 0.14 | -26.83 | 11.85 | 49.09 | 41.87 | 9.04 |
| F47 | 43.306 | 4.852 | 47 | 1.26 | 0.138 | -26.28 | 10.7 | 28.61 | 66.94 | 4.45 |
| F58 | 43.302 | 4.852 | 58 | 1.24 | 0.142 | -26.26 | 10.18 | 56.43 | 40.8 | 2.77 |
| G31 | 43.31 | 4.84 | 31 | 1.44 | 0.147 | -26.59 | 11.42 | 23.61 | 67.64 | 8.75 |
| G47 | 43.305 | 4.84 | 47 | 1.3 | 0.143 | -26.41 | 10.62 | 36.21 | 57.83 | 5.96 |
| G57 | 43.301 | 4.84 | 57 | 1.2 | 0.129 | -26.23 | 10.86 | 57.23 | 39.65 | 3.12 |
| G65 | 43.296 | 4.84 | 65 | 1.15 | 0.13 | -25.97 | 10.33 | 53.97 | 44.75 | 1.28 |
| H30 | 43.312 | 4.826 | 30 | 1.27 | 0.13 | -26.45 | 11.36 | 47.72 | 43.17 | 9.11 |
| H45 | 43.307 | 4.828 | 45 | 1.1 | 0.101 | -26.41 | 11.63 | 33.03 | 65.17 | 1.8 |
| H56 | 43.302 | 4.828 | 56 | 1.41 | 0.142 | -26.62 | 11.55 | 52.35 | 41.7 | 5.95 |
| I32 | 43.314 | 4.815 | 32 | 1.18 | 0.121 | -26.08 | 11.39 | 30.62 | 63.58 | 5.8 |
| I42 | 43.309 | 4.814 | 42 | 1.22 | 0.129 | -26.18 | 11.05 | 51.77 | 44.51 | 3.72 |
| I50 | 43.305 | 4.814 | 51 | 1.23 | 0.132 | -26.12 | 10.89 | 51.51 | 39.12 | 9.37 |
| I58 | 43.3 | 4.814 | 58 | 1.13 | 0.117 | -26.21 | 11.24 | n.a. | n.a. | n.a. |
| I68 | 43.291 | 4.814 | 68 | 1.14 | 0.12 | -26.2 | 11.08 | 57.88 | 41.22 | 0.9 |
| J28 | 43.318 | 4.801 | 28 | 1.2 | 0.11 | -26.32 | 12.38 | n.a. | n.a. | n.a. |
| J36 | 43.313 | 4.803 | 36 | 1.14 | 0.126 | -26.11 | 10.55 | 31.08 | 64.45 | 4.47 |
| J46 | 43.309 | 4.802 | 46 | 1.15 | 0.123 | -26.13 | 10.9 | 34.55 | 61.87 | 3.58 |
| J52 | 43.304 | 4.802 | 52 | 1.09 | 0.12 | -25.85 | 10.66 | 49.21 | 46.84 | 3.95 |
| J63 | 43.295 | 4.802 | 63 | 1.17 | 0.126 | -26.05 | 10.89 | n.a. | n.a. | n.a. |
| J70 | 43.286 | 4.802 | 72 | 1.16 | 0.129 | -25.9 | 10.52 | 57.98 | 39.73 | 2.28 |
| K28 | 43.318 | 4.789 | 28 | 1.4 | 0.113 | -26.39 | 14.5 | 20.97 | 67.15 | 11.88 |
| K43 | 43.309 | 4.789 | 43 | 1.03 | 0.112 | -25.87 | 10.65 | n.a. | n.a. | n.a. |
| K57 | 43.3 | 4.79 | 57 | 1.12 | 0.11 | -26.21 | 11.43 | 46.94 | 51.6 | 1.46 |
| K65 | 43.291 | 4.79 | 65 | 1.12 | 0.128 | -26.02 | 10.24 | 44.15 | 53.37 | 2.48 |
| K72 | 43.281 | 4.79 | 72 | 1.1 | 0.123 | -26.01 | 10.42 | 59.53 | 39.29 | 1.18 |
| <i>S-W stations</i> | | | | | | | | | | |
| CSB100 | 3.258 | 42.417 | 100 | 0.24 | 0.04 | -22.99 | 7.22 | n.a. | n.a. | n.a. |
| CSB112 | 3.284 | 42.416 | 112 | 0.24 | 0.04 | -23 | 7.26 | n.a. | n.a. | n.a. |
| CSB66 | 3.185 | 42.417 | 66 | 0.91 | 0.12 | -24.14 | 8.77 | n.a. | n.a. | n.a. |
| CSB84 | 3.215 | 42.417 | 84 | 0.71 | 0.09 | -24.15 | 8.85 | n.a. | n.a. | n.a. |
| CSB92 | 3.233 | 42.417 | 92 | 0.58 | 0.08 | -23.61 | 8.23 | n.a. | n.a. | n.a. |
| CSD100 | 3.259 | 42.397 | 100 | 0.49 | 0.07 | -23.53 | 8.45 | n.a. | n.a. | n.a. |
| CSD107 | 3.287 | 42.397 | 107 | 0.34 | 0.09 | -23.18 | 7.75 | n.a. | n.a. | n.a. |
| CSD58 | 3.197 | 42.397 | 58 | 0.84 | 0.1 | -23.77 | 9.54 | n.a. | n.a. | n.a. |
| CSD91 | 3.24 | 42.397 | 91 | 0.39 | 0.05 | -23.65 | 8.42 | n.a. | n.a. | n.a. |
| PR1 | 3.838 | 42.686 | 294 | 0.51 | 0.08 | -22.74 | 7.26 | 55.41 | 26.68 | 17.91 |
| T74 | 3.21 | 42.663 | 74 | 0.84 | 0.12 | -23.56 | 8.36 | n.a. | n.a. | n.a. |
| HTU282 | 3.983 | 42.887 | 282 | 0.43 | 0.07 | -22.48 | 7.51 | n.a. | n.a. | 72.91 |

n.a = not available

Table 7.2. Station locations, elemental, isotopic compositions and grain-size data of surficial shelf sediments in the Gulf of Lions, April 2005

| core | latitude (° N) | longitude (° E) | water depth (m) | OC (%) | TN (%) | $\delta^{13}\text{C}_{\text{OC}}$ (‰) | C:N (atomic) | clay (%) | silt (%) | sand (%) |
|----------------------------------|----------------|-----------------|-----------------|--------|--------|---------------------------------------|--------------|----------|----------|----------|
| <i>Rhône prodelta</i> | | | | | | | | | | |
| E33 | 43.314 | 4.865 | 35 | 2.01 | 0.24 | -27.49 | 9.95 | 45.22 | 52.82 | 1.96 |
| F31 | 43.312 | 4.852 | 26 | 2.03 | 0.24 | -27.69 | 9.89 | n.a. | n.a. | n.a. |
| F32 | 43.31 | 4.851 | 35 | 1.96 | 0.23 | -27.68 | 9.92 | 44.71 | 52.22 | 3.07 |
| G20 | 43.312 | 4.841 | 23 | 2.02 | 0.24 | -27.58 | 9.63 | n.a. | n.a. | n.a. |
| G31 | 43.309 | 4.839 | 35 | 2.05 | 0.24 | -27.58 | 9.8 | 53.73 | 44.4 | 1.87 |
| RB41 | 43.316 | 4.874 | 42 | 1.94 | 0.23 | -27.19 | 9.78 | 45.2 | 52.93 | 1.86 |
| RB49 | 43.313 | 4.874 | 49 | 1.84 | 0.22 | -27.12 | 9.88 | n.a. | n.a. | n.a. |
| RB55 | 43.309 | 4.874 | 53 | 1.69 | 0.21 | -27.04 | 9.49 | 45.4 | 53.2 | 1.4 |
| RB60 | 43.306 | 4.874 | 60 | 1.37 | 0.16 | -26.31 | 10.03 | 45.61 | 51.9 | 2.49 |
| RB65 | 43.302 | 4.874 | 65 | 1.39 | 0.17 | -26.12 | 9.75 | 45.61 | 51.9 | 2.49 |
| RB69 | 43.299 | 4.875 | 68 | 1.31 | 0.16 | -26.2 | 9.81 | 48.58 | 49.71 | 1.71 |
| RC35 | 43.316 | 4.869 | 35 | 2.01 | 0.23 | -27.75 | 10 | n.a. | n.a. | n.a. |
| RC50 | 43.311 | 4.869 | 47 | 2 | 0.25 | -27.01 | 9.3 | n.a. | n.a. | n.a. |
| RD36 | 43.314 | 4.861 | 29 | 2.05 | 0.24 | -27.54 | 9.82 | n.a. | n.a. | n.a. |
| RD38 | 43.314 | 4.859 | 36 | 1.96 | 0.22 | -27.49 | 10.17 | 35.23 | 62.46 | 2.31 |
| RD43 | 43.312 | 4.859 | 37 | 1.96 | 0.24 | -27.63 | 9.59 | n.a. | n.a. | n.a. |
| RD53 | 43.308 | 4.859 | 48 | 1.68 | 0.2 | -26.91 | 9.96 | n.a. | n.a. | n.a. |
| RD60 | 43.304 | 4.859 | 59 | 1.56 | 0.19 | -26.81 | 9.72 | 42.18 | 55.53 | 2.29 |
| RD65 | 43.3 | 4.859 | 63 | 1.72 | 0.18 | -27.6 | 10.86 | 45.79 | 52.88 | 1.32 |
| RD71 | 43.296 | 4.858 | 70 | 1.38 | 0.16 | -26.25 | 10.28 | 46.8 | 50.83 | 2.37 |
| <i>Mid-shelf mud belt</i> | | | | | | | | | | |
| SA65 | 42.83 | 3.23 | 66 | 0.92 | 0.19 | -23.02 | 5.57 | 51.21 | 48.38 | 0.41 |
| SB77 | 42.9 | 3.32 | 79 | 0.86 | 0.17 | -22.97 | 5.85 | 61.8 | 35.16 | 3.04 |
| SC63 | 43.01 | 3.32 | 64 | 0.83 | 0.18 | -22.85 | 5.51 | 48.8 | 49.87 | 1.33 |
| SD79 | 43.05 | 3.47 | 81 | 0.85 | 0.18 | -22.98 | 5.67 | 66.24 | 33.35 | 0.41 |
| SE62 | 43.13 | 3.5 | 63 | 0.89 | 0.17 | -23.66 | 5.97 | 59.48 | 39.45 | 1.07 |
| SF75 | 43.17 | 3.63 | 77 | 0.81 | 0.16 | -23.41 | 6 | 39.77 | 54.22 | 6.01 |
| SG61 | 43.25 | 3.71 | 64 | 0.86 | 0.14 | -22.94 | 6.98 | 38.13 | 60.03 | 1.84 |
| SH79 | 43.27 | 3.82 | 80 | 0.94 | 0.23 | -23.11 | 4.87 | 45.24 | 51.97 | 2.79 |
| SI65 | 43.34 | 3.89 | 66 | 0.83 | 0.15 | -23.39 | 6.4 | 59.07 | 39.77 | 1.16 |
| SJ78 | 43.32 | 4 | 79 | 0.89 | 0.18 | -23.06 | 5.78 | 40.56 | 53.58 | 5.86 |
| SK63 | 43.33 | 4.11 | 65 | 0.81 | 0.17 | -23.25 | 5.6 | 59.65 | 39.56 | 0.79 |
| SL72 | 43.29 | 4.2 | 74 | 0.85 | 0.17 | -23.45 | 5.89 | n.a. | n.a. | n.a. |
| SL91 | 43.02 | 4.2 | 91 | 0.46 | 0.11 | -23.27 | 4.81 | n.a. | n.a. | n.a. |
| SM61 | 43.27 | 4.32 | 64 | 0.79 | 0.15 | -23.61 | 6.08 | 44.92 | 45.93 | 9.15 |
| SM87 | 43.05 | 4.32 | 92 | 0.63 | 0.15 | -23.34 | 4.88 | n.a. | n.a. | n.a. |
| SN76 | 43.22 | 4.36 | 78 | 0.9 | 0.18 | -23.59 | 5.77 | 54.08 | 42.85 | 3.08 |
| SN85 | 43.08 | 4.37 | 91 | 0.63 | 0.14 | -23.63 | 5.24 | n.a. | n.a. | n.a. |
| SO66 | 43.23 | 4.51 | 67 | 0.89 | 0.17 | -23.94 | 6 | 20.58 | 78.93 | 0.49 |
| SO80 | 43.13 | 4.51 | 84 | 0.87 | 0.18 | -23.65 | 5.53 | 54.8 | 43.44 | 1.77 |
| SP77 | 43.22 | 4.65 | 70 | 0.99 | 0.17 | -24.45 | 6.83 | 51.73 | 46.14 | 2.13 |
| SQ67 | 43.24 | 4.65 | 66 | 1.04 | 0.18 | -24.37 | 6.78 | 51.57 | 46 | 2.43 |
| SR61 | 43.27 | 4.73 | 63 | 1.06 | 0.17 | -25.07 | 7.28 | n.a. | n.a. | n.a. |
| SS80 | 43.26 | 4.78 | 82 | 1.16 | 0.18 | -25.33 | 7.36 | 52.4 | 47.2 | 0.4 |

n.a = not available

Table 7.3. Molecular composition of surficial sediment samples. S = syringyl phenols; V = vanillyl phenols; C = cinnamyl phenols; Λ = (S+V+C) B = benzoic acids; P = p-hydroxybenzenes, October 2004

| core | S mg/100 mg OC | V mg/100 mg OC | C mg/100 mg OC | Λ mg/100 mg OC | % CuO products | B mg/100 mg OC | % CuO products | P mg/100 mg OC | % CuO products |
|------------------------------|----------------------|----------------------|----------------------|------------------------------|-------------------|----------------------|-------------------|----------------------|-------------------|
| <i>Rhône prodelta</i> | | | | | | | | | |
| E33 | 1.93 | 1.79 | 0.35 | 4.07 | 79.74% | 0.39 | 7.59% | 0.65 | 12.67% |
| E48B | 1.27 | 1.27 | 0.20 | 2.74 | 80.49% | 0.19 | 5.56% | 0.48 | 13.94% |
| E56 | 1.16 | 1.34 | 0.26 | 2.76 | 73.35% | 0.39 | 10.40% | 0.61 | 16.24% |
| E65 | 1.58 | 1.69 | 0.39 | 3.66 | 76.82% | 0.40 | 8.39% | 0.70 | 14.79% |
| F32 | 1.30 | 1.72 | 0.23 | 3.26 | 78.08% | 0.22 | 5.33% | 0.69 | 16.59% |
| F47 | 0.85 | 1.47 | 0.30 | 2.63 | 74.96% | 0.23 | 6.57% | 0.65 | 18.47% |
| F58 | 1.03 | 1.30 | 0.21 | 2.54 | 76.16% | 0.23 | 6.75% | 0.57 | 17.09% |
| G31 | 1.45 | 1.78 | 0.29 | 3.53 | 78.75% | 0.25 | 5.67% | 0.70 | 15.59% |
| G47 | 1.46 | 1.91 | 0.27 | 3.64 | 77.76% | 0.24 | 5.09% | 0.80 | 17.15% |
| G57 | 1.01 | 1.29 | 0.20 | 2.51 | 75.65% | 0.20 | 6.00% | 0.61 | 18.34% |
| G65 | 0.92 | 1.22 | 0.17 | 2.30 | 71.62% | 0.23 | 7.21% | 0.68 | 21.17% |
| H30 | n.a. | n.a. | n.a. | n.a. | n.a. | n.a. | n.a. | n.a. | n.a. |
| H45 | n.a. | n.a. | n.a. | n.a. | n.a. | n.a. | n.a. | n.a. | n.a. |
| H56 | n.a. | n.a. | n.a. | n.a. | n.a. | n.a. | n.a. | n.a. | n.a. |
| H62 | n.a. | n.a. | n.a. | n.a. | n.a. | n.a. | n.a. | n.a. | n.a. |
| I32 | 1.02 | 1.42 | 0.17 | 2.61 | 75.74% | 0.22 | 6.30% | 0.62 | 17.96% |
| I42 | n.a. | n.a. | n.a. | n.a. | n.a. | n.a. | n.a. | n.a. | n.a. |
| I50 | 1.18 | 1.48 | 0.23 | 2.90 | 76.79% | 0.23 | 6.04% | 0.65 | 17.17% |
| I58 | n.a. | n.a. | n.a. | n.a. | n.a. | n.a. | n.a. | n.a. | n.a. |
| I68 | 1.00 | 1.28 | 0.21 | 2.49 | 74.40% | 0.24 | 7.06% | 0.62 | 18.54% |
| J28 | 1.54 | 1.72 | 0.31 | 3.57 | 79.79% | 0.26 | 5.83% | 0.64 | 14.38% |
| J36 | 1.63 | 1.35 | 0.26 | 3.24 | 78.15% | 0.23 | 5.44% | 0.68 | 16.40% |
| J46 | 1.11 | 1.30 | 0.26 | 2.67 | 77.35% | 0.26 | 7.65% | 0.52 | 15.00% |
| J52 | 1.07 | 1.28 | 0.27 | 2.62 | 77.52% | 0.27 | 8.05% | 0.49 | 14.43% |
| J63 | 1.21 | 1.51 | 0.27 | 2.99 | 73.95% | 0.41 | 10.21% | 0.64 | 15.85% |
| J70 | 0.98 | 1.13 | 0.23 | 2.33 | 76.39% | 0.25 | 8.10% | 0.47 | 15.51% |
| K28 | 1.81 | 1.71 | 0.28 | 3.79 | 80.22% | 0.30 | 6.26% | 0.64 | 13.52% |
| K43 | n.a. | n.a. | n.a. | n.a. | n.a. | n.a. | n.a. | n.a. | n.a. |
| K57 | n.a. | n.a. | n.a. | n.a. | n.a. | n.a. | n.a. | n.a. | n.a. |
| K65 | 0.96 | 1.16 | 0.19 | 2.31 | 72.92% | 0.21 | 6.78% | 0.64 | 20.30% |
| K72 | 0.64 | 1.05 | 0.13 | 1.81 | 73.68% | 0.19 | 7.86% | 0.45 | 18.46% |
| <i>S-W stations</i> | | | | | | | | | |
| T74 | n.a. | n.a. | n.a. | n.a. | n.a. | n.a. | n.a. | n.a. | n.a. |
| CSB66 | n.a. | n.a. | n.a. | n.a. | n.a. | n.a. | n.a. | n.a. | n.a. |
| CSB100 | n.a. | n.a. | n.a. | n.a. | n.a. | n.a. | n.a. | n.a. | n.a. |
| CSB84 | n.a. | n.a. | n.a. | n.a. | n.a. | n.a. | n.a. | n.a. | n.a. |
| CSB92 | n.a. | n.a. | n.a. | n.a. | n.a. | n.a. | n.a. | n.a. | n.a. |
| CSB112 | 0.37 | 0.44 | 0.11 | 0.80 | 68.80% | 0.17 | 14.89% | 0.19 | 16.31% |
| CSD58 | n.a. | n.a. | n.a. | n.a. | n.a. | n.a. | n.a. | n.a. | n.a. |
| CSD91 | n.a. | n.a. | n.a. | n.a. | n.a. | n.a. | n.a. | n.a. | n.a. |
| CSD100 | n.a. | n.a. | n.a. | n.a. | n.a. | n.a. | n.a. | n.a. | n.a. |
| CSD107 | n.a. | n.a. | n.a. | n.a. | n.a. | n.a. | n.a. | n.a. | n.a. |
| HTU282 | n.a. | n.a. | n.a. | n.a. | n.a. | n.a. | n.a. | n.a. | n.a. |
| PR1 | 0.14 | 0.26 | 0.03 | 0.44 | 58.00% | 0.11 | 14.32% | 0.21 | 27.68% |

Table 7.4. Molecular composition of surficial sediment. S = syringyl phenols; V = vanillyl phenols; C = cinnamyl phenols; Λ = (S+V+C) B = benzoic acids; P = p-hydroxybenzenes, April 2005

| Core | S | V | C | Λ | | B | | P | |
|----------------------------------|--------------|--------------|--------------|--------------|----------------|--------------|----------------|--------------|----------------|
| | mg/100 mg OC | mg/100 mg OC | mg/100 mg OC | mg/100 mg OC | % CuO products | mg/100 mg OC | % CuO products | mg/100 mg OC | % CuO products |
| <i>Rhône prodelta</i> | | | | | | | | | |
| E33 | 1.06 | 1.21 | 0.19 | 2.46 | 72.69% | 0.21 | 6.11% | 0.72 | 21.20% |
| F31 | n.a. | n.a. | n.a. | n.a. | n.a. | n.a. | n.a. | n.a. | n.a. |
| F32 | 1.18 | 1.32 | 0.23 | 2.73 | 73.20% | 0.24 | 6.35% | 0.76 | 20.45% |
| G20 | n.a. | n.a. | n.a. | n.a. | n.a. | n.a. | n.a. | n.a. | n.a. |
| G31 | 1.00 | 1.19 | 0.20 | 2.40 | 74.00% | 0.22 | 6.81% | 0.62 | 19.20% |
| RB41 | 1.14 | 1.37 | 0.22 | 2.72 | 75.31% | 0.24 | 6.73% | 0.65 | 17.96% |
| RB49 | n.a. | n.a. | n.a. | n.a. | n.a. | n.a. | n.a. | n.a. | n.a. |
| RB55 | 1.08 | 1.25 | 0.21 | 2.54 | 73.59% | 0.27 | 7.78% | 0.64 | 18.63% |
| RB60 | 1.22 | 1.51 | 0.24 | 2.96 | 75.68% | 0.27 | 6.99% | 0.68 | 17.33% |
| RB65 | n.a. | n.a. | n.a. | n.a. | n.a. | n.a. | n.a. | n.a. | n.a. |
| RB69 | 1.01 | 1.30 | 0.20 | 2.52 | 75.27% | 0.24 | 7.29% | 0.58 | 17.44% |
| RC35 | n.a. | n.a. | n.a. | n.a. | n.a. | n.a. | n.a. | n.a. | n.a. |
| RC50 | n.a. | n.a. | n.a. | n.a. | n.a. | n.a. | n.a. | n.a. | n.a. |
| RD36 | n.a. | n.a. | n.a. | n.a. | n.a. | n.a. | n.a. | n.a. | n.a. |
| RD38 | 1.22 | 1.44 | 0.21 | 2.87 | 73.24% | 0.23 | 5.95% | 0.82 | 20.81% |
| RD43 | n.a. | n.a. | n.a. | n.a. | n.a. | n.a. | n.a. | n.a. | n.a. |
| RD53 | 1.07 | 1.40 | 0.18 | 2.66 | 70.77% | 0.26 | 6.92% | 0.84 | 22.32% |
| RD60 | 1.15 | 1.42 | 0.22 | 2.79 | 75.62% | 0.28 | 7.55% | 0.62 | 16.82% |
| RD65 | 1.15 | 1.29 | 0.19 | 2.63 | 70.67% | 0.24 | 6.33% | 0.86 | 22.99% |
| RD71 | 0.99 | 1.18 | 0.18 | 2.36 | 71.38% | 0.25 | 7.64% | 0.69 | 20.98% |
| <i>Mid-shelf mud belt</i> | | | | | | | | | |
| SA65 | 0.24 | 0.26 | 0.09 | 0.59 | 71.38% | 0.17 | 7.64% | 0.32 | 20.98% |
| SB77 | 0.11 | 0.14 | 0.04 | 0.29 | 50.81% | 0.10 | 17.34% | 0.18 | 31.84% |
| SC63 | n.a. | n.a. | n.a. | n.a. | n.a. | n.a. | n.a. | n.a. | n.a. |
| SD79 | 0.12 | 0.15 | 0.04 | 0.30 | 53.73% | 0.08 | 15.22% | 0.17 | 31.05% |
| SE62 | n.a. | n.a. | n.a. | n.a. | n.a. | n.a. | n.a. | n.a. | n.a. |
| SF75 | 0.28 | 0.32 | 0.10 | 0.70 | 71.35% | 0.10 | 10.38% | 0.18 | 18.27% |
| SG61 | n.a. | n.a. | n.a. | n.a. | n.a. | n.a. | n.a. | n.a. | n.a. |
| SH79 | n.a. | n.a. | n.a. | n.a. | n.a. | n.a. | n.a. | n.a. | n.a. |
| SI65 | n.a. | n.a. | n.a. | n.a. | n.a. | n.a. | n.a. | n.a. | n.a. |
| SJ78 | 0.21 | 0.18 | 0.00 | 0.39 | 50.00% | 0.09 | 11.15% | 0.30 | 38.85% |
| SK63 | n.a. | n.a. | n.a. | n.a. | n.a. | n.a. | n.a. | n.a. | n.a. |
| SL72 | 0.11 | 0.15 | 0.03 | 0.29 | 51.72% | 0.11 | 19.66% | 0.16 | 28.61% |
| SL91 | 0.12 | 0.10 | 0.03 | 0.25 | 42.86% | 0.15 | 25.16% | 0.19 | 31.98% |
| SM61 | n.a. | n.a. | n.a. | n.a. | n.a. | n.a. | n.a. | n.a. | n.a. |
| SM87 | n.a. | n.a. | n.a. | n.a. | n.a. | n.a. | n.a. | n.a. | n.a. |
| SN76 | 0.12 | 0.17 | 0.03 | 0.32 | 53.37% | 0.18 | 29.99% | 0.10 | 16.63% |
| SN85 | 0.16 | 0.28 | 0.04 | 0.48 | 59.99% | 0.14 | 17.32% | 0.18 | 22.69% |
| SO66 | 0.22 | 0.34 | 0.08 | 0.64 | 63.32% | 0.14 | 13.90% | 0.23 | 22.78% |
| SO80 | 0.19 | 0.35 | 0.06 | 0.60 | 54.86% | 0.22 | 20.38% | 0.27 | 24.76% |
| SP77 | 0.39 | 0.60 | 0.08 | 0.91 | 64.28% | 0.16 | 11.34% | 0.35 | 24.38% |
| SQ67 | n.a. | n.a. | n.a. | n.a. | n.a. | n.a. | n.a. | n.a. | n.a. |
| SR61 | n.a. | n.a. | n.a. | n.a. | n.a. | n.a. | n.a. | n.a. | n.a. |

8. Conclusions

A multi-proxy study was conducted to investigate source, transport, and deposition of OM in the Adriatic Sea and Gulf of Lions. Surface sediments and suspended material were collected along the sediment dispersal system. CuO oxidation, elemental, $\delta^{13}\text{C}$ and $\Delta^{14}\text{C}$ analyses were carried out to characterize the organic material. Based on our results, we can conclude that changes in biogeochemical surficial distributions reflect elevated dynamism of continental margins. This study highlights the remarkable interaction between sediment transport processes and organic biogeochemical trends in both Adriatic Sea and Gulf of Lions, in particular for the prodeltaic regions. Different biogeochemical distributions in both systems reflect either differing sediment transport dynamics (clinoform vs mid-shelf mud deposit) or importance of contributions from minor (i.e. Apennine) rivers to the Adriatic system (delivery of sediment via point vs line sources). The following is a summary of salient conclusions for each study area.

1) Adriatic Sea

- Based on the information obtained from PCA analysis, the western Adriatic sediments can be grouped into three main biogeochemical partitions: proximal Po prodelta, distal Po prodelta, and Adriatic mud-wedge. High variability in elemental, isotopic, and biomarker data was measured in the Po prodelta area, whereas the region south of the Po region exhibited a narrower range of values.
- The OM collected in the water column is compositionally heterogeneous, with contributions from marine phytoplankton, riverine-estuarine phytoplankton, and soil-derived OM. In the Po prodelta area, elemental and isotopic compositions suggest that

the phytoplankton (marine and riverine-estuarine) are the major OC constituent in the surface water column, ranging from ~50-80%. In the lowermost layer (1 m above the seafloor) the soil-derived OC is the most important OC source, ranging from ~50-70%. Along the Adriatic shelf, primary production is influenced by land-derived nutrients that promote phytoplankton growth which in turn influence the isotopic composition in the water column. At the same time, a fraction of fine, isotopically depleted, terrestrial material travels southward suspended within the WAAC. The dilution of marine-derived OC with terrigenous material, located in the distal stations, generates a marked longitudinal $\delta^{13}\text{C}_{\text{OC}}$ gradient seaward.

- Soil-derived OC is the main component of the material supplied by the Biferno and Po rivers, on average ~74 %. Riverine phytoplankton and plant fragments are additional important sources, accounting for ~19 and ~8%, respectively.
- The surficial sediments were highly influenced by terrigenous material, which is dominated by soil-derived OM (from ~ 50-94%). Frequent physical reworking and reoxidation of surficial sediments results in an efficient reactor where refractory soil-derived OC, delivered by the Po and Appennine rivers, is rapidly accumulated and preserved. Significant contributions of plant fragments are geographically limited in the Po prodelta, which exhibits the highest plant-fragment fraction in the proximal prodelta area, ~ 5%. Along the shelf, the 3,5-Bd/V and Pd:[Vd+Sd] ratios indicate humified soil-derived OM, confirming the absence of noteworthy plant fragment contributions. The riverine-estuarine phytoplankton is confined within the Po prodelta area, where the highest contribution on average is exhibited in the proximal Po prodelta area, ~9%.

2) Po prodelta area

- During the 100-year flood, the discharge of highly-concentrated and flocculated sediment into the relatively calm basin lead to rapid deposition of fine material. Fine sediment, because of its higher surface area, is particularly rich in humified, soil-derived OC relative to the coarse fraction. Following the initial emplacement of the flood deposit, surficial sediments coarsened. Lignin-rich vascular plant fragments are associated with coarse material because of their hydraulic behavior. As a result, the evolution of the surficial flood deposit with time resulted in the preferential concentration of fresh, modern woody debris in the seabed, at the expense of aged, humified, soil-derived OC. Based on the correlation between CuO oxidation lignin products and ^{14}C age, the higher the content of fresh, lignin-rich vascular plant fragments, the younger the OM.
- Although large part of the OC contribution from the Po is aged, the river also delivers a small fraction of modern OC which incorporates anthropogenic ^{14}C , produced by nuclear weapons testing.
- Over the course of 2 years, the algal-derived OC contribution was negligible. It is probable that oxygen exposure time controls algal OC preservation. As bioturbation and resuspension create an oscillating oxic/anoxic environment, episodic physical and biological mixing affects the degradation of fresh algal compounds in prodeltaic sediments.

3) Gulf of Lions

- The terrestrial composition in the prodelta surficial sediments varied seasonally: physical reworking of new sediment has an active role in the preferential transport of the finest material which in turn impacted the $\delta^{13}\text{C}$, Λ , N/C values as well as the grain size distribution in the surficial sediments.
- Surficial concentrations of plant debris, coupled with coarse-sized particles, reflected lateral sorting in the benthic boundary layer. Wood fragments, rich in organic matter and lignin, hydraulically behave like very fine sand and are retained within the prodelta area.
- Soil-derived OM adsorbed onto fine fraction, lignin-poor particles, is selectively transported out of the prodelta along the main sediment dispersal system. Therefore a two-end-member mixing model among soil-derived OM and marine phytoplankton, might be adequate to quantification of terrigenous and marine contribution in this continental margin.
- The advected material that reaches the slope and the head of the canyons has lost its original terrestrial signature and is mainly marine. Along the dispersal system, the terrestrial OM adsorbed onto the fine material is either degraded by microbial activity and/or diluted by marine OM. The geochemical surficial distributions observed suggest a relatively elevated retention time for the sediments within the proximal and distal prodelta area, allowing for significant microbial degradation and marine dilution.

Bibliography

- Aller, R.C. 1998. Mobile deltaic and continental shelf muds as suboxic, fluidized bed reactors. *Marine Chemistry* 61, 143-155.
- Aller, R.C., Blair, N.E., 2004. Early diagenetic remineralization of sedimentary organic C in the Gulf of Papua deltaic complex (Papua New Guinea): Net loss of terrestrial C and diagenetic fractionation of C isotopes. *Geochimica et Cosmochimica Acta*, 68:1815-1825.
- Berner R. A., 1989. Biogeochemical cycles of carbon and sulfur and their effect on atmospheric oxygen over phanerozoic time. *Palaeogeography, Palaeoclimatology, Palaeoecology* 75, 97–122.
- Bianchi, T.S., Mitra, S., McKee, B. A., 2002. Sources of terrestrially-derived organic carbon in lower Mississippi River and Louisiana shelf sediments: Implications for differential sedimentation and transport at the coastal margin. *Marine Chemistry*, 77:211–223.
- Blair, N. E., Leithold, E. L., Ford, S. T., Peeler, K. A., Holmes J. C., and Perkey D. W., 2003. The persistence of memory: The fate of ancient sedimentary organic carbon in a modern sedimentary system. *Geochimica et Cosmochimica Acta* 67, 63–74.
- Boldrin, A., Langone, L., Miserocchi S., Turchetto M., Acri A., 2005. Po River plume on the Adriatic continental shelf: observations on dispersion and sedimentation dynamics of dissolved and suspended matter during different river discharge rates. *Marine Geology*, 222–223:135–158.
- Cattaneo, A., Correggiari, A., Langone, L., Trincardi, F., 2003, The late-Holocene Gargano subaqueous delta, Adriatic shelf: Sediment pathways and supply fluctuations. *Marine Geology* 193/1-2, 61-91.
- Cloern, J. E., Cole, B. E., Wong, R. L. J., Alpine, A. E., 1985. Temporal dynamics of estuarine phytoplankton: a case study of San Francisco Bay. *Hydrobiologia* 29: 153-176
- Correggiari, A., Trincardi, F., Langone, L., Roveri, M., 2001, Styles of failure in late Holocene highstand prodelta wedges on the Adriatic shelf. *Journal of Sedimentary Research, part B* 71, 218-236.
- Degobbis, D., Gilmartin, M., Revelante, N., 1986. An annotated nitrogen budget calculation for the northern Adriatic Sea. *Marine Chemistry* 20, 159–177.
- Degobbis, D., Gilmartin, M., 1990. Nitrogen, phosphorous and biogenic silicon budgets for the northern Adriatic Sea. *Oceanologia Acta* 13, 31– 43.
- Dittmar, T., Lara R.J., 2001. Molecular evidence for lignin degradation in sulfate reducing mangrove sediments (Amazônia, Brazil). *Geochimica et Cosmochimica Acta* 65, 1403-1414.
- Faganeli, J., Malei, J., Pezdič, J., Malačič, V., 1988. C:N:P ratios and stable C isotopic ratios as indicators of sources of organic matter in the Gulf of Trieste (northern Adriatic). *Oceanologia Acta* 11, 377– 382.

- Fain, A. M. V., Ogston, A. S., Sternberg, R. W. Sediment transport event analysis on the western Adriatic continental shelf, *Continental Shelf Research*, doi:10.1016/j.csr.2005.03.007
- Fernandes, M. B., Elias V. O., Cardoso J. N., Carvalho M.S., 1999. Sources and fate of n-alkanols and sterols in sediments of the Amazon shelf. *Organic geochemistry* 30, 1075-1087.
- Fox, J.M., Hill, P.S., Milligan, T.G., Boldrin, A., 2004. Flocculation and sedimentation on the Po River Delta. *Marine Geology*. 203, 95– 107.
- Fry, B. and Sherr E.B.,1984. $\delta^{13}\text{C}$ measurements as indicators of carbon flow in marine and freshwater ecosystems. *Marine Science* 27, 13–47.
- Frignani, M., Langone, L., Ravaioli, M., Sorgente, D., Alvisi, F., Albertazzi, S., 2005. Fine sediment mass balance in the western Adriatic continental shelf over a century time scale. *Marine Geology* 222/223, 113–133.
- Geyer, W.R., Hill, P.S., and Kineke, G. C., 2004. The transport and dispersal of sediment by buoyant coastal flows. *Continental Shelf Research*, 24:927-949.
- Giordani, P., Helder, W., Koning, E., Miserocchi, S., Danovaro, R., & Malaguti A., 2002. Gradients of pelagic–benthiccoupling and carbon budgets in the Adriatic and northern Ionian Sea. *Journal of Marine Systems* 33–34, 365–387.
- Goñi M.A. and Hedges J.I., 1992. Lignin dimers: Structures, distribution, and potential geochemical applications. *Geochimica et Cosmochimica Acta* 56, 4025–4043.
- Goñi M. A. and Hedges J.I., 1995. Sources and reactivities of marine derived organic matter in coastal sediments as determined by alkaline CuO oxidation. *Geochimica et Cosmochimica Acta* 59, 2965–2981.
- Goñi, M.A., Ruttenger, K.C., Eglinton, T.I., 1998. A reassessment of the sources and importance of land-derived organic matter in surface sediments from the Gulf of Mexico. *Geochimica et Cosmochimica Acta* 62, 3055–3075.
- Goñi M.A. and Montgomery S., 2000. Alkaline CuO oxidation with a microwave digestion system. Lignin analyses of geochemical samples. *Analytical Chemistry* 72, 3116–3121.
- Goñi M. A., Yunker M. B., Macdonald R. W., and Eglinton T. I., 2000. Distribution and sources of organic biomarkers in arctic sediments from the Mackenzie River and Beaufort Shelf. *Marine Chemistry* 71, 23–51.
- Goñi, M.A., Teixeira, M.J., and Perkey D.W., 2003. Sources and distribution of organic matter in a river-dominated estuary (Winyah Bay, SC, USA). *Estuarine Coastal and Shelf Science*, 57, 1023-1048.
- Goñi, M. A., Monacci, N., Gisewhite. R., Andrea Ogston, A., Crockett, J., Nittrouer, C., 2006. Distribution and sources of particulate organic matter in the water column and sediments of the Fly River Delta, Gulf of Papua (Papua New Guinea), *Estuarine, Coastal and Shelf Science* 69: 225-245

- Goñi M. A., Yunker, M. B., Macdonald, R. W., and Eglinton, T. I. (2005) The supply and preservation of ancient and modern components of organic carbon in the Canadian Beaufort Shelf of the Arctic Ocean. *Marine Chemistry* 93, 53-73.
- Gordon, E.S., Goñi, M.A., 2003. Sources and distribution of terrigenous organic matter delivered by the Atchafalaya River to sediments in the northern Gulf of Mexico. *Geochimica et Cosmochimica Acta* 67, 2359–2375.
- Hedges J. I. and Mann D. C., 1979. The lignin geochemistry of marine sediments from the southern Washington coast. *Geochimica et Cosmochimica Acta* 43, 1809–1818.
- Hedges J. I., Keil R. G., 1995. Sedimentary organic matter preservation: An assessment and speculative synthesis. *Marine Chemistry* 49, 81–115.
- Hedges, J. I., Oades, J.M., 1997. Comparative organic geochemistries of soils and sediments. *Organic Geochemistry* 27, 319–361.
- Hedges, J.I., Keil, R.G. and Benner, R., 1997. What happens to terrestrial organic matter in the ocean? *Organic Geochemistry* 27, 195–212.
- Keil, R.G., Tsamakis, E., Giddings J.C., and Hedges J.I., 1998. Biochemical distributions (amino acids, neutral sugars, and lignin phenols) among size classes of modern marine sediments from the Washington Coast. *Geochimica et Cosmochimica Acta* 62, 1347-1364.
- Kristensen, E. and Andersen, F.Ø., 1987. Determination of organic carbon in marine sediments: a comparison of two CHN-analyzer methods. *Journal of Experimental Marine Biology and Ecology* 109, 15-23
- Leithold, E. L. and Hope, R.S. 1999. Deposition and modification of a flood layer on the northern California shelf: lessons from and about the fate of terrestrial particulate organic carbon. *Marine Geology* 154, 183-195
- Leithold, E. L., N. E. Blair, and D. W. Perkey, 2006. Geomorphologic controls on the age of particulate organic carbon from small mountainous and upland rivers. *Global Biogeochemical Cycles*, 20, GB3022, doi:10.1029/2005GB002677.
- Ludwig, W. 2001. The age of river carbon. *Nature* 409: 466-467.
- Mayer, P. A., 1994. Preservation of elemental and isotopic source identification of sedimentary organic matter. *Chemical Geology* 144, 289–302.
- Mayer, L. M., Keil, R. G., Macko, S. A., Joye, S. B., Ruttenberg, K. C. & Aller, R. C., 1998. Importance of suspended particulates in riverine delivery of bioavailable nitrogen to coastal zones. *Global Biogeochemical Cycles* 12, 573–579.
- Malanotte Rizzoli, P., Bergamasco, A., 1983. The dynamics of the coastal region of the Northern Adriatic Sea. *Journal of Physical Oceanography* 13, 1105-1130.

- Martinotti, W., Camusso, M., Guzzi, L., Patrolecco, L., Pettine, M., 1997. C, N and their stable isotopes in suspended and sedimented matter from the Po estuary (Italy). *Water Air Soil Pollution* 99, 325– 332.
- Millie, D. F., G. L. Fahnenstiel, Steven E. Lohrenz, H. J. Carrick, T. Johengen, and O. M. E. Schofield, 2003. Physical-biological coupling in southeastern Lake Michigan: Influence of episodic sediment resuspension on phytoplankton. *Aquatic Ecology* 37, 393-408.
- Miserocchi, S., Langone, L., Tesi, T., 2007. Content and isotopic composition of organic carbon within a flood layer in the Po River prodelta (Adriatic Sea). *Continental Shelf Research*, doi:10.1016/j.csr.2005.05.005
- Nelson, B.W., 1970. Hydrography, sediment dispersal, and recent historical development of the Po river delta. In: Morgan, J.P. (Ed.), *Deltaic Sedimentation: Modern and Ancient*, Soc. Paleontologists and Mineralogists, New York, pp. 152– 184.
- Ogrinc, N., Fontolan, G., Faganeli, J., Covelli S., 2005. Carbon and nitrogen isotope compositions of organic matter in coastal marine sediments (the Gulf of Trieste, N Adriatic Sea): Indicators of sources and preservation. *Marine Chemistry*, 95, 163–181.
- Opsahl, S., and R. Benner. 1995. Early diagenesis of vascular plant tissues: lignin and cutin decomposition and biogeochemical implications. *Geochimica Cosmochimica Acta* 59, 4889-4904
- Palinkas, C.M., Nittrouer C.A., 2006. Cliniform sedimentation along the Apennine River shelf, Adriatic Sea. *Marine Geology*, *Marine Geology* 234, 245–260
- Penna N., Capellacci S., Ricci F., 2004. The influence of the Po River discharge on phytoplankton bloom dynamics along the coastline of Pesaro (Italy) in the Adriatic Sea. *Marine Pollution Bulletin* 48, 321–326
- Pettine, M., Patrolecco, L., Camuso, M., Crescenzo, S., 1998. Transport of carbon and nitrogen to the northern Adriatic Sea by the Po River. *Estuarine Coastal Shelf Science* 46, 127–142.
- Prahl F.G., 1985. Chemical evidence of differential particle dispersal in the southern Washington coastal environment. *Geochimica Cosmochimica Acta* 49, 2533–2539.
- Prahl, F. G., Ertel, J. R., Goñi, M. A., Sparrow, M. A., Eversmeyer, B., 1994. Terrestrial organic carbon contributions to sediments on the Washington margin. *Geochimica et Cosmochimica Acta* 58, 3035–3048.
- Prahl F., DeLange G.J., Scholten S., and Cowie G.L., 1997. A case of post-depositional aerobic degradation of terrestrial organic matter in turbidite deposits from the Madeira Abyssal Plain. *Organic Geochemistry* 27, 141–152.
- Puig, P., Ogston, A., Guillen, J., Fain, A., Palanques, A. Sediment transport processes from the topset to the forest of a crenulated cliniform. *Continental Shelf Research*, doi:10.1016/j.csr.2006.11.005

- Schneider, B., Schlitzer, B., Fischer, G., Nöthig E., 2003. Depth-dependent elemental compositions of particulate organic matter (POM) in the ocean. *Global Biogeochemical Cycles*, 17-2: 1-16.
- Syvistski, J.P.M, Kettner, A.J. On the flux of water and sediment into the Northern Adriatic Sea. *Continental Shelf Research*, doi:10.1016/j.csr.2005.08.029.
- Stevens, A.W., Wheatcroft, R.A., Wiberg, P.L. Sediment erodibility along the western Adriatic margin, Italy. *Continental Shelf Research*, in press.
- Teeri J. A. and Stowe L. G., 1976. Climatic patterns and the distribution of C4 grasses in North America. *Oecologia* 23, 1–12.
- Tesi, T., Miserocchi, S. Langone, L., Boni, L., Guerrini, F. 2006a. Sources, fate and distribution of organic matter on the western Adriatic continental shelf, Italy. *Water, Air and Soil pollution: Focus* 6, 593–603.
- Tesi T, Miserocchi S, Goñi MA, Langone L, 2006b. Comparative organic geochemistries in surficial sediments from the Rhône (France) and Po (Italy) prodelta area. *Ocean Science Meeting, Honolulu (Hi) 20-24 February, OS16A-34*
- Tesi T, Miserocchi S, Goñi MA, Langone L. Origin and distribution of organic material in the western Mediterranean Sea, Gulf of Lions, France. *Marine chemistry*, in press, doi: 10.1016/j.marchem.2007.01.005.
- Tesi T, Miserocchi S, Goñi MA, Langone L. Organic carbon dynamics along the Western Adriatic shelf in surficial sediments and particulate material. *Estuarine coastal and shelf science*, in press. *Estuarine, Coastal and Shelf Science*.
- Traykovski, P., Geyer, W.R. Observations and modeling of wave induced fluid-mud gravity flows on the Po prodelta. *Continental Shelf Research*, doi:10.1016/j.csr.2005.07.008.
- Wainright, S.C., Hopkinson Jr., C.S. 1997. Effects of sediment resuspension on organic matter processing in coastal environments: a simulation model. *Journal of Marine Systems* 11, 353-368.
- Verardo, D.J., Froehlich, P.N., and McIntyre, A., 1990. Determination of organic carbon and nitrogen in marine sediments using the Carlo Erba NA-1500 Analyzer. *Deep-Sea Research*, 37 157-165.
- Zavatarelli, M., Pinardi, N., Kourafalou, V.H., Maggiore, A., 2002. Diagnostic and prognostic model studies of the Adriatic Sea general circulation: Seasonal variability. *Journal of Geophysical Research*, 107(C1), 3004, doi:10.1029/2000JC000210.